UNIVERSIDADE DE SÃO PAULO
FACULDADE DE CIÊNCIAS FARMACÊUTICAS
PROGRAMA DE PÓS-GRADUAÇÃO EM FARMÁCIA
(FÁRMACO E MEDICAMENTOS)
ÁREA DE PRODUÇÃO E CONTROLE DE FÁRMACOS

MARIANA YASUE SAITO MIYAGI

Development and evaluation of flubendazole inhalable nanoparticles for lung cancer treatment

São Paulo
2023

UNIVERSIDADE DE SÃO PAULO
FACULDADE DE CIÊNCIAS FARMACÊUTICAS
PROGRAMA DE PÓS-GRADUAÇÃO EM FARMÁCIA
(FÁRMACO E MEDICAMENTOS)
ÁREA DE PRODUÇÃO E CONTROLE DE FÁRMACOS

MARIANA YASUE SAITO MIYAGI

Development and evaluation of flubendazole inhalable nanoparticles for lung cancer treatment

Versão Corrigida

Tese apresentada à Faculdade de Ciências Farmacêuticas da Universidade de São Paulo para obtenção do título de Doutora em Ciências.

Orientador: Prof. Dr. Gabriel Lima Barros de Araujo
Coorientador: Prof. Dr. Tetsuya Ozeki

São Paulo
2023

Mariana Yasue Saito Miyagi

Development and evaluation of flubendazole inhalable nanoparticles for lung cancer treatment
Tese apresentada à Faculdade de Ciências Farmacêuticas da Universidade de São Paulo para a obtenção do título de Doutora em Ciências.

Comissão Julgadora

Prof. Dr. Gabriel Lima Barros de Araujo
orientador/presidente

_____
1o. Examinador

_____
2o. Examinador

_____
3o. Examinador

_____
4o. Examinador

São Paulo, _____ de _____ de 2023.

DEDICATION

To my dear parents who gave me all the tools one can need to grow and be happy.

To Rodrigo, my husband, the one who completes me and was there for me during this journey's ups and downs.

ACKNOWLEDGEMENTS

"Happiness requires struggle."

"Happiness is not something you achieve.
It's not something you do or someplace you get to.
Happiness is something you inhabit."

"True happiness occurs only when you find the problems
you enjoy having and enjoy solving."

Mark Manson

PREFACE

This thesis is an original work elaborated by Mariana Yasue Saito Miyagi under the supervision of Prof. Gabriel de Araujo at the University of São Paulo.

The motivations for starting this project are described in Chapter 1. Chapter 2 aims to encompass all intersection areas between the targeted cancer and the proposed innovative pharmaceutical form, and grounded in pharmaceutical technology is presented as a state-of-the-art review. As the focused area is an incipient field, Chapter 3 is a yet to be published critical review that discusses the main challenges that must be overcome to make feasible the translation of oral inhaled chemotherapy from the bench to the bedside.

Chapter 4 briefly states the rationale for screening that is not usually published since it compiles a few rather obvious and unsuccessful approaches. The author still finds that it pertinent to be included in this work as one might find it useful during his or her early research.

A version of Chapter 5 was published in International Journal of Pharmaceutics, 2023. DOI number: 10.1016/j.ijpharm.2023.123324 by Mariana Yasue Saito Miyagi; Rafael de Oliveira Faria; Gabriel Batista de Souza; Claudiana Lameu; Tatsuaki Tagami; Tetsuya Ozeki; Vinícius Danilo Nonato Bezzon; Megumi Nishitani Yukuyama; Nadia Araci Bou-Chacra and Gabriel Lima Barros de Araujo. As the first author, I was responsible for conceptualization, investigation, formal analysis, visualization, writing, project administration and review and editing. The data presented in Chapters 4 and 5 was originated from the collaboration between Pharmaceutical Technology & Solid State Research Group under supervision of Prof. Gabriel de Araujo at the University of São Paulo; Laboratório de Estudos dos Mecanismos Moleculares da Metástase under supervision of Prof. Claudiana Lameu at the University of São Paulo; and Drug Delivery and Nano Pharmaceutics Laboratory under supervision of Prof. Tetsuya Ozeki at the Nagoya City University.

The conclusion of this work is presented in Chapter 6 and future directions in Chapter 8, with the expectation to convey to the reader the interesting perspectives of the orally inhaled therapy for cancer.

RESUMO

MIYAGI, M. Y. S. Desenvolvimento e avaliação de nanopartículas inalatórias de flubendazol para tratamento de câncer de pulmão. 2023. 133f. Tese (Doutorado) – Faculdade de Ciências Farmacêuticas, Universidade de São Paulo, São Paulo, 2023.

O câncer de pulmão é a principal causa de morte relacionada ao câncer. Além de novas abordagens inovadoras, estratégias práticas que melhorem a eficácia dos medicamentos já disponíveis são necessárias. A administração inalatória de quimioterapia é uma alternativa promissora para aumentar a eficácia, reduzir a toxicidade, melhorando a qualidade de vida dos pacientes de uma forma mais abrangente do que a imunoterapia. Por se tratar de uma abordagem nova em um campo de pesquisa incipiente, há muitos desafios a serem superados antes de ter tal produto no mercado. Depois de avaliar o cenário atual, uma formulação de pó seco inalatório foi proposta para reposicionar o flubendazol, um medicamento anti-helmíntico pouco solúvel e com grande potencial contra uma variedade de linhagens de câncer. Os nanocristais de flubendazol foram obtidos através de nanopreciptação e o pó seco foi produzido por secagem por atomização. Através do planejamento fatorial fracionado, os parâmetros de secagem por atomização foram otimizados e o impacto da formulação nas propriedades de aerolização foi esclarecido. As limitações de concentração foram mapeadas através da metodologia de superfície de resposta e uma concentração de 15% de flubendazol foi viabilizada com a adição de 20% de L-leucina levando a um tamanho de partícula de flubendazol de 388,6 nm, diâmetro aerodinâmico médio de massa de 2,9 μm, 50,3% FPF, dose emitida de 83,2% e o triplo da solubilidade inicial. Embora a citotoxicidade desta formulação em células A549 tenha sido limitada, a formulação apresentou um efeito sinérgico quando associada ao paclitaxel, conduzindo a uma redução surpreendente de 1000 vezes no IC50. Em comparação com 3 ciclos de paclitaxel isoladamente, um modelo de tratamento combinado de 3 ciclos aumentou o limiar de citotoxicidade em 25% para a mesma dose. Nosso estudo sugere, pela primeira vez, que os nanocristais de flubendazol entregues como DPI apresentam alto potencial como adjuvantes para aumentar a potência dos agentes citotóxicos e reduzir os efeitos adversos.

Palavras-chaves: inalatório, nanopartículas, *spray drying*, delineamento experimental, câncer de pulmão.

ABSTRACT

Lung cancer is the leading cause of cancer-related death. In addition to new innovative approaches, practical strategies that improve the efficacy of already available drugs are urgently needed. Inhalable administration of chemotherapy is a promising alternative to increase efficacy, reduce toxicity, and improve patients' quality of life in a more embracing way than immunotherapy. Since it is a new approach in an incipient field of research, there are many challenges to be overcome before having such a product on the market. After evaluating the current scenario, an inhalable dry powder formulation was proposed to reposition flubendazole, a poorly soluble anthelmintic drug with potential against a variety of cancer lineages. Flubendazole nanocrystals were obtained through nanoprecipitation, and dry powder was produced by spray drying. Through fractional factorial design, the spray drying parameters were optimized and the impact of formulation on aerosolization properties was clarified. The loading limitations were clarified through response surface methodology, and a 15% flubendazole loading was feasible through the addition of 20% L-leucine, leading to a flubendazole particle size of 388.6 nm, median mass aerodynamic diameter of 2.9 μm, 50.3% FPF, emitted dose of 83.2% and triple the initial solubility. Although the cytotoxicity of this formulation in A549 cells was limited, the formulation showed a synergistic effect when associated with paclitaxel, leading to a surprising 1000-fold reduction in the IC50. Compared to 3 cycles of paclitaxel alone, a 3-cycle model combined treatment increased the threshold of cytotoxicity by 25% for the same dose. Our study suggests, for the first time, that orally inhaled flubendazole nanocrystals show high potential as adjuvants to increase cytotoxic agents' potency and reduce adverse effects.

Keywords: pulmonary delivery, nanoparticles, spray drying, design of experiments, lung cancer.

LIST OF FIGURES

LIST OF TABLES

LIST OF ABBREVIATIONS AND ACRONYMS

ACI	Andersen Cascade Impactor
ANVISA	Agência Nacional de Vigilância Sanitária (Brazilian Health Regulatory Agency)
API	Active Pharmaceutical Ingredient
BCS	Biopharmaceutical Classification System
CI	Combination Index
Cmax	Maximal Plasma Concentration
COPD	Chronic Obstructive Pulmonary Disease
DLS	Dynamic Light Scattering
DMSO	Dimethyl Sulfoxide
DoE	Design Of Experiments
DPI	Dry Powder Inhaler
DPPC	1,2-Dipalmitoyl-sn-glycero-3-phosphocholine
DSC	Differential Scanning Calorimetry
DSPC	1,2-Distearoyl-sn-glycero-3-phosphocholine
DVS	Dynamic Vapor Sorption
ED	Emitted Dose
EGFR	Epidermal Growth Factor Receptor
EMA	European Medicines Agency
EPR	Enhanced Permeation and Retention
FBZ	Flubendazole
FBZ SD NC	Flubendazole Spray Dried Nanocrystal
FDA	Food and Drug Administration
FPF	Fine Particle Fraction
GEMM	Genetically engineered mouse models
GSD	Geometric Standard Deviation
HSA	Highest Single Agent
IC_{50}	Half Maximal Inhibitory Concentration
INCA	Instituto Nacional de Câncer (Brazilian National Cancer Institute)

Inlet T	Inlet Temperature
MMAD	Mass Median Aerodynamic Diameter
NGI	Next Generation Impactor
NLC	Nanostructured Lipid Carriers
NSCLC	Non-small Cell Lung Cancer
OPC	Oropharyngeal Consortium
pMDI	Pressurized Metered-dose Inhaler
SCLC	Small Cell Lung Cancer
SD	Spray Dried
SEM	Scanning Electron Microscopy
SIMPATEC-USP	Simplified Impactor Developed at the University of São Paulo
SLN	Solid Lipid Nanoparticles
PBS	Phosphate-buffered saline
PDI	Polydispersity Index
PD-1	Programmed Cell Death Protein 1
Pe	Peclet Number
PEG	Polyethylene Glycol
PLGA	Poly (lactic-co-glycolic acid)
PVP K30	Polyvinylpyrrolidone K30
PVA	Polyvinyl Alcohol
PXRD	Powder X-Ray Diffraction
QbD	Quality by Design
QTPP	Quality Target Product Profile
RH	Relative Humidity
Tg	Glass Transition Temperature
TKIs	Tyrosine Kinase Inhibitors
Tm	Melting Temperature
TPGS	D-tocopherol acid polyethylene glycol succinate
WHO	World Health Organization

TABLE OF CONTENTS

CHAPTER 1   GENERAL INTRODUCTION

1.1 INTRODUCTION

Lung cancer is the leading cause of death worldwide and the fifth most diagnosed cancer in Brazil. In 2020 Brazilian National Cancer Institute (INCA) reported more than 16,000 new cases, and 28,618 deaths (INCA - INSTITUTO NACIONAL DE CÂNCER, 2022). The main causes include tobacco and occupational exposure to carcinogens as asbestos, arsenic, and cadmium, and the risk is related to genetic factors and environmental exposure (INCA - INSTITUTO NACIONAL DE CÂNCER, 2022b). Lung cancer is a silent disease that when cough and coughing up blood, chest pain, and dyspnea symptoms are detected (ARBOUR; RIELY, 2019) the disease is no longer in its initial stages (MIDTHUN, 2016). It is estimated that 84% are diagnosed in advanced stages in Brazil, leading to a five-year relative survival rate of 18% (INCA - INSTITUTO NACIONAL DE CÂNCER, 2022b). If detected early, in localized stages, the survival rate can increase to 59% (SUNG et al., 2021a). Treatment is stage-specific, with surgery resection and radiotherapy indicated for the initial stages (CORTÉS; URQUIZU; CUBERO, 2015). Although immunotherapy shows important advances, it is estimated that less than 50% of NSCLC patients would be eligible for this treatment (ARBOUR; RIELY, 2019; LEE, 2019). Therefore, chemotherapy has an important role in all stages of the disease, administered alone or in association with other therapies (CORTÉS; URQUIZU; CUBERO, 2015).

Chemotherapy is mainly administered intravenously, but in this route, less than 6% of the initial dose reaches the lungs, as the majority accumulates in the liver, spleen, and kidneys, reducing efficiency and increasing adverse effects (AI et al., 2018; KUZMOV; MINKO, 2015; NEWMAN, 2018). Nausea, diarrhea, myelosuppression, and neural and cardiovascular toxicity are some of the effects that can impact on impair patients' quality of life and compliance with the treatment (FELIU et al., 2020; ZWITTER, 2018). The inhalation route is widely known for asthma treatment, but it has been increasingly explored for vaccines and other diseases such as diabetes due to convenience and non-invasiveness, highly vascularized epithelia, and absence of first-pass metabolism (HAMISHEHKAR; RAHIMPOUR; JAVADZADEH, 2012). Formulations can be administered as solutions or suspensions through nasal spray or nebulization; or by powders, through oral inhalation with dry powder inhaler (DPI) or pressurized metered dose inhaler (pMDI) (HADIWINOTO; LIP KWOK; LAKERVELD, 2018a; HAMISHEHKAR; RAHIMPOUR; JAVADZADEH, 2012). Inhaled therapy for the treatment of lung cancer is a promising approach, once it allows the delivery of higher concentrations of the drug directly to intended the site action, minimizing toxicity and side

effects, contributing to the overall efficacy (MASELLI; KEYT; RESTREPO, 2017). DPI appears to be preferable amongst other devices for the convenience of size and way of handling, and also for its superior chemical and microbiological stability due to the dry state and reduced humidity content (HAMISHEHKAR; RAHIMPOUR; JAVADZADEH, 2012). The most important quality attributes of this type of formulation, is the particle shape, once it impacts the particle aerodynamics flow, and particle size around 1–3 μm, once it must reach the lower airways (bronchi, bronchioles, and alveolus) for absorption (HADIWINOTO; LIP KWOK; LAKERVELD, 2018a; TAKI *et al.*, 2016). Although different technologies can be used to obtain the particles with the desired characteristics, spray drying is the process that attracts attention due to its versatility, possibility to be performed as a one-step continuous process (HADIWINOTO; LIP KWOK; LAKERVELD, 2018a).

Spray drying is a process that briefly produces a dry powder from a liquid phase by atomizing the solution or suspension into a chamber with a heated gas, where the solvent is immediately removed, and the powder collected in a recipient (HADIWINOTO; LIP KWOK; LAKERVELD, 2018a). The particles obtained with this one-step process technology show a spherical shape due to the constant airflow inside the chamber and also present relatively good uniform particle size distribution (HADIWINOTO; LIP KWOK; LAKERVELD, 2018a). It can be applied to the development of different systems, such as microspheres or microcapsules, by varying the atomized solution or suspension (GUTERRES; BECK; POHLMANN, 2009). When combining spray drying with precipitation it is possible to obtain nanoparticles, as demonstrated by Ozeki, T. and colleagues with the development of a two-solution mixing type of spray nozzle (OZEKI *et al.*, 2012). The mixture of the organic solution of the poorly water-soluble drug and the aqueous solution of the carrier occurs inside the nozzle (TAKI *et al.*, 2016). As the solvent composition changes, the drug precipitates as nanocrystals and is dried before the crystal growth is complete, allowing the formation of nanoparticles in microparticles (TAKI *et al.*, 2016). These nanoparticles can also be obtained through simple spray nozzles by spray drying of a previously prepared nanosuspension, as demonstrated in Figure 1.1.

Figure 1.1. Schematic representation of spray drying process and nanoparticles in microparticles as final dry powder product.
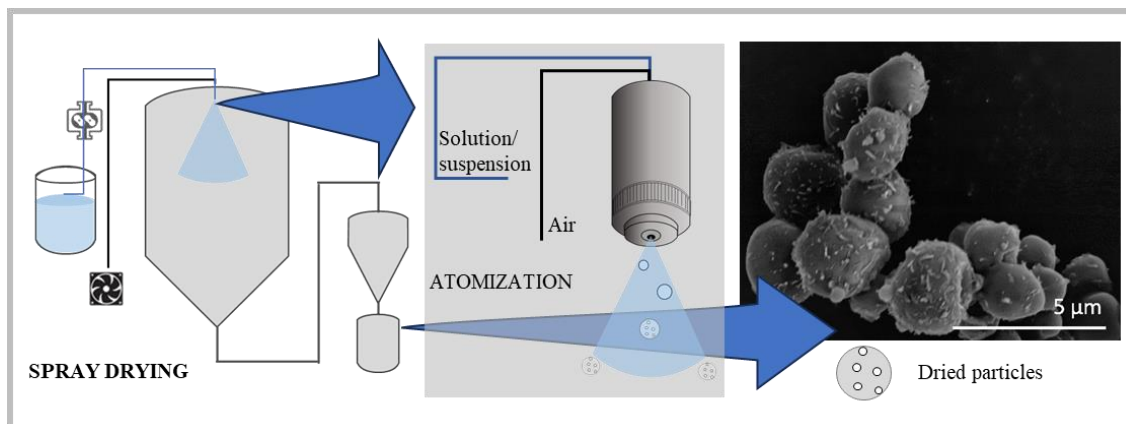
Source: elaborated by the author.

Nanocrystals can be defined as nanoscale particles which are composed mainly by pure API, and can present crystalline (organized) structure or can be found in an amorphous state (CHEN *et al.*, 2017). The significant size reduction and consequent increase in particle surface enhances solubility, rate of dissolution, increasing bioavailability and reducing the amount of dose required to therapeutic effect and patient-to-patient variability (BHATIA, 2016). The improvement of the dissolution rate by reduction in the particle size can be explained by the Noyes-Whitney equation (BUCKTON; BEEZER, 1992), according to which since nanosized particles present enlarged surface area, enhancing the dissolution rate (KAKRAN *et al.*, 2012). In recent years, nanocrystals gained prominence as a promising technology for the development of inhalable formulations aiming to improve targeting and bioavailability of drugs with poor solubility for several applications, including cancer treatment. Hu et al. formulated spray-dried nanocrystals of curcumin powders for inhalation with great aerodynamic properties achieving enhanced drug dissolution and plasma concentration with high levels of lung deposition, demonstrating the potentiality of this innovative technology for lung cancer treatment. The same group also demonstrated the feasibility of the use of nanocrystals for sustained pulmonary delivery of highly lipophilic antitumor drugs with improved drug release, retention, and local availability, opening a new front for DPIs development (HU *et al.*, 2017). Consequently, the development of the nanocrystal-based platform for inhaled systems has great potential to accelerate the development of new options for chemotherapy through drug repositioning.

Flubendazole belongs to benzimidazole anthelmintic class and is indicated for the treatment of intestinal nematodes (MACKENZIE; LANSING, 2014), acting by specific binding to the β-tubulin subunit of microtubule (ČÁŇOVÁ; ROZKYDALOVÁ; RUDOLF, 2017).

Microtubules cytoskeleton are highly dynamic structures composed of αβ-tubulin heterodimers that are important to many vital cell functions, including correct segregation of chromosomes during mitosis (LACHAU-DURAND *et al.*, 2019; PARKER *et al.*, 2017). The failure in this process initiates apoptosis cascade leading to cell death (PARKER *et al.*, 2017). Although it is not an approved indication, many studies have demonstrated its potential for the treatment of different types of cancer, including breast cancer, leukemia, neuroblastoma and non-small-cell lung cancer (NSCLC) (ČÁŇOVÁ; ROZKYDALOVÁ; RUDOLF, 2017; PARKER *et al.*, 2017). For NSCLC, high βIII-tubulin expression conferred resistance to the treatment with vinca alkaloids, a chemotherapeutic class of tubulin-binding agent, resulting in patients poor survival and recovery from surgical resection (PARKER *et al.*, 2017). Although the mechanism of action is the same as vinca alkaloids, flubendazole seems to bind to a different tubulin site, presenting an important alternative for the treatment of these patients (SPAGNUOLO *et al.*, 2010). Flubendazole is usually administered orally at doses of approximately 5 mg/kg, 3 times per day, achieving maximal plasma concentration lower than 5 ng/ml even after 2 g ingestion, which is considered very limited (ČÁŇOVÁ; ROZKYDALOVÁ; RUDOLF, 2017). Once the low bioavailability is the main limitation for the use of flubendazole in cancer treatment (VIALPANDO *et al.*, 2016), new approaches for the development of alternative formulations that improve its poor solubility (0.005 mg/mL) (GABRIEL L. B. DE ARAUJO *et al.*, 2018; VIALPANDO *et al.*, 2016) and targeting the systemic or local delivery must be explored to repurpose flubendazole for lung cancer.

1.2 HYPOTHESIS

Flubendazole (FBZ) is a well-established class II drug, approved for human use since 1980 (LACHAU-DURAND *et al.*, 2019) with known safety that shows potential for the treatment of lung cancer. However, the clinical application of FBZ is compromised due to its low aqueous solubility and consequent very poor bioavailability. We believe that the development of a nanocrystalline DPI formulation by spray drying will improve solubility of FBZ and increase delivery to the lungs and is an interesting approach to repurpose poorly soluble drugs for cancer.

1.3 OBJECTIVE

1.3.1 Overall objective

The aim of this present study is the development and characterization of an inhalable dry powder formulation of flubendazole nanocrystals with suitable physicochemical and aerodynamic properties for delivery to the lungs.

1.3.2 Specific objective

- Obtention of flubendazole nanoparticles.
- Obtention of dry powder formulation with suitable characteristics for inhaled delivery.
- Optimization of formulation and process parameters through quality by design (QbD) approach.
- Physicochemical characterization of optimized formulation.
- Efficacy evaluation *in vitro*.

1.4 REFERENCES

AI, X.; GUO, X.; WANG, J.; STANCU, A. L.; JOSLIN, P. M. N.; ZHANG, D.; ZHU, S. Targeted Therapies for Advanced Non-Small Cell Lung Cancer. v. 9, p. 19, 2018.

ARBOUR, K. C.; RIELY, G. J. Systemic Therapy for Locally Advanced and Metastatic Non–Small Cell Lung Cancer: A Review. **JAMA**, v. 322, n. 8, p. 764, 27 ago. 2019.

BHATIA, S. Nanoparticles Types, Classification, Characterization, Fabrication Methods and Drug Delivery Applications. *Em*: BHATIA, S. **Natural Polymer Drug Delivery Systems**. Cham: Springer International Publishing, 2016. p. 33–93.

BUCKTON, G.; BEEZER, A. E. The Relationship between Particle Size and Solubility. **International Journal of Pharmaceutics**, v. 82, n. 3, p. R7–R10, maio 1992.

ČÁŇOVÁ, K.; ROZKYDALOVÁ, L.; RUDOLF, E. Anthelmintic Flubendazole and Its Potential Use in Anticancer Therapy. **Acta Medica (Hradec Kralove, Czech Republic)**, v. 60, n. 1, p. 5–11, 2017.

CHEN, M.-L.; JOHN, M.; LEE, S. L.; TYNER, K. M. Development Considerations for Nanocrystal Drug Products. **The AAPS Journal**, v. 19, n. 3, p. 642–651, maio 2017.

CORTÉS, Á. A.; URQUIZU, L. C.; CUBERO, J. H. Adjuvant Chemotherapy in Non-Small Cell Lung Cancer: State-of- the-Art. **Translational lung cancer research**, v. 4, n. 2, p. 7, 2015.

FELIU, J.; HEREDIA-SOTO, V.; GIRONÉS, R.; JIMÉNEZ-MUNARRIZ, B.; SALDAÑA, J.; GUILLÉN-PONCE, C.; MOLINA-GARRIDO, M. J. Management of the Toxicity of Chemotherapy and Targeted Therapies in Elderly Cancer Patients. **Clinical and Translational Oncology**, v. 22, n. 4, p. 457–467, abr. 2020.

GABRIEL L. B. DE ARAUJO; FABIO FURLAN FERREIRA; CARLOS E. S. BERNARDES; JULIANA A. P. SATO; OTÁVIO M. GIL; DALVA L. A. DE FARIA; RAIMAR LOEBENBERG; STEPHEN R. BYRN; DANIELA D. M. GHISLENI; NADIA A. BOU-CHACRA; TEREZINHA J. A. PINTO; SELMA G. ANTONIO; HUMBERTO G. FERRAZ; DMITRY ZEMLYANOV; DÉBORA S. GONÇALVES; MANUEL E. MINAS DA PIEDADE. A New Thermodynamically Favored Flubendazole/Maleic Acid Binary Crystal Form: Structure, Energetics, and in Silico PBPK Model-Based Investigation. **A New Thermodynamically Favored Flubendazole/Maleic Acid Binary Crystal Form: Structure, Energetics, and in Silico PBPK Model-Based Investigation**, v. 18, n. 9, p. 2377–2386, 2018.

GUTERRES, S. S.; BECK, R. C. R.; POHLMANN, A. R. Spray-Drying Technique to Prepare Innovative Nanoparticulated Formulations for Drug Administration: A Brief Overview. **Brazilian Journal of Physics**, v. 39, n. 1a, p. 205–209, abr. 2009.

HADIWINOTO, G. D.; LIP KWOK, P. C.; LAKERVELD, R. A Review on Recent Technologies for the Manufacture of Pulmonary Drugs. **Therapeutic Delivery**, v. 9, n. 1, p. 47–70, jan. 2018.

HAMISHEHKAR, H.; RAHIMPOUR, Y.; JAVADZADEH, Y. The Role of Carrier in Dry Powder Inhaler. *Em*: SEZER, A. D. **Recent Advances in Novel Drug Carrier Systems**. [s.l.] InTech, 2012.

HU, X.; YANG, F.-F.; WEI, X.-L.; YAO, G.-Y.; LIU, C.-Y.; ZHENG, Y.; LIAO, Y.-H. Curcumin Acetate Nanocrystals for Sustained Pulmonary Delivery: Preparation, Characterization and In Vivo Evaluation. **Journal of Biomedical Nanotechnology**, v. 13, n. 1, p. 99–109, 1 jan. 2017.

INCA - INSTITUTO NACIONAL DE CÂNCER. **Câncer de pulmão**. [s.l: s.n.]. Disponível em: <https://www.gov.br/inca/pt-br/assuntos/cancer/tipos/pulmao>. Acesso em: 22 ago. 2023.

KAKRAN, M.; SHEGOKAR, R.; SAHOO, N. G.; AL SHAAL, L.; LI, L.; MÜLLER, R. H. Fabrication of Quercetin Nanocrystals: Comparison of Different Methods. **European Journal of Pharmaceutics and Biopharmaceutics**, v. 80, n. 1, p. 113–121, jan. 2012.

KUZMOV, A.; MINKO, T. Nanotechnology Approaches for Inhalation Treatment of Lung Diseases. **Journal of Controlled Release**, v. 219, p. 500–518, dez. 2015.

LACHAU-DURAND, S.; LAMMENS, L.; VAN DER LEEDE, B.; VAN GOMPEL, J.; BAILEY, G.; ENGELEN, M.; LAMPO, A. Preclinical Toxity and Pharmacokinetics of a New Orally Bioavailable Flubendazole Formulation and the Impact for Clinical Trials and Risk/Benefit to Patients. **PLOS Neglected Tropical Diseases**, v. 13, n. 1, p. e0007026, 16 jan. 2019.

LEE, S. H. Chemotherapy for Lung Cancer in the Era of Personalized Medicine. **Tuberculosis and Respiratory Diseases**, v. 82, n. 3, p. 179, 2019.

28

MACKENZIE, C.; LANSING, E. A REVIEW OF FLUBENDAZOLE AND ITS POTENTIAL AS A MACROFILARIACIDE. p. 67, [s.d.]

MASELLI, D.; KEYT, H.; RESTREPO, M. Inhaled Antibiotic Therapy in Chronic Respiratory Diseases. **International Journal of Molecular Sciences**, v. 18, n. 5, p. 1062, 16 maio 2017.

MIDTHUN, D. E. Early Detection of Lung Cancer. **F1000Research**, v. 5, p. 739, 25 abr. 2016.

NEWMAN, S. P. Delivering Drugs to the Lungs: The History of Repurposing in the Treatment of Respiratory Diseases. **Advanced Drug Delivery Reviews**, v. 133, p. 5–18, ago. 2018.

OZEKI, T.; AKIYAMA, Y.; TAKAHASHI, N.; TAGAMI, T.; TANAKA, T.; FUJII, M.; OKADA, H. Development of a Novel and Customizable Two-Solution Mixing Type Spray Nozzle for One-Step Preparation of Nanoparticle-Containing Microparticles. **Biological and Pharmaceutical Bulletin**, v. 35, n. 11, p. 1926–1931, 2012.

PARKER, A. L.; TEO, W. S.; MCCARROLL, J. A.; KAVALLARIS, M. An Emerging Role for Tubulin Isotypes in Modulating Cancer Biology and Chemotherapy Resistance. **International Journal of Molecular Sciences**, v. 18, n. 7, p. 1434, 4 jul. 2017.

SPAGNUOLO, P. A.; HU, J.; HURREN, R.; WANG, X.; GRONDA, M.; SUKHAI, M. A.; DI MEO, A.; BOSS, J.; ASHALI, I.; BEHESHTI ZAVAREH, R.; FINE, N.; SIMPSON, C. D.; SHARMEEN, S.; ROTTAPEL, R.; SCHIMMER, A. D. The Antihelmintic Flubendazole Inhibits Microtubule Function through a Mechanism Distinct from Vinca Alkaloids and Displays Preclinical Activity in Leukemia and Myeloma. **Blood**, v. 115, n. 23, p. 4824–4833, 10 jun. 2010.

SUNG, H.; FERLAY, J.; SIEGEL, R. L.; LAVERSANNE, M.; SOERJOMATARAM, I.; JEMAL, A.; BRAY, F. Global Cancer Statistics 2020: GLOBOCAN Estimates of Incidence and Mortality Worldwide for 36 Cancers in 185 Countries. **CA: A Cancer Journal for Clinicians**, v. 71, n. 3, p. 209–249, 2021.

TAKI, M.; TAGAMI, T.; FUKUSHIGE, K.; OZEKI, T. Fabrication of Nanocomposite Particles Using a Two-Solution Mixing-Type Spray Nozzle for Use in an Inhaled Curcumin Formulation. **International Journal of Pharmaceutics**, v. 511, n. 1, p. 104–110, set. 2016.

VIALPANDO, M.; SMULDERS, S.; BONE, S.; JAGER, C.; VODAK, D.; VAN SPEYBROECK, M.; VERHEYEN, L.; BACKX, K.; BOEYKENS, P.; BREWSTER, M. E.; CEULEMANS, J.; NOVOA DE ARMAS, H.; VAN GEEL, K.; KESSELAERS, E.; HILLEWAERT, V.; LACHAU-DURAND, S.; MEURS, G.; PSATHAS, P.; VAN HOVE, B.; VERRECK, G.; VOETS, M.; WEUTS, I.; MACKIE, C. Evaluation of Three Amorphous Drug Delivery Technologies to Improve the Oral Absorption of Flubendazole. **Journal of Pharmaceutical Sciences**, v. 105, n. 9, p. 2782–2793, set. 2016.

ZWITTER, M. Toxicity and Quality of Life in Published Clinical Trials for Advanced Lung Cancer. **Supportive Care in Cancer**, v. 26, n. 10, p. 3453–3459, out. 2018.

CHAPTER 2   LITERATURE REVIEW

2.1   LUNG CANCER

Lung cancer is the leading cause of death by cancer worldwide, with an estimated 2.2 million new cases and 1.8 million deaths only in 2018 (SUNG *et al.*, 2021a). In Brazil, 28,618 deaths in 2020 were reported in 2020 (INCA - INSTITUTO NACIONAL DE CÂNCER, 2022b), and as the fifth most diagnosed cancer, it is estimated 32,560 new cases for the three-year period from 2023 to 2025 (INCA - INSTITUTO NACIONAL DE CÂNCER, 2022a). The main cause is attributed to tobacco, which is responsible for two-thirds of lung cancer deaths (SUNG *et al.*, 2021a). Genetic factors, pulmonary fibrosis, ionizing radiation, and occupational exposure to carcinogens as asbestos, arsenic, and cadmium also increase the risk (CLARK; ALSUBAIT, 2023; INCA - INSTITUTO NACIONAL DE CÂNCER, 2022b). The incidence rate has been decreasing due to reduction of tobacco demand (INCA - INSTITUTO NACIONAL DE CÂNCER, 2022b; SUNG *et al.*, 2021a), but earlier diagnosis are key to decrease mortality. Lung cancer is a silent disease that when symptoms such as cough with blood, chest pain and dyspnea are detected, the disease is no longer in its initial stages (MIDTHUN, 2016). It is estimated that more than 50% of patients are already diagnosed in metastatic stages of the disease (ARBOUR; RIELY, 2019), which to a low 5-year survival rate of 0 to 6%, compared to the 59% 5-year survival of patients in localized stages (SUNG *et al.*, 2021a). In Brazil, 84% are diagnosed in advanced stages in Brazil (INCA - INSTITUTO NACIONAL DE CÂNCER, 2022b).

Figure 2.1. Lung cancer mortality rate in 2020.
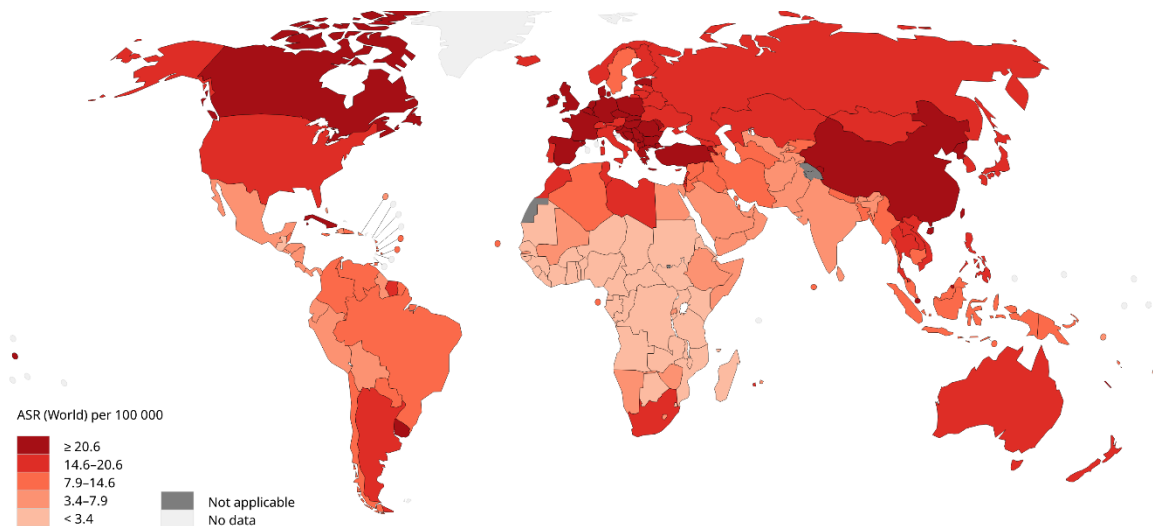
Source: (WORLD HEALTH ORGANIZATION,2020)

Lung cancer is divided into the following major subgroups (Figure 2.2): small cell lung cancer (SCLC) and non-small cell lung cancer (NSCLC), the latter representing approximately 85% of diagnoses and can be divided into adenocarcinoma, squamous cell carcinoma, and large cell lung cancer (DUMA; SANTANA-DAVILA; MOLINA, 2019). SCLC arises in the central airways and it is suggested that it originates from pulmonary neuroendocrine cells (CHEUNG; NGUYEN, 2015). Adenocarcinoma is the predominant type of NSCLC, constituting nearly 40% of lung cancer types (DUMA; SANTANA-DAVILA; MOLINA, 2019) and arises from distal airways (CHEUNG; NGUYEN, 2015) from alveolar cells (DUMA; SANTANA-DAVILA; MOLINA, 2019). Squamous cell carcinomas tend to arise from proximal airways from basal progenitors, with cellular origin not yet identified, possibly club cells (clara cells) (CHEUNG; NGUYEN, 2015). Large cell carcinomas represent 5 to 10% of lung cancer types (DUMA; SANTANA-DAVILA; MOLINA, 2019) and are actually a diagnosis of exclusion, for undifferentiated NSCLC and therefore could not be classified as previously mentioned types (PARDO *et al.*, 2009) due to absence of therapeutically relevant alterations and lack of immunohistochemistry defining markers (CLARK; ALSUBAIT, 2023). Advances in immunohistochemical and genetic characterizations support reassignments of large cell carcinomas sue to squamous, glandular, or neuroendocrine differentiations (CLARK; ALSUBAIT, 2023).

Figure 2.2. Lung cancer classification by histological type and common region of origin.
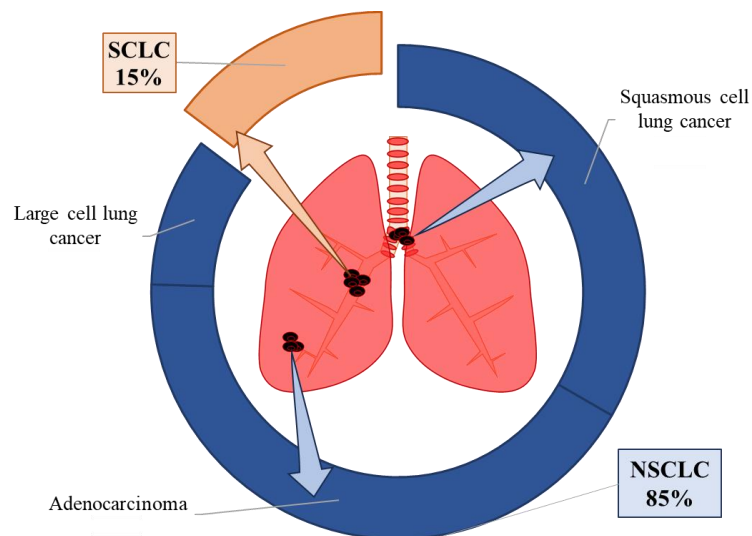
Source: elaborated by the author.

Treatment are stage-specific (SASE *et al.*, 2021) and depends on comorbidities, and molecular characteristics: for NSCLC, for example, complete surgical resection is indicated for patients in initial stages (I and II) and radiotherapy (CORTÉS; URQUIZU; CUBERO, 2015) or stereotactic ablative body radiotherapy (NASIM; SABATH; EAPEN, 2019), when the first is contraindicated. Stage III comprises tumors located in the lungs and regional lymph nodes and presents low curative potential (<20%) through indicated multimodal therapy: chemotherapy, surgery, and radiotherapy (ARBOUR; RIELY, 2019). Chemotherapy is also required for stage II patients after the resection procedure, advanced and metastatic stages (DUMA; SANTANA-DAVILA; MOLINA, 2019; LU *et al.*, 2019; NASIM; SABATH; EAPEN, 2019). For metastatic stage IV aiming attenuation of symptoms and increasing survival, the standard treatment was platinum doublet (carboplatin or cisplatin) in association with gemcitabine, vinorelbine, taxanes (paclitaxel or docetaxel) or pemetrexed (DUMA; SANTANA-DAVILA; MOLINA, 2019). Regardless of the histologic subtype, a progressing regime over 6 cycles is not indicated since several trials have shown lack of improvement in the overall survival (DUMA; SANTANA-DAVILA; MOLINA, 2019). Figure 2.3. summarizes treatment indications according to disease stages.

Figure 2.3. Lung cancer treatment indications based on disease stage.
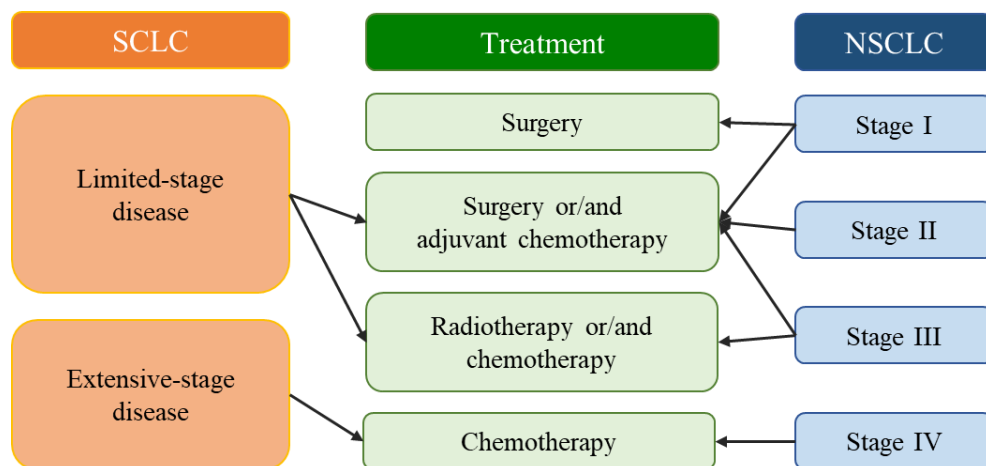
Source: adapted with permission from (SASE et al., 2021).

Targeted therapy with epidermal growth factor receptor tyrosine kinase inhibitors (EGFR TKIs), as erlotinib and gefitinib, has demonstrated significant improvements in adverse effects, the overall survival and progression free survival for metastatic stages of NSCLC when compared to platinum-based chemotherapy (DUMA; SANTANA-DAVILA; MOLINA, 2019). A randomized, open-label, phase 3 trial demonstrated that associations of platinum-based

treatments with immunotherapy such as atezolizumab or durvalumab provided longer overall survival rate to extensive stage SCLC patients (PAZ-ARES *et al.*, 2019). Pembrolizumab, a monoclonal antibody that binds to programmed cell death protein 1 (PD-1), became the first-line choice for monotherapy for NSCLC patients with high expression of PD-L1 (DUMA; SANTANA-DAVILA; MOLINA, 2019). For NSCLC patients with EGFR exon 19 deletions or exon 21 L858R mutations, osimertinib is FDA-approved first-line treatment, after demonstrating improvement in progression-free survival of 8-9 months in comparison to first-generation EGFR TKIs (erlotinib and gefitinib) (DUMA; SANTANA-DAVILA; MOLINA, 2019). Figure 2.4. illustrates advances in treatment for NSCLC. Immunotherapy has proven that the cure for some patients with metastatic stage is possible, but unfortunately, targeted agents and immunotherapy have not exhibited the same improvements for early stage cases (DUMA; SANTANA-DAVILA; MOLINA, 2019). Also, although immunotherapy represents a breakthrough for lung cancer treatment, it is estimated that not more than 50% of NSCLC patients would be eligible (ARBOUR; RIELY, 2019; LEE, 2019). Thus, discovery of new drugs, and strategies such as local delivery that can quickly contribute to increasing the efficiency of existing chemotherapy regimens, need to be explored to benefit all the patients.

Figure 2.4. Timeline of treatment of metastatic and non-metastatic non-small cell lung cancer (NSCLC).
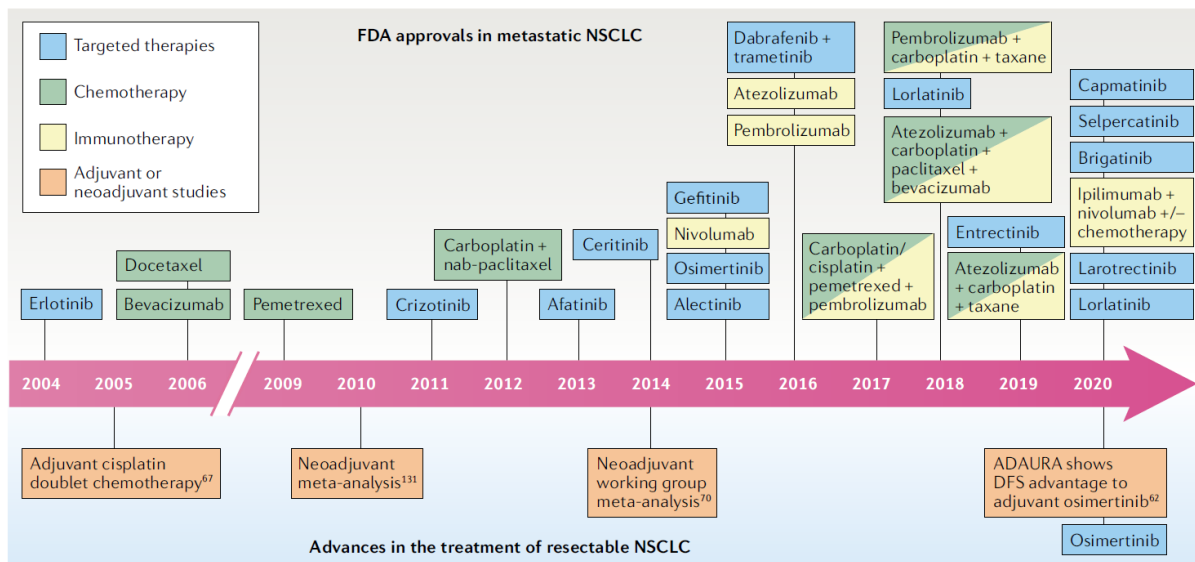
Source: (CHAFT *et al.*, 2021).

2.2 DRUG REPURPOSING AND FLUBENDAZOLE

Development of new drugs is a slow process that takes approximately 10 to 17 years, which demands extensive evaluation of efficacy, safety, pharmacokinetics and pharmacodynamics that results in huge costs estimated in USD2–3 billion (ZHANG *et al.*, 2020). Unfortunately, only 5% of oncology drugs that enter human trials (clinical trials phase I) end up approved (ZHANG *et al.*, 2020). Drug repurposing (or repositioning) is an alternative strategy for the discovery of new drugs for a specific disease based on the identification of new uses of already approved drugs (DOUMAT *et al.*, 2023). The known safety and pharmacokinetic profile, but mostly the target-defined antineoplastic compound can significantly reduce cost and risk-associated investments (ZHANG *et al.*, 2020). Chloroquine and quinacrine, antimalarial agents; disulfiram, approved for alcohol abuse treatment; and itraconazole, an antifungal agent; are examples of drugs in current evaluation for repurposing for lung cancer that evolved to clinical trials (ZHANG *et al.*, 2020).

Benzimidazole is a heterocyclic aromatic compound whose structure is one of the most frequent among Food and Drug Administration (FDA) approved drugs (LEE; TAN; OON, 2023). Its structure containing electron-rich nitrogen heterocycles facilitates substitution, originating derivates with distinct biological activities as antimicrobial, anti-hypertensive, anti-diabetic, and potentially anticancer agents (LEE; TAN; OON, 2023). Flubendazole (FBZ), methyl N-[6-(4-fluorobenzoyl)-1H-benzimidazol-2-yl]carbamate (Figure 2.5), belongs to benzimidazole carbamates anthelmintic class, and is widely used in veterinary medicine for parasitic worms infections (ČÁŇOVÁ; ROZKYDALOVÁ; RUDOLF, 2017). It is approved for human use in Europe and commercialized under the name of Fluvermal® (ČÁŇOVÁ; ROZKYDALOVÁ; RUDOLF, 2017) as tablets or oral suspension. It acts by preferentially binding to β-tubulin subunit of nematodes inhibiting polymerization (ČÁŇOVÁ *et al.*, 2018). Since this mechanism is similar to other well stablished chemotherapeutics, the benzimidazole class attracted attention of the scientific community for drug repurposing in the last years specially for cancer treatment.

Microtubule cytoskeleton are highly dynamic structures composed of αβ-tubulin heterodimers that are important for many vital cellular functions, including integrity of cell shape, intracellular transport and correct segregation of chromosomes during mitosis (O'NEILL, 2016). Failure in this process initiates the apoptosis cascade leading to cell death. (PARKER *et al.*, 2017). Interestingly, drugs capable of interfering with this process have been explored for the treatment of many diseases such as infections and cancer (MÜHLETHALER *et al.*, 2021).

A computational and crystallographic fragment screening approach identified 27 distinct sites of tubulin binding sites (MÜHLETHALER *et al.*, 2021), from which three are recognized as the most pharmacologically relevant: taxol; vinblastine or vinca alkaloids; and colchicine (O'NEILL, 2016). Taxol binding agents act by binding in the lumen of the polymer promoting polymerization and stabilization; while vinblastine and colchicine (benzimidazole-derived anthelmintics) are destabilizing agents since exhibit affinity for the tubulin dimer and inhibit further polymerization (MORRIS; FORNIER, 2008; O'NEILL, 2016). Many taxol and vinblastine site targeting agents (as vincristine, vinblastine, vinorelbine, paclitaxel and docetaxel) have been approved by FDA for cancer chemotherapy, but colchicine itself has a narrow therapeutic index and consequently limited application (TIAN *et al.*, 2018).

FBZ is a destabilizing agent that specifically binds to the colchicine domain that was tested against a large variety of cell lines and showed promising anticancer activity (MICHAELIS *et al.*, 2015a). Preparations of water-soluble FBZ by conjugation with cyclodextrins exhibited cytotoxicity for neuroblastoma cultures in nanomolar concentrations, including cell lines with acquired resistance to drugs as taxanes, vinca alkaloid, docetaxel, paclitaxel, and cisplatin (MICHAELIS *et al.*, 2015a). FBZ displayed activity against leukemia and myeloma primary patient samples, and OCI-AML2 cells resistant to vinblastine (SPAGNUOLO *et al.*, 2010). Moreover, intraperitoneal injection of 20 or 50 mg FBZ/kg (in 0.9% NaCl and 0.01% Tween-80) delayed tumor growth in mouse xenograft models of leukemia and myeloma (SPAGNUOLO *et al.*, 2010). When administered by intraperitoneal injection of flubendazole (10 and 20 mg/kg, possibly as a solution containing DMSO) showed inhibition of human non-small cell lung carcinoma (NSCLC) cell growth in a mice xenograft model (XIE *et al.*, 2021).

Figure 2.5. Flubendazole molecular structure.
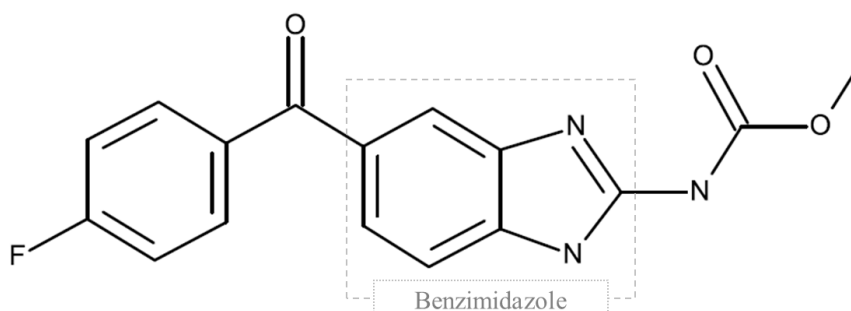
Source: (MINDA *et al.*, 2021)

The first reported experiments sponsored by WHO in the 1970's that discovered FBZ as the highly effective microfilaricide were performed by parenteral administration (GEARY; MACKENZIE; SILBER, 2019; LACHAU-DURAND *et al.*, 2019). But the pain caused by subcutaneous administration, and inflammation induced by intramuscular injection impaired these administration routes, arousing concerns over parenteral administration (SAINAS *et al.*, 2018) and led to the development of an oral formulation by Janssen Pharmaceuticals, which was first approved for human use in 1980 for treatment of intestinal nematodes (LACHAU-DURAND *et al.*, 2019; MACKENZIE; LANSING, 2014). FBZ tolerance has been well known and established for humans for oral administration, as no toxicity is reported after ingestion of 2 g of the drug, or repeated treatment with 50 mg/kg daily for 24 months (SPAGNUOLO *et al.*, 2010). In animals, toxicity was substantially studied in different models, with no important adverse effects, at a maximal plasmatic concentration of 1.12 g/mL in mice (SPAGNUOLO *et al.*, 2010). For veterinary indications, flubendazole is usually administered orally at doses of approximately 5 mg/kg, 3 times per day, achieving maximal plasma concentration lower than 5 ng/ml even after 2 g ingestion, which is considered very limited (ČÁŇOVÁ; ROZKYDALOVÁ; RUDOLF, 2017). With known pharmacokinetic and toxicity profiles, the use of this important drug repurposing candidate for cancer is impaired by its physicochemical characteristics. FBZ is Biopharmaceutical Classification System (BCS) class II type of drug, since it presents high permeability and low aqueous solubility (GABRIEL L. B. DE ARAUJO *et al.*, 2018; VIALPANDO *et al.*, 2016). Therefore, new approaches for the development of alternative formulations that improve its low solubility (0,005 mg/mL) (GABRIEL L. B. DE ARAUJO *et al.*, 2018; VIALPANDO *et al.*, 2016) must be explored to enhance its approved use and enable repurposing for cancer.

2.3   NANOTECHNOLOGY

An interesting approach to improve the solubility of the drug is the particle size reduction. At the nanometric scale, the increase in the ratio of surface area per volume of particle is more significant than for sizes above 1 μm (SHEGOKAR; MÜLLER, 2010). This larger surface area translates into higher interaction of solvent molecules and smaller diffusion distance, which in addition to a decrease in intermolecular forces by rearrangement in the crystalline state, results in increased saturation solubility (MIRZA; AHIRRAO; KSHIRSAGAR, 2017). The dissolution rate is also enhanced by two factors, as explained by the Noyes-Whitney equation: surface area

and saturation solubility (BUCKTON; BEEZER, 1992). The consequent increase in bioavailability could reduce the dose required for the therapeutic effect (BHATIA, 2016).

Nanotechnology involves the manipulation of particles in submicron range, characterization and application of different materials in a wide range of areas, from research, diagnosis (paramagnetic nanoparticles, quantum dots) and therapeutics to biomedical tools (silver and gold nanoparticles) (BHATIA, 2016). Nevertheless, the precise definition of nanoparticles in terms of size is not a consensus (PARK, 2013). Rather than limiting the definition to ranges from the atomic level at around 0.2 nm to around 100 nm, FDA and EMA are in agreement suggesting that the application of nanotechnology must also be regarding the observation of changes in physical, chemical and biological properties of materials even for particles up to 1 μm (FLÜHMANN *et al.*, 2019). Aside from solubility, the small size of nanoparticles destined for cancer treatments favors passive accumulation, since they penetrate more easily through the highly vascularized tumors (AFTAB *et al.*, 2018). This phenomenon known as enhanced permeation and retention (EPR) occurs due to intense metabolism and expressive angiogenesis, tumors exhibit high concentration of new vessels with wider fenestrations that can vary commonly from 1-100 nm even up to 4.7 μm (GOLOMBEK et al., 2018). Thus, the passive diffusion and favored accumulation in the interstitial space of the tumor vasculature by lack of lymphatic or blood recovery (MATSUMURA; MAEDA, 1986), some nanoparticles can exhibit slow release with increased time of exposure at the tumor site, contributing to greater efficacy and less toxicity (AFTAB et al., 2018). Nanoparticles also show advantages regarding clearance mechanisms and evasion. Since opsonization is antigen-size dependent, nano-sized particles could have higher chances of evading capture by phagocytosis resulting in prolonged retention in comparison to micro-size range particles (ELSAYED; ABOUGHALY, 2016). To promote targeted delivery, increase permeation, prolong release time or protect from degradation, drugs can be encapsulated, involved in a polymeric or lipidic matrix; or conjugated to other molecules, originating different types of nanoparticles (Figure 2.6), such as liposomes, nanostructured carriers, nanoemulsions (MÜLLER; GOHLA; KECK, 2011a).

Figure 2.6. Schematic classification of types of nanomaterials. SLN: solid lipid nanoparticles; NLC: nanostructured lipid carriers (NLC)
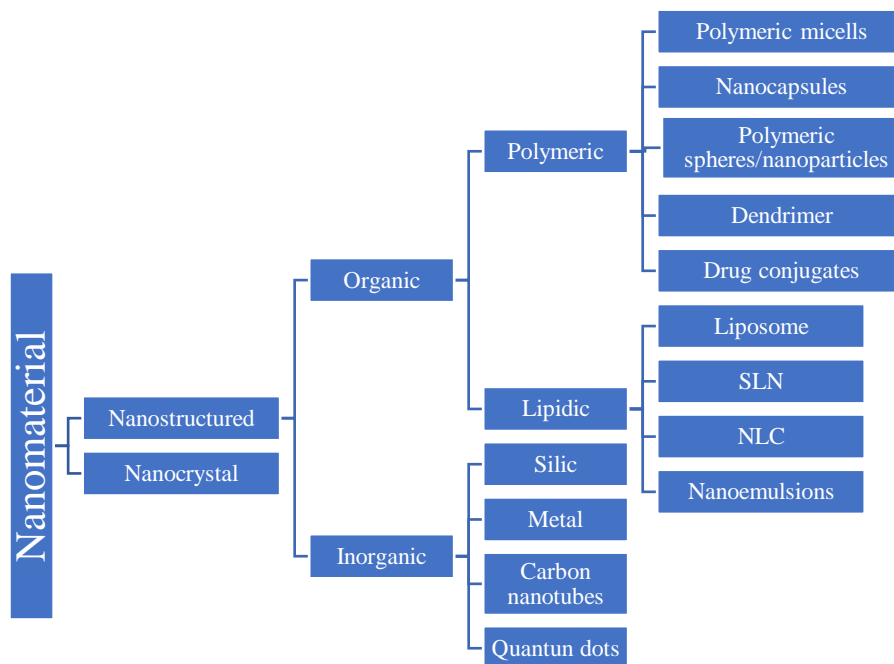
Source: Elaborated by the author. Adapted with permission from (BHATIA, 2016).

Many studies describe the obtention of complex nanoparticles with remarkable improvements. Liposomes, for example, consist of self-assembling vesicular structures that contain aqueous solution encapsulated by one or multiple concentric phospholipid membranes in the range of 50 to1000 nm that can deliver either lipophilic drugs entrapped within the membrane or hydrophilic substances solubilized in the interior solution (LAOUINI *et al.*, 2012; MEHTA, 2016). They have been proven to be biocompatible and biodegradable and can promote sustained release, enhance intracellular uptake, besides protecting the active pharmaceutical ingredient (API) by encapsulation (MEHTA, 2016). They represent a successful nano-based drug delivery system and have presented many approved formulations like Doxil® and DaunoXome® on the market since 1995 and 1900, respectively (LAOUINI *et al.*, 2012). They can incorporate hydrophilic drugs in the core, but comparatively, the amount of hydrophobic drugs incorporated is smaller (DAN, 2017). The main challenge of nanoparticles obtention is reaching the desired size while maintaining the system stability to avoid aggregation (MÜLLER; GOHLA; KECK, 2011a), resulting in average drug loadings of 10% (PARK, 2013).

Nanocrystals can be defined as nanoscale particles which are composed mainly by pure API, and can present crystalline (organized) structure or can be found in amorphous state (CHEN *et al.*, 2017). They were discovered in the early 1960s reaching the market in the 2000s, and can be obtained essentially from two approaches: bottom-up or top-down strategies (CHEN *et al.*, 2017; MÜLLER; GOHLA; KECK, 2011a). In bottom-up approaches, the drug is initially solubilized and added to an anti-solvent, promoting its precipitation; while in top-down approaches, the drug is subjected to a process such as high-pressure grinding or homogenization to break the particles down to the nanoscale (CHEN *et al.*, 2017). Over 80 applications of nanocrystal products were filled for FDA evaluation from 1973 to 2015, most consisting in BSC class II drugs, with improved bioavailability and reduced food related absorption effect (CHEN *et al.*, 2017). Anticancer drugs represented 24% of the applications (CHEN *et al.*, 2017). Conventional oral and intravenous were the predominant routes of administration, with 65% and 20%, respectively, while interestingly, inhalation represented 2% of submissions (CHEN *et al.*, 2017). In recent years, inhaled delivery systems gained prominence as a promising technology for cancer treatment.

2.4 INHALED THERAPY FOR LUNG CANCER

Inhalation for medicinal treatment of asthma has been practiced over thousand years BC in China by use of opium incense and in Egypt, with black henbane plant vapors containing atropine (SANDERS, 2007). However, only through 1867's edition of British Pharmacopoeia was it formally recognized as medical therapy for specific drugs for the treatment of cough, tuberculosis, bronchitis, pharyngitis, and laryngitis (STEIN; THIEL, 2017). In the 19th century, intense innovation in pharmaceutical industry contributed to improve convenience of inhalation therapy with the development of sprays, nebulizers and inhalers (EL-SHERBINY; EL-BAZ; YACOUB, 2015; SANDERS, 2007). Important markers of further innovation in devices, delivery of higher doses and treatment diversification, were introduction of anesthetic gases in the 1840s, beta agonists and corticosteroids in the 1900s, migraine headache treatment with ergotamine in 1959, and more recently, insulin, antibiotics, vaccines and also treatment for osteoporosis (STEIN; THIEL, 2017).

Enabling local delivery of higher drug doses is particularly promising for the treatment of cancer since lower doses with targeted delivery could improve patients' quality of life (MASELLI; KEYT; RESTREPO, 2017). It is non-invasive, avoids first-pass metabolism, reduces systemic exposure, and presents interesting physiological conditions for absorption due

to the thin epithelium, large surface area of highly vascularized alveoli tissue (EL-SHERBINY; EL-BAZ; YACOUB, 2015; GRONEBERG *et al.*, 2003). An inhaled chemotherapy treatment was first mentioned in the late 1960's, with the first clinical report published in 1968 (KUZMOV; MINKO, 2015; ROSIÈRE *et al.*, 2019a). Well-established drugs such as cisplatin, doxorubicin and paclitaxel have already been formulated as an inhaled solution or powder (WAUTHOZ; ROSIÈRE; AMIGHI, 2021). Liposomal cisplatin administered by nebulization proved to be tolerable in patients with NSCLC (WITTGEN *et al.*, 2007), and for patients with osteosarcoma, when administered in lipid form by nebulization, with minimal systemic exposure (CHOU *et al.*, 2013). Levet V. et al. developed a formulation of cisplatin as a 24 hours prolonged release inhaled powder, with potential for adjuvant therapy and for the prevention of micrometastases (LEVET *et al.*, 2016). Zhong developed a pH-dependent release dendrimer-conjugated doxorubicin powder inhaler formulation (ZHONG, 2018). Highly complex systems, such as the multifunctional nanolipid carriers developed by Taratula et al. containing a drug such as doxorubicin or paclitaxel, siRNA to suppress pump and non-pump resistance mechanisms, and a luteinizing hormone-releasing analog to target lung cancer cells have shown high efficiency in an animal model (TARATULA *et al.*, 2013). When compared to intravenous administration, inhaled routes showed greater antitumor activity and lower drug exposure in healthy organs (TARATULA *et al.*, 2013). Inhaled formulations can be delivered either as a liquid, by nebulizers, nasal sprays and soft mist inhalers, or as oral powders, by pressurized metered dose inhalers (pMDIs) and dry powder inhalers (DPIs) (HADIWINOTO; LIP KWOK; LAKERVELD, 2018a; HAMISHEHKAR; RAHIMPOUR; JAVADZADEH, 2012). DPIs are preferable amongst other inhalable devices (Table 2.1) for the convenience of size and way of handling, superior chemical and microbiological stability due to the reduced humidity content and no need for reconstitution, not requiring cold chain (HAMISHEHKAR; RAHIMPOUR; JAVADZADEH, 2012) or propellant in the formulation. Also, specifically regarding cancer treatment, it is more suitable for administering higher drug doses of poorly soluble drugs in short periods of administration, and are not dependent on specialized hospital facilities, due to less exposure of the drug to the environment (ROSIÈRE *et al.*, 2019a). Unfortunately, no DPI product has still been tested in clinical trials for cancer treatment (SEYHAN, 2019), and some key points will be discussed later in chapter 3. In contrast, the inhalable drugs that did evolved to human clinical trials, mostly by nebulization, proved to be generally viable and safe, but failed in phase I or II at best, mainly due to dose-limiting toxicity, without clear efficacy superiority to conventional routes (ROSIÈRE *et al.*, 2019a). Some promising outcomes were significant increase in survival rate with carboplatin treatment using one third of the common

intravenously administered dose in phase II clinical trial and absence or reduced systemic toxicities (ROSIÈRE *et al.*, 2019a).

Table 2.1. Comparison of Inhalation Methods for Therapeutic Delivery: Dry Powder Inhalers (DPIs), Nebulizers, and Pressurized Metered-Dose Inhalers (pMDIs).

Aspects	Dry Powder Inhalers (DPIs)	Nebulizers	Pressurized Metered-Dose Inhalers (pMDIs)
Principle	Devices that promote the perforation of a capsule or an inner reservoir, as a blister, that contains the inhalable powder upon the actuation of a valve. The dose is dispersed by the turbulence generated by patient's aspiration.	Generates aerosol from a liquid formulation delivering the drug directly through patients breathing.	Device containing the drug substance is dissolved or suspended, in a liquid propellant stored under pressure. The dose is dispensed upon coordinated actuation of a metering valve in the form of aerosols and inhalation.
Portability	Portable and convenient	Bulky and less portable	Portable and convenient
Inhalation Technique	Requires good inhalation technique	Easy to use for patients with limited hand coordination	Requires proper coordination between actuation and inhalation
Age Suitability	Suitable for patients of all ages	Suitable for patients with limited lung capacity or physical limitations	Suitable for patients of all ages
Administration Time	Quick and efficient drug delivery	Long administration time	Quick and efficient drug delivery
Equipment	No power source required	Requires power source	No power source required
Medication Flexibility	Wide range of medication options	Limited dose flexibility	Wide range of medication options
Maintenance	Lower risk of contamination	Regular maintenance and cleaning	Regular maintenance and cleaning
Cost	Cost-effective	More expensive equipment and higher medication cost	Cost-effective
Drug Stability	Improved drug stability (usually drugs are more stable in dry powder form)	Drug stability may vary depending on the formulation (liquid form may be required for certain drugs)	Drug stability may vary depending on the formulation (propellant-driven delivery)
Medication Waste	Lower medication waste	Higher medication waste	Higher medication waste

Source: elaborated by the author. Data from obtained from: (BAILEY; BERKLAND, 2009; DHAND, 2017; FDA, 2018; HADIWINOTO; LIP KWOK; LAKERVELD, 2018a; ROSIÈRE *et al.*, 2019b)

The efficiency of delivering particles to the site of action depends directly on their aerodynamic characteristics modulated by size, shape, density and surface roughness (LIN *et al.*, 2015a). Particles larger than 6 μm are retained by mucus and ciliary movements in the upper respiratory tract, which consists of the nasal cavity and pharynx, and are eliminated by coughing or swallowing (EL-SHERBINY; EL-BAZ; YACOUB, 2015). On the other hand, particles smaller than 1.0 μm are mostly exhaled (HADIWINOTO; LIP KWOK; LAKERVELD, 2018a). Therefore, particles whose average size is between 1 and 5 μm can more easily reach the central and distal tracts, while smaller particles can reach the alveoli and regions of the bronchioles (LOIRA-PASTORIZA; TODOROFF; VANBEVER, 2014). Those particles can be absorbed and internalized by cells, phagocytosed by macrophages or even cross the epithelial barrier and reach the systemic circulation or lymphatic system. (EL-SHERBINY; EL-BAZ; YACOUB, 2015; FERNÁNDEZ TENA; CASAN CLARÀ, 2012; KUZMOV; MINKO, 2015). The drug fraction that reaches the lymphatic system may even contribute to redistribution to more peripheral areas, with important potential for the treatment of metastases in lymph nodes (MANGAL *et al.*, 2017a).

Currently, many inhaled products are obtained by simply mixing a micronized active with an inert carrier such as lactose (RUDÉN *et al.*, 2019), but different technologies can be employed in order to modulate the desired characteristics: jet milling, spray drying, spray freeze drying and supercritical fluid, and which principles are summarized in Table 2.2 (LIN *et al.*, 2015b). Among them, spray drying technology can be highlighted by the scalability, cost and versatility for controlled obtention of low density particles of different shapes and sizes (ARPAGAUS, 2018; LIN *et al.*, 2015b; VEHRING, 2008). It is widely used for manufacturing of known inhaled products such as tobramycin (TOBI® podhaler®, Novartis) and mannitol (Aridol®, Pharmaxis) (ZHOU *et al.*, 2015).

Table 2.2. Technologies used to obtain inhaled powders and respective advantages and challenges.

Technology	Product characteristics	Advantages	Challenges
Jet milling	• Irregular particles.	• Simple operation; • No use of solvents; • Feasible process for heat sensitive materials.	• Highly cohesive particles; • High energy demand.
Spray drying	• Spherical particles; • Low density; • Allow obtention of amorphous particles	• One-step continuous process; • Versatility, allowing obtention of complex particles.	• Risk of degradation for heat sensible products; • Potential alteration of the crystalline structure; • Possible stability risk in case of amorphous state.
Spray freeze drying	• Allow obtention of amorphous particles; • High porosity.	• Uniform particle size • Potential improvement of dissolution (due to porosity)	• High energy demand; • Slow process.
Supercritical fluid	• Allow obtention of amorphous particles.	• Easy solvent separation; • No use of organic solvents.	• Scale-up problems

Source: elaborated by the author. Data obtained from (CHOW *et al.*, 2007; HADIWINOTO; LIP KWOK; LAKERVELD, 2018a).

2.5   SPRAY DRYING

Spray drying was patented in 1872 as a process optimized for promoting drying simultaneously with atomization (PERCY, 1872). Briefly, a liquid phase is atomized into a chamber with a heated gas, where the solvent is immediately removed and the final product is a ready to use dried powder (HADIWINOTO; LIP KWOK; LAKERVELD, 2018a). It was initially applied to the dairy industry (C. ANANDHARAMAKRISHNAN, PADMA ISHWARYA S., 2015), but since then it has been used in the manufacture of a wide range of materials, such as polymers, metals, food ingredients and pharmaceutical excipients (PARIKH, 2008). In the last 25 years its application has also been explored not only as a technology for drying materials, but for particle engineering in order to increase local drug delivery and its bioavailability, for production and stabilization of nanoparticles (ARPAGAUS *et al.*, 2018; ELSAYED; ABOUGHALY, 2016; PARIKH, 2008; VEHRING, 2008). Process parameters and formulation components directly impact on final product physical properties (C. ANANDHARAMAKRISHNAN, PADMA ISHWARYA S., 2015), and in order to modulate those characteristics, a deeper understanding of the process is required.

During atomization, the product as solution or suspension is fed into the heated chamber by a pump, and sprayed into many droplets, increasing liquid surface contact with the heated gas, and promoting a drastic reduction in the drying time (AL-KHATTAWI *et al.*, 2018). As the drying time is proportional to the square of particle dimension, it is reduced to a few seconds,

allowing drying to be carried with minimum heat exposure (C. ANANDHARAMAKRISHNAN, PADMA ISHWARYA S., 2015). This step can be influenced by liquid product characteristics, viscosity, surface tension, and flow rate; and equipment design and parameters, as nozzle design and atomization pressure (C. ANANDHARAMAKRISHNAN, PADMA ISHWARYA S., 2015). The composition of the solution or suspension, as solid concentration, and molecular weight can impact on viscosity (AL-KHATTAWI *et al.*, 2018). At a constant atomization pressure, the higher the viscosity, the bigger the droplet size, and thus the final powder particle size. This impact of solids concentrations can be more expressive for nanoparticle preparations with diluted solutions (1-5%), in comparison to higher concentrations (>10%), commonly applied in food industry to improve process throughput (BAGHDAN et al., 2019; TORRICO GUZMÁN; SUN; MEENACH, 2019; VICENTE et al., 2013). In these cases, atomization pressure could exert increased influence (BAGHDAN et al., 2019; TORRICO GUZMÁN; SUN; MEENACH, 2019; VICENTE et al., 2013). There are different types of atomizers, but the most commonly found in the pharmaceutical industry are pressure nozzles, for larger scales, and two-fluid nozzles, particularly interesting for production of smaller particles and high viscosity feeds (VICENTE et al., 2013).

Moisture evaporation is the most critical step in particle formation, and influences directly on particle morphology (C. ANANDHARAMAKRISHNAN, PADMA ISHWARYA S., 2015). After droplet formation, the particles tend to be more concentrated in the surface due to surface adsorption (VEHRING, 2008). When exposed to the heated air, the droplet temperature increases until reaching equilibrium evaporation temperature, the surface concentration is saturated as the solvent evaporates and the particles tend to move in the opposite direction, towards the center, and particle starts to shrink (C. ANANDHARAMAKRISHNAN, PADMA ISHWARYA S., 2015). During this phase, the evaporation rate is proportional to the surface area, and the main parameter for particle drying and obtained morphology can be explained with Peclet Number concept (C. ANANDHARAMAKRISHNAN, PADMA ISHWARYA S., 2015; VEHRING, 2008). Peclet number is the ratio between drying rate of a droplet and diffusion rate of solutes from the edge to the center of a droplet (C. ANANDHARAMAKRISHNAN, PADMA ISHWARYA S., 2015; VEHRING, 2008). Although the prediction of shell formation and final morphology are still not clear, it is reported that the increase in solid concentration can result in a more resistant particle (C. ANANDHARAMAKRISHNAN, PADMA ISHWARYA S., 2015; VEHRING, 2008). Depending on the properties of solution components, a sticky state can be reached during evaporation due to increase in surface viscosity, leading to agglomeration by droplets or dried

particles collision (C. ANANDHARAMAKRISHNAN, PADMA ISHWARYA S., 2015). Besides molecular weight of a polymer, for example, this stickiness is also related to the glass transition temperature (*Tg*) of the components, which can be considered as a critical attribute during formulation design (C. ANANDHARAMAKRISHNAN, PADMA ISHWARYA S., 2015). Since diffusion and evaporation rates changes through the process, not only for equipment design but also by formulation as with mixture of solvents, other shapes can be obtained as well (VEHRING, 2008). For example, if a thin shell is formed retaining, restraining moisture removal by a diffusion controlled process, inflated particles can be observed, whose shape can turn out hollow, irregular or can break apart (C. ANANDHARAMAKRISHNAN, PADMA ISHWARYA S., 2015; VICENTE *et al.*, 2013).

Lastly, particle separation from the drying gas is often based on inertia: the air carrying dried particles enter cyclones, are subjected to the vortex that forces the deposition by impaction on the cyclone walls (BOHR; RUGE; BECK-BROICHSITTER, 2014). The efficiency of drying and residual moisture can impact adhesion to equipment inner walls, affecting process yield and product stability.

An interesting example of an engineered spray dried particle marketed product is TOBI® podhaler (tobramycin DPI). Manufactured with the patented technology Pulmosphere™, its small porous particles consist of lipids, diastereoylphosphatidyldicoline and calcium chloride, resulting in lower cohesion, contributing to better dispersibility and aerosolization performance (MEHTA, 2019). iSPERSE™ technology involves spraying drugs in aqueous or organic solution with excipients such as magnesium stearate and leucine, producing denser small particles with good dispersibility (MEHTA, 2019). It was employed for the production of DPI from itraconazole (Pulmazol), in order to overcome problems of low solubility and increase dose at the site of action, and is currently under phase II clinical trial for the treatment of aspergillosis (PULMATRIX INC., 2021). Previous studies used nanoprecipitation processess through spray drying for the obtention of inhalable dry powders. Curcumin nano-in-micro particles, composed of PLGA and mannitol with PVA used as stabilizer, were obtained for aiming inhaled photodynamic therapy, and exhibited 64.94% of fine particle fraction (FPF) and 233.41 nm after redispersion and satisfactory uptake by A549 lung cancer cells (BAGHDAN *et al.*, 2019). Amorphous paclitaxel nanoparticles of 200 nm were prepared by single emulsion followed by solvent evaporation and spray drying with mannitol as carrier (TORRICO GUZMÁN; SUN; MEENACH, 2019). The obtained nanoparticles exhibited higher particle size of paclitaxel 270.6 nm PDI of 0.33, 3% drug loading, FPF of 66% and 97% RF, and 70% reduction in the IC50 after 48 hours of exposure for A549 cells (TORRICO GUZMÁN; SUN;

MEENACH, 2019). Hence, spray drying is a scalable and versatile technology that is suitable for the development of nanocrystals for inhalation.

2.6 REFERENCES

AFTAB, S.; SHAH, A.; NADHMAN, A.; KURBANOGLU, S.; AYSIL OZKAN, S.; DIONYSIOU, D. D.; SHUKLA, S. S.; AMINABHAVI, T. M. Nanomedicine: An Effective Tool in Cancer Therapy. **International Journal of Pharmaceutics**, v. 540, n. 1–2, p. 132–149, abr. 2018.

AL-KHATTAWI, A.; BAYLY, A.; PHILLIPS, A.; WILSON, D. The Design and Scale-up of Spray Dried Particle Delivery Systems. **Expert Opinion on Drug Delivery**, v. 15, n. 1, p. 47–63, 2 jan. 2018.

ARBOUR, K. C.; RIELY, G. J. Systemic Therapy for Locally Advanced and Metastatic Non–Small Cell Lung Cancer: A Review. **JAMA**, v. 322, n. 8, p. 764, 27 ago. 2019.

ARPAGAUS, C. Pharmaceutical Particle Engineering via Nano Spray Drying - Process Parameters and Application Examples on the Laboratory-Scale. **International Journal of Medical Nano Research**, v. 5, n. 1, 31 dez. 2018. Disponível em: <https://www.clinmedjournals.org/articles/ijmnr/international-journal-of-medical-nano-research-ijmnr-5-026.php?jid=ijmnr>. Acesso em: 8 set. 2019.

ARPAGAUS, C.; COLLENBERG, A.; RÜTTI, D.; ASSADPOUR, E.; JAFARI, S. M. Nano Spray Drying for Encapsulation of Pharmaceuticals. **International Journal of Pharmaceutics**, v. 546, n. 1–2, p. 194–214, jul. 2018.

BAGHDAN, E.; DUSE, L.; SCHÜER, J. J.; PINNAPIREDDY, S. R.; POURASGHAR, M.; SCHÄFER, J.; SCHNEIDER, M.; BAKOWSKY, U. Development of Inhalable Curcumin Loaded Nano-in-Microparticles for Bronchoscopic Photodynamic Therapy. **European Journal of Pharmaceutical Sciences**, v. 132, p. 63–71, abr. 2019.

BAILEY, M. M.; BERKLAND, C. J. Nanoparticle Formulations in Pulmonary Drug Delivery. **Medicinal Research Reviews**, v. 29, n. 1, p. 196–212, jan. 2009.

BHATIA, S. Nanoparticles Types, Classification, Characterization, Fabrication Methods and Drug Delivery Applications. *Em*: BHATIA, S. **Natural Polymer Drug Delivery Systems**. Cham: Springer International Publishing, 2016. p. 33–93.

BUCKTON, G.; BEEZER, A. E. The Relationship between Particle Size and Solubility. **International Journal of Pharmaceutics**, v. 82, n. 3, p. R7–R10, maio 1992.

C. ANANDHARAMAKRISHNAN, PADMA ISHWARYA S. **Spray Drying Techniques for Food Ingredient Encapsulation**. [s.l.] John Wiley & Sons, Ltd, 2015. 312 p.

ČÁŇOVÁ, K.; ROZKYDALOVÁ, L.; RUDOLF, E. Anthelmintic Flubendazole and Its Potential Use in Anticancer Therapy. **Acta Medica (Hradec Kralove, Czech Republic)**, v. 60, n. 1, p. 5–11, 2017.

ČÁŇOVÁ, K.; ROZKYDALOVÁ, L.; VOKURKOVÁ, D.; RUDOLF, E. Flubendazole Induces Mitotic Catastrophe and Apoptosis in Melanoma Cells. **Toxicology in Vitro**, v. 46, p. 313–322, fev. 2018.

CHAFT, J. E.; RIMNER, A.; WEDER, W.; AZZOLI, C. G.; KRIS, M. G.; CASCONE, T. Evolution of Systemic Therapy for Stages I–III Non-Metastatic Non-Small-Cell Lung Cancer. **Nature Reviews Clinical Oncology**, v. 18, n. 9, p. 547–557, set. 2021.

CHEN, M.-L.; JOHN, M.; LEE, S. L.; TYNER, K. M. Development Considerations for Nanocrystal Drug Products. **The AAPS Journal**, v. 19, n. 3, p. 642–651, maio 2017.

CHEUNG, W. K. C.; NGUYEN, D. X. Lineage Factors and Differentiation States in Lung Cancer Progression. **Oncogene**, v. 34, n. 47, p. 5771–5780, 19 nov. 2015.

CHOU, A. J.; GUPTA, R.; BELL, M. D.; RIEWE, K. O.; MEYERS, P. A.; GORLICK, R. Inhaled Lipid Cisplatin (ILC) in the Treatment of Patients with Relapsed/Progressive Osteosarcoma Metastatic to the Lung. **Pediatric Blood & Cancer**, v. 60, n. 4, p. 580–586, 2013.

CHOW, A. H. L.; TONG, H. H. Y.; CHATTOPADHYAY, P.; SHEKUNOV, B. Y. Particle Engineering for Pulmonary Drug Delivery. **Pharmaceutical Research**, v. 24, n. 3, p. 411–437, mar. 2007.

CLARK, S. B.; ALSUBAIT, S. Non–Small Cell Lung Cancer. *Em*: **StatPearls**. Treasure Island (FL): StatPearls Publishing, 2023.

CORTÉS, Á. A.; URQUIZU, L. C.; CUBERO, J. H. Adjuvant Chemotherapy in Non-Small Cell Lung Cancer: State-of- the-Art. **Translational lung cancer research**, v. 4, n. 2, p. 7, 2015.

DAN, N. Core–Shell Drug Carriers: Liposomes, Polymersomes, and Niosomes. *Em*: ANDRONESCU, E.; GRUMEZESCU, A. M. **Nanostructures for Drug Delivery**. Amsterdam, The Netherlands: Elsevier, 2017. p. 63–105.

DHAND, R. Inhaled Drug Therapy 2016: The Year in Review. **Respiratory Care**, v. 62, n. 7, p. 978–996, jul. 2017.

DOUMAT, G.; DAHER, D.; ZERDAN, M. B.; NASRA, N.; BAHMAD, H. F.; RECINE, M.; POPPITI, R. Drug Repurposing in Non-Small Cell Lung Carcinoma: Old Solutions for New Problems. **Current Oncology**, v. 30, n. 1, p. 704–719, 5 jan. 2023.

DUMA, N.; SANTANA-DAVILA, R.; MOLINA, J. R. Non–Small Cell Lung Cancer: Epidemiology, Screening, Diagnosis, and Treatment. **Mayo Clinic Proceedings**, v. 94, n. 8, p. 1623–1640, ago. 2019.

ELSAYED, I.; ABOUGHALY, M. H. H. Inhalable Nanocomposite Microparticles: Preparation, Characterization and Factors Affecting Formulation. **Expert Opinion on Drug Delivery**, v. 13, n. 2, p. 207–222, fev. 2016.

EL-SHERBINY, I. M.; EL-BAZ, N. M.; YACOUB, M. H. Inhaled Nano- and Microparticles for Drug Delivery. **Global Cardiology Science and Practice**, v. 2015, n. 1, p. 2, jan. 2015.

FDA. **Metered Dose Inhaler (MDI) and Dry Powder Inhaler (DPI) Products - Quality Considerations** abr. 2018. Disponível em: <https://www.fda.gov/media/70851/download>. Acesso em: 28 jan. 2020.

FERNÁNDEZ TENA, A.; CASAN CLARÀ, P. Deposition of Inhaled Particles in the Lungs. **Archivos de Bronconeumología (English Edition)**, v. 48, n. 7, p. 240–246, jul. 2012.

FLÜHMANN, B.; NTAI, I.; BORCHARD, G.; SIMOENS, S.; MÜHLEBACH, S. Nanomedicines: The Magic Bullets Reaching Their Target? **European Journal of Pharmaceutical Sciences**, v. 128, p. 73–80, fev. 2019.

GABRIEL L. B. DE ARAUJO; FABIO FURLAN FERREIRA; CARLOS E. S. BERNARDES; JULIANA A. P. SATO; OTÁVIO M. GIL; DALVA L. A. DE FARIA; RAIMAR LOEBENBERG; STEPHEN R. BYRN; DANIELA D. M. GHISLENI; NADIA A. BOU-CHACRA; TEREZINHA J. A. PINTO; SELMA G. ANTONIO; HUMBERTO G. FERRAZ; DMITRY ZEMLYANOV; DÉBORA S. GONÇALVES; MANUEL E. MINAS DA PIEDADE. A New Thermodynamically Favored Flubendazole/Maleic Acid Binary Crystal Form: Structure, Energetics, and in Silico PBPK Model-Based Investigation. **A New Thermodynamically Favored Flubendazole/Maleic Acid Binary Crystal Form: Structure, Energetics, and in Silico PBPK Model-Based Investigation**, v. 18, n. 9, p. 2377–2386, 2018.

GEARY, T. G.; MACKENZIE, C. D.; SILBER, S. A. Flubendazole as a Macrofilaricide: History and Background. **PLOS Neglected Tropical Diseases**, v. 13, n. 1, p. e0006436, 16 jan. 2019.

GOLOMBEK, S. K.; MAY, J.-N.; THEEK, B.; APPOLD, L.; DRUDE, N.; KIESSLING, F.; LAMMERS, T. Tumor Targeting via EPR: Strategies to Enhance Patient Responses. **Advanced Drug Delivery Reviews**, v. 130, p. 17–38, maio 2018.

GRONEBERG, D. A.; WITT, C.; WAGNER, U.; CHUNG, K. F.; FISCHER, A. Fundamentals of Pulmonary Drug Delivery. **Respiratory Medicine**, v. 97, n. 4, p. 382–387, abr. 2003.

HADIWINOTO, G. D.; LIP KWOK, P. C.; LAKERVELD, R. A Review on Recent Technologies for the Manufacture of Pulmonary Drugs. **Therapeutic Delivery**, v. 9, n. 1, p. 47–70, jan. 2018.

HAMISHEHKAR, H.; RAHIMPOUR, Y.; JAVADZADEH, Y. The Role of Carrier in Dry Powder Inhaler. *Em*: SEZER, A. D. **Recent Advances in Novel Drug Carrier Systems**. [s.l.] InTech, 2012.

INCA - INSTITUTO NACIONAL DE CÂNCER. **Estimativa 2023 : incidência de câncer no Brasil**. [s.l: s.n.]. Disponível em: <https://www.inca.gov.br/sites/ufu.sti.inca.local/files/media/document/estimativa-2023.pdf>. Acesso em: 22 ago. 2023a.

INCA - INSTITUTO NACIONAL DE CÂNCER. **Câncer de pulmão**. [s.l: s.n.]. Disponível em: <https://www.gov.br/inca/pt-br/assuntos/cancer/tipos/pulmao>. Acesso em: 22 ago. 2023b.

KAKRAN, M.; SHEGOKAR, R.; SAHOO, N. G.; AL SHAAL, L.; LI, L.; MÜLLER, R. H. Fabrication of Quercetin Nanocrystals: Comparison of Different Methods. **European Journal of Pharmaceutics and Biopharmaceutics**, v. 80, n. 1, p. 113–121, jan. 2012.

KUZMOV, A.; MINKO, T. Nanotechnology Approaches for Inhalation Treatment of Lung Diseases. **Journal of Controlled Release**, v. 219, p. 500–518, dez. 2015.

LACHAU-DURAND, S.; LAMMENS, L.; VAN DER LEEDE, B.; VAN GOMPEL, J.; BAILEY, G.; ENGELEN, M.; LAMPO, A. Preclinical Toxicity and Pharmacokinetics of a New Orally Bioavailable Flubendazole Formulation and the Impact for Clinical Trials and Risk/Benefit to Patients. **PLOS Neglected Tropical Diseases**, v. 13, n. 1, p. e0007026, 16 jan. 2019.

LAOUINI, A.; JAAFAR-MAALEJ, C.; LIMAYEM-BLOUZA, I.; SFAR, S.; CHARCOSSET, C.; FESSI, H. Preparation, Characterization and Applications of Liposomes: State of the Art. **Journal of Colloid Science and Biotechnology**, v. 1, n. 2, p. 147–168, 1 dez. 2012.

LEE, S. H. Chemotherapy for Lung Cancer in the Era of Personalized Medicine. **Tuberculosis and Respiratory Diseases**, v. 82, n. 3, p. 179, 2019.

LEE, Y. T.; TAN, Y. J.; OON, C. E. Benzimidazole and Its Derivatives as Cancer Therapeutics: The Potential Role from Traditional to Precision Medicine. **Acta Pharmaceutica Sinica B**, v. 13, n. 2, p. 478–497, fev. 2023.

LEVET, V.; ROSIÈRE, R.; MERLOS, R.; FUSARO, L.; BERGER, G.; AMIGHI, K.; WAUTHOZ, N. Development of Controlled-Release Cisplatin Dry Powders for Inhalation against Lung Cancers. **International Journal of Pharmaceutics**, v. 515, n. 1, p. 209–220, 30 dez. 2016.

LIN, Y.-W.; WONG, J.; QU, L.; CHAN, H.-K.; ZHOU, Q. Powder Production and Particle Engineering for Dry Powder Inhaler Formulations. **Current Pharmaceutical Design**, v. 21, n. 27, p. 3902–3916, 17 set. 2015a.

LIN, Y.-W.; WONG, J.; QU, L.; CHAN, H.-K.; ZHOU, Q. Powder Production and Particle Engineering for Dry Powder Inhaler Formulations. **Current Pharmaceutical Design**, v. 21, n. 27, p. 3902–3916, 17 set. 2015b.

LOIRA-PASTORIZA, C.; TODOROFF, J.; VANBEVER, R. Delivery Strategies for Sustained Drug Release in the Lungs. **Advanced Drug Delivery Reviews**, v. 75, p. 81–91, ago. 2014.

LU, T.; YANG, X.; HUANG, Y.; ZHAO, M.; LI, M.; MA, K.; YIN, J.; ZHAN, C.; WANG, Q. Trends in the Incidence, Treatment, and Survival of Patients with Lung Cancer in the Last Four Decades. **Cancer Management and Research**, v. Volume 11, p. 943–953, jan. 2019.

MACKENZIE, C.; LANSING, E. A REVIEW OF FLUBENDAZOLE AND ITS POTENTIAL AS A MACROFILARIACIDE. p. 67, 2014.

MANGAL, S.; GAO, W.; LI, T.; ZHOU, Q. Pulmonary Delivery of Nanoparticle Chemotherapy for the Treatment of Lung Cancers: Challenges and Opportunities. **Acta Pharmacologica Sinica**, v. 38, n. 6, p. 782–797, jun. 2017.

MASELLI, D.; KEYT, H.; RESTREPO, M. Inhaled Antibiotic Therapy in Chronic Respiratory Diseases. **International Journal of Molecular Sciences**, v. 18, n. 5, p. 1062, 16 maio 2017.

MATSUMURA, Y.; MAEDA, H. A New Concept for Macromolecular Therapeutics in Cancer Chemotherapy: Mechanism of Tumoritropic Accumulation of Proteins and the Antitumor Agent Smancs. p. 7, dez. 1986.

MEHTA, P. Dry Powder Inhalers: A Focus on Advancements in Novel Drug Delivery Systems. **Journal of Drug Delivery**, v. 2016, p. 1–17, 2016.

MEHTA, P. P. Dry powder inhalers: upcoming platform technologies for formulation development. **Therapeutic Delivery**, v. 10, n. 9, p. 551–554, 1 set. 2019.

MICHAELIS, M.; AGHA, B.; ROTHWEILER, F.; LÖSCHMANN, N.; VOGES, Y.; MITTELBRONN, M.; STARZETZ, T.; HARTER, P. N.; ABHARI, B. A.; FULDA, S.; WESTERMANN, F.; RIECKEN, K.; SPEK, S.; LANGER, K.; WIESE, M.; DIRKS, W. G.; ZEHNER, R.; CINATL, J.; WASS, M. N.; CINATL, J. Identification of Flubendazole as Potential Anti-Neuroblastoma Compound in a Large Cell Line Screen. **Scientific Reports**, v. 5, n. 1, p. 8202, 3 fev. 2015.

MIDTHUN, D. E. Early Detection of Lung Cancer. **F1000Research**, v. 5, p. 739, 25 abr. 2016.

MINDA, D.; MIOC, A.; BANCIU, C.; SOICA, C.; RACOVICEANU, R.; MIOC, M.; MACASOI, I.; AVRAM, S.; VOICU, A.; MOTOC, A.; TRANDAFIRESCU, C. Cyclodextrin Dispersion of Mebendazole and Flubendazole Improves In Vitro Antiproliferative Activity. **Processes**, v. 9, n. 12, p. 2185, 3 dez. 2021.

MORRIS, P. G.; FORNIER, M. N. Microtubule Active Agents: Beyond the Taxane Frontier. **Clinical Cancer Research**, v. 14, n. 22, p. 7167–7172, 15 nov. 2008.

MÜHLETHALER, T.; GIOIA, D.; PROTA, A. E.; SHARPE, M. E.; CAVALLI, A.; STEINMETZ, M. O. Comprehensive Analysis of Binding Sites in Tubulin. **Angewandte Chemie International Edition**, v. 60, n. 24, p. 13331–13342, 2021.

MÜLLER, R. H.; GOHLA, S.; KECK, C. M. State of the Art of Nanocrystals – Special Features, Production, Nanotoxicology Aspects and Intracellular Delivery. **European Journal of Pharmaceutics and Biopharmaceutics**, v. 78, n. 1, p. 1–9, maio 2011.

NASIM, F.; SABATH, B. F.; EAPEN, G. A. Lung Cancer. **Medical Clinics of North America**, v. 103, n. 3, p. 463–473, maio 2019.

O'NEILL, M. Characterization of the Effects of Flubendazole, a Benzimidazole Anthelmintic, on Filarial Nematodes. 2016.

PARDO, J.; MARTINEZ-PEÑUELA, A. M.; SOLA, J. J.; PANIZO, A.; GÚRPIDE, A.; MARTINEZ-PEÑUELA, J. M.; LOZANO, M. D. Large Cell Carcinoma of the Lung: An Endangered Species? **Applied Immunohistochemistry & Molecular Morphology**, v. 17, n. 5, p. 383, out. 2009.

PARIKH, D. M. Advances in Spray Drying Technology: New Applications for a Proven Process. **American Pharmaceutical Review**, p. 6, jan. 2008.

PARK, K. Facing the Truth about Nanotechnology in Drug Delivery. **ACS Nano**, v. 7, n. 9, p. 7442–7447, 24 set. 2013.

PARKER, A. L.; TEO, W. S.; MCCARROLL, J. A.; KAVALLARIS, M. An Emerging Role for Tubulin Isotypes in Modulating Cancer Biology and Chemotherapy Resistance. **International Journal of Molecular Sciences**, v. 18, n. 7, p. 1434, 4 jul. 2017.

PAZ-ARES, L. *et al.* Durvalumab plus Platinum–Etoposide versus Platinum–Etoposide in First-Line Treatment of Extensive-Stage Small-Cell Lung Cancer (CASPIAN): A Randomised, Controlled, Open-Label, Phase 3 Trial. **The Lancet**, v. 394, n. 10212, p. 1929–1939, nov. 2019.

PERCY, S. R. UNITED STATES PATENT US125406A. **UNITED STATES PATENT OFFICE**, p. 2, abr. 1872.

PULMATRIX INC. **Study in Adult Asthmatic Patients With Allergic Bronchopulmonary Aspergillosis - NCT03960606**ClinicalTrials.gov, 27 ago. 2021. Disponível em: <https://clinicaltrials.gov/ct2/show/study/NCT03960606?term=PUR1900&draw=2&rank=2>.

ROSIÈRE, R.; BERGHMANS, T.; DE VUYST, P.; AMIGHI, K.; WAUTHOZ, N. The Position of Inhaled Chemotherapy in the Care of Patients with Lung Tumors: Clinical Feasibility and Indications According to Recent Pharmaceutical Progresses. **Cancers**, v. 11, n. 3, p. 329, 7 mar. 2019a.

ROSIÈRE, R.; BERGHMANS, T.; DE VUYST, P.; AMIGHI, K.; WAUTHOZ, N. The Position of Inhaled Chemotherapy in the Care of Patients with Lung Tumors: Clinical Feasibility and Indications According to Recent Pharmaceutical Progresses. **Cancers**, v. 11, n. 3, p. 329, 7 mar. 2019b.

RUDÉN, J.; FRENNING, G.; BRAMER, T.; THALBERG, K.; AN, J.; ALDERBORN, G. Linking Carrier Morphology to the Powder Mechanics of Adhesive Mixtures for Dry Powder Inhalers via a Blend-State Model. **International Journal of Pharmaceutics**, v. 561, p. 148–160, abr. 2019.

SAINAS, S.; DOSIO, F.; BOSCHI, D.; LOLLI, M. L. **Targeting Human Onchocerciasis: Recent Advances Beyond Ivermectin | Elsevier Enhanced Reader**. Disponível em: <https://reader.elsevier.com/reader/sd/pii/S0065774318300010?token=9A992C0B321494B6B207C1C

43FD13D424C07712AB9D4CE60C1D82556622C8E83805D7870F10D75747831CBF6C4B81249&o
riginRegion=us-east-1&originCreation=20230215140151>. Acesso em: 15 fev. 2023.

SANDERS, M. Inhalation Therapy: An Historical Review. **Primary Care Respiratory Journal**, v. 16, n. 2, p. 71–81, 13 mar. 2007.

SASE, K.; FUJISAKA, Y.; SHOJI, M.; MUKAI, M. Cardiovascular Complications Associated with Contemporary Lung Cancer Treatments. **Current Treatment Options in Oncology**, v. 22, n. 8, p. 71, 10 jun. 2021.

SEYHAN, A. A. Lost in Translation: The Valley of Death across Preclinical and Clinical Divide – Identification of Problems and Overcoming Obstacles. **Translational Medicine Communications**, v. 4, n. 1, p. 18, dez. 2019.

SPAGNUOLO, P. A.; HU, J.; HURREN, R.; WANG, X.; GRONDA, M.; SUKHAI, M. A.; DI MEO, A.; BOSS, J.; ASHALI, I.; BEHESHTI ZAVAREH, R.; FINE, N.; SIMPSON, C. D.; SHARMEEN, S.; ROTTAPEL, R.; SCHIMMER, A. D. The Antihelmintic Flubendazole Inhibits Microtubule Function through a Mechanism Distinct from Vinca Alkaloids and Displays Preclinical Activity in Leukemia and Myeloma. **Blood**, v. 115, n. 23, p. 4824–4833, 10 jun. 2010.

STEIN, S. W.; THIEL, C. G. The History of Therapeutic Aerosols: A Chronological Review. **Journal of Aerosol Medicine and Pulmonary Drug Delivery**, v. 30, n. 1, p. 20–41, fev. 2017.

SUNG, H.; FERLAY, J.; SIEGEL, R. L.; LAVERSANNE, M.; SOERJOMATARAM, I.; JEMAL, A.; BRAY, F. Global Cancer Statistics 2020: GLOBOCAN Estimates of Incidence and Mortality Worldwide for 36 Cancers in 185 Countries. **CA: A Cancer Journal for Clinicians**, v. 71, n. 3, p. 209–249, 2021.

TARATULA, O.; KUZMOV, A.; SHAH, M.; GARBUZENKO, O. B.; MINKO, T. Nanostructured Lipid Carriers as Multifunctional Nanomedicine Platform for Pulmonary Co-Delivery of Anticancer Drugs and SiRNA. **Journal of Controlled Release**, v. 171, n. 3, p. 349–357, nov. 2013.

TIAN, Z.; CHU, Y.; WANG, H.; ZHONG, L.; DENG, M.; LI, W. Biological Activity and Interaction Mechanism of the Diketopiperazine Derivatives as Tubulin Polymerization Inhibitors. **RSC Advances**, v. 8, n. 2, p. 1055–1064, 2 jan. 2018.

TORRICO GUZMÁN, E. A.; SUN, Q.; MEENACH, S. A. Development and Evaluation of Paclitaxel-Loaded Aerosol Nanocomposite Microparticles and Their Efficacy Against Air-Grown Lung Cancer Tumor Spheroids. **ACS Biomaterials Science & Engineering**, v. 5, n. 12, p. 6570–6580, 9 dez. 2019.

VEHRING, R. Pharmaceutical Particle Engineering via Spray Drying. **Pharmaceutical Research**, v. 25, n. 5, p. 999–1022, maio 2008.

VIALPANDO, M.; SMULDERS, S.; BONE, S.; JAGER, C.; VODAK, D.; VAN SPEYBROECK, M.; VERHEYEN, L.; BACKX, K.; BOEYKENS, P.; BREWSTER, M. E.; CEULEMANS, J.; NOVOA DE ARMAS, H.; VAN GEEL, K.; KESSELAERS, E.; HILLEWAERT, V.; LACHAU-DURAND, S.; MEURS, G.; PSATHAS, P.; VAN HOVE, B.; VERRECK, G.; VOETS, M.; WEUTS, I.; MACKIE, C. Evaluation of Three Amorphous Drug Delivery Technologies to Improve the Oral Absorption of Flubendazole. **Journal of Pharmaceutical Sciences**, v. 105, n. 9, p. 2782–2793, set. 2016.

VICENTE, J.; PINTO, J.; MENEZES, J.; GASPAR, F. Fundamental Analysis of Particle Formation in Spray Drying. **Powder Technology**, v. 247, p. 1–7, out. 2013.

WAUTHOZ, N.; ROSIÈRE, R.; AMIGHI, K. Inhaled Cytotoxic Chemotherapy: Clinical Challenges, Recent Developments, and Future Prospects. **Expert Opinion on Drug Delivery**, v. 18, n. 3, p. 333–354, 4 mar. 2021.

WITTGEN, B. P. H.; KUNST, P. W. A.; BORN, K. van der; WIJK, A. W. van; PERKINS, W.; PILKIEWICZ, F. G.; PEREZ-SOLER, R.; NICHOLSON, S.; PETERS, G. J.; POSTMUS, P. E. Phase I Study of Aerosolized SLIT Cisplatin in the Treatment of Patients with Carcinoma of the Lung. **Clinical Cancer Research**, v. 13, n. 8, p. 2414–2421, 15 abr. 2007.

WORLD HEALTH ORGANIZATION. Estimated age-standardized mortality rates (World) in 2020, lung, both sexes, all ages. Cancer Today. GLOBOCAN. 2020. Available at: <https://gco.iarc.fr/today/home>.

XIE, X.; CAI, X.; TANG, Y.; JIANG, C.; ZHOU, F.; YANG, L.; LIU, Z.; WANG, L.; ZHAO, H.; ZHAO, C.; HUANG, X. Flubendazole Elicits Antitumor Effects by Inhibiting STAT3 and Activating Autophagy in Non-Small Cell Lung Cancer. **Frontiers in Cell and Developmental Biology**, v. 9, p. 680600, 26 ago. 2021.

ZHANG, Z.; ZHOU, L.; XIE, N.; NICE, E. C.; ZHANG, T.; CUI, Y.; HUANG, C. Overcoming Cancer Therapeutic Bottleneck by Drug Repurposing. **Signal Transduction and Targeted Therapy**, v. 5, n. 1, p. 1–25, 2 jul. 2020.

ZHONG, Q. Co-Spray Dried Mannitol/Poly(Amidoamine)-Doxorubicin Dry-Powder Inhaler Formulations for Lung Adenocarcinoma: Morphology, In Vitro Evaluation, and Aerodynamic Performance. **AAPS PharmSciTech**, v. 19, n. 2, p. 531–540, fev. 2018.

ZHOU, Q. (Tony); LEUNG, S. S. Y.; TANG, P.; PARUMASIVAM, T.; LOH, Z. H.; CHAN, H.-K. Inhaled Formulations and Pulmonary Drug Delivery Systems for Respiratory Infections. **Advanced Drug Delivery Reviews**, v. 85, p. 83–99, maio 2015.

CHAPTER 3   FROM BENCH TO BEDSIDE: WHICH GAPS NEED TO BE FULFILLED TO ACTUALLY DELIVER INHALED THERAPY FOR CANCER PATIENTS?

3.1 INTRODUCTION

With estimated 2.2 million new cases, lung cancer was responsible for 18% of the total cancer deaths in 2020 and remains the type of cancer that causes most deaths in the world (SUNG *et al.*, 2021a). Late diagnosis and poor prognosis contribute to the 5-year survival rate of 10% to 20%, and although prevention programs are promoted around the world, it is expected that the burden of cancer will increase by 47% in 2040 due to aging and population growth (SUNG *et al.*, 2021a). Therefore, unless resources and effort are managed to create and improve treatments, the mortality rate also tends to grow in the same proportion.

Inhalable therapies have been used for many years for asthma and other respiratory issues, but recently its application for systemic delivery has been receiving increasing interest as an alternative to oral administration in several therapeutic uses, as diabetes (Exubera® - Pfizer and Affreza® - MannKind Corporation), migraine (Migranal® - Novartis), endometriosis (Synarel® - Searle), osteoporosis (Miacalcin®NS - Novartis) and vaccines (HADIWINOTO; LIP KWOK; LAKERVELD, 2018a). The advantages of this route over intravenous and oral administration especially regarding a cancer treatment include non-invasiveness, reduced systemic toxicity and favored physiological conditions due to the thin and large surface area of highly vascularized alveoli tissue (EL-SHERBINY; EL-BAZ; YACOUB, 2015; GRONEBERG *et al.*, 2003). It is reported that after an intravenous administration, often less than 6% of the dose can reach the lungs, whereas the majority is more likely to accumulate in the liver, kidney and spleen, reducing treatment effectiveness and inducing severe toxicity, from allergic reactions, diarrhea, vomiting and nausea to myelosuppression, neuro and cardiovascular toxicity (AI *et al.*, 2018; KUZMOV; MINKO, 2015; NEWMAN, 2018). In contrast, the direct delivery reduces metabolization and retention in healthy tissues, allowing accumulation of higher amount of drugs in the site of action, contributing to the overall increase in efficacy (EL-SHERBINY; EL-BAZ; YACOUB, 2015; GRONEBERG *et al.*, 2003).

An inhaled chemotherapy treatment was first mentioned in the late 1960's, with the first clinical report published in 1968 (KUZMOV; MINKO, 2015; ROSIÈRE *et al.*, 2019a). Most of the experience acquired since was due to studies using animal models, reporting tumor size reduction (KIM *et al.*, 2012; ROA *et al.*, 2011) and lower concentration of the drug in healthy tissues (XIE *et al.*, 2010; ZHU *et al.*, 2019). The clinical trials conducted in humans have proven the approach feasible and safe in most of the cases, but all of them failed in phase I or II at best, mainly by dose-limiting toxicity (ROSIÈRE *et al.*, 2019a). The main pharmaceutical forms of inhalable formulations are solutions and suspensions, that are delivered as nasal sprays, soft

mist inhalers or nebulizers, and dry powders (HADIWINOTO; LIP KWOK; LAKERVELD, 2018a), administered by pressurized metered-dose inhaler (pMDI) or dry powder inhaler (DPI) (HAMISHEHKAR; RAHIMPOUR; JAVADZADEH, 2012). DPI are preferable amongst other inhalable devices for the convenience of size and way of handling, superior chemical and microbiological stability due to the reduced humidity content and no need for reconstitution, not requiring cold chain (HAMISHEHKAR; RAHIMPOUR; JAVADZADEH, 2012) or propellant in the formulation.

Local delivery of a small amount of drug with maximized effectiveness and minimum adverse effects is the target for any formulation scientist, especially for chemotherapy. For lung cancer, the cancer with the highest mortality rate worldwide (SUNG *et al.*, 2021b), the perfect solution could naturally be an inhalable formulation. Yet, no inhalable treatment targeting lung cancer is available on the market (ROSIÈRE *et al.*, 2019b). Many studies describe different complex engineered particles that can be delivered by solution or powder (DPI, pMDI), and many highlight DPI advantages over other forms of delivery, but none evolved to clinical trials (ROSIÈRE *et al.*, 2019b). What are the challenges that stand in the way of the development of dry powders for inhalation and cancer treatment? If the development of inhalable chemotherapy is infant, what is already known and what needs to be explored? This chapter focuses on answering to those questions to establish a feasible strategy to the development of local delivery for lung cancer treatment.

3.2 FORMULATION

For DPIs, the main pillars for an effective delivery are formulation, device, and patient (THALBERG *et al.*, 2023). Formulation plays an important role in the delivery since its physicochemical characteristics are essential to reach deep lungs and bypass physiologic barriers to assure an effective delivery. Optimization of particle size, shape, and surface properties, enhances the probability of delivering the desired dose to the targeted site. Moreover, other characteristics such as roughness or porosity also influence particle interactions with lung cells and can impact on cellular uptake, adhesion, and subsequent pharmacological effects.

3.2.1 Lung physiology

The challenge is the intricate lung physiology. After a brief atomization, high doses of poorly soluble drugs can be delivered directly to the site of action avoiding first pass metabolism, reaching a huge and highly vascularized alveolar surface area of 70 and 160 m^2

that facilitates absorption (WEBER; ZIMMER; PARDEIKE, 2014). But due to the branched structure of the respiratory tract, aspirated particles are first selected by size. The majority of the particles bigger than 6 μm are retained in the upper respiratory tract, that consists of nasal cavity, pharynx, and larynx, by mucociliary clearance and are eliminated either by coughing or swallowing (EL-SHERBINY; EL-BAZ; YACOUB, 2015). Particles of size mainly between 1 and 5 μm settle in central and distant tracts, while smaller ones are mainly eliminated by exhalation (HADIWINOTO; LIP KWOK; LAKERVELD, 2018a), but can also settle in alveolar and tracheo-bronchial region (LOIRA-PASTORIZA; TODOROFF; VANBEVER, 2014).

To protect exogenous substances from directly accessing the systemic circulation, the upper and central respiratory tract is constituted by a monolayer of epithelial cells, ciliated and goblet cells (YUE *et al.*, 2022). The latter produces mucus, composed by 80% phospholipids (roughly half of them being dipalmitoyl phosphatidylcholine, DPPC), 5-10% neutral lipids (mainly cholesterol), and 5-10% proteins (CZECHTIZKY *et al.*, 2022). The mucus thickness of approximately 10-30 μm in the thickness of trachea, and 2-5 μm in the bronchus, with a clearance rate of 4-20 mm/min (YUE *et al.*, 2022) can potentially decrease efficacy. Particles that can rapidly permeate through the mucus layer might be retained for a longer period in the lung (DING *et al.*, 2021). Since mucus is hydrophilic and presents a negative charge, positively charged particles are more likely to interact with sialic acid residues of mucins and thus have more difficulty to penetrate the barrier (HE *et al.*, 2022; KNAP *et al.*, 2022). In contrast, neutrally or negatively charged particles can avoid electrostatic interaction and permeate easier. Also, hydrophilic nanoparticles are reported to also be more inert, since the hydration layer would provide surface protection to prevent interaction with the mucus (WANG *et al.*, 2022b). PEG coating confers neutral charge to particles and is reported to improve diffusion through mucus barrier (DING *et al.*, 2021). TPGS (D-tocopherol acid polyethylene glycol succinate) promoted higher penetration of curcumin nanocrystals through mucus layer, proved by confocal imaging in vitro and increased bioavailability, due to electrostatic repulsion from PEG hydrophilic chains (HUANG *et al.*, 2022).

After deposition, the size and morphology of the undissolved particles also impacts susceptibility to clearance by macrophages, whose optimal range for phagocytosis is 2-3 μm (BARANOV *et al.*, 2021). Alveolar macrophages are the major immune cells in the lung, responsible for innate immune defense, clearance of pathogens and debris, maintaining tissue homeostasis, and modulation of inflammatory responses (ALLARD; PANARITI; MARTIN, 2018). To ensure exposure of the drug to cancer cells, it is crucial to prevent sequestration of

the drug by alveolar macrophages, as their engulfment can result in degradation and reduced effectiveness. Alveolar macrophages typically face challenges in engulfing particles larger than 10 μm and smaller than approximately 1 μm in diameter, although the exact threshold may vary depending on particle characteristics and lung conditions (BARANOV *et al.*, 2021). Particle shape also plays an important role in phagocytosis and subsequent activation of inflammatory cascade for degradation. Experimental evidence and theoretical predictions indicate that spherical particles are more efficiently ingested compared to particles with extreme irregularly shaped particles, as needles (BARANOV *et al.*, 2021). Rounder and smoother particles consistently showed higher efficiency of uptake compared to elongated or stretched shapes, but were also reported to show lower inflammasome triggering (BARANOV *et al.*, 2021).

Ideally, local acting drug particles would reach the tumor region and be internalized by cancer cells. But if readily solubilized, they could also have increased pulmonary absorption by healthy cells, reaching limiting dose toxicity due to high concentration peaks in lung fluids and tissues (ROSIÈRE *et al.*, 2019a); or rapidly permeate to blood vessels, reaching systemic circulation leading to adverse effects (OKUDA; OKAMOTO, 2020). In contrast, particles with low solubility or high molecular weight would be more susceptible to enzymatic degradation, or phagocytosis with subsequent lysosomal degradation and mucociliary clearance (OKUDA; OKAMOTO, 2020). Moreover, particles deposited in the alveolar region can be cleared to the lymphatic system, revealing an interesting target for metastatic cancers (PRAPHAWATVET; PETERS; WILLIAMS, 2020). It is reported that increased molecular weight particles, greater than 10-20 kDa, are more likely to be transferred to lymph nodes after macrophage sequestration (PRAPHAWATVET; PETERS; WILLIAMS, 2020). Also, radio labeled solid lipid nanoparticles (SLN) were observed in axillary and inguinal lymph nodes after inhaled administration (PRAPHAWATVET; PETERS; WILLIAMS, 2020).

Many approaches of complex formulations that can modulate charge, add tumor targeted ligands, and confer controlled released characteristics have been investigated, resulting in remarkable improvements *in vitro* and *in vivo*. But unfortunately, the pace of toxicity research studies and excipients approval for actual availability for the market do not follow the same pace.

3.2.2 Toxicity knowledge of excipients

Inhalation is recognized as a medical therapy since 1867 by British Pharmacopoeia for treatment of cough, tuberculosis, bronchitis, pharyngitis, and laryngitis (SANDERS, 2007; STEIN; THIEL, 2017), but excipient options for pulmonary delivery are still very limited

compared to oral or parenteral formulations (Table 3.1). The majority of dry powder formulations is obtained by mixing micronized API with lactose as carrier and often magnesium stearate as force control agent to reduce cohesive forces between particles and enhance inhalable fraction (YE; MA; ZHU, 2022b). However, as particle engineering is applied to improve physicochemical characteristics, new excipients are explored to meet new requirements.

α-lactose monohydrate is the most used carrier, but its susceptibility to degradation, hygroscopicity and complex solid state comprising 2 anomers, 2 anhydrous polymorphs, 1 hydrate and amorphous phase (PINTO *et al.*, 2021), stimulated the use of other excipients as mannitol, trehalose and pullulan to improve process and product properties (ZILLEN *et al.*, 2021). D-mannitol is a non-reducing sugar alcohol approved for inhalation that exhibited improvement FPF for some adhesive mixtures, and has been explored as a soluble matrix for nanoparticles in microparticles (ZILLEN *et al.*, 2021). Trehalose is also a non-reducing sugar, but unlike mannitol, it presents an amorphous state, which is explored for stabilization of protein structure and preserving other biologics integrity (CHANG; CHAN, 2022). A recent polysaccharide explored for stabilization of amorphous APIs through spray-drying due to its high glass transition temperature (261°C) is pullulan (CHANG; CHAN, 2022). Although both trehalose and pullulan are generally regarded as safe excipients, they are yet to be approved for pulmonary administration (ZILLEN *et al.*, 2021).

Examples of other excipients that have been extensively explored in preclinical research, are leucine and Poly (lactic-co-glycolic acid) (PLGA). Leucine is an essential amino acid reported to improve FPF, ED, and moisture uptake (LI, 2017). It is already approved for intravenous administration, and although not approved by FDA for inhalation yet, clinical trials indicate low toxicity risk (ZILLEN *et al.*, 2021). PLGA is one of the most explored biodegradable polymers for inhalation that confers sustained release and maintains higher concentrations in the lung (SHAH *et al.*, 2020). But its half-life of approximately 60 days can potentially lead to inflammation due to accumulation after repeated administration (YE; MA; ZHU, 2022b). PLGA like other ligands engineered for targeted nanoparticle delivery as epidermal growth factor receptor, vascular endothelial growth factor and transferrin have unknown elimination fate (ALHAJJ *et al.*, 2018). Toxicity of these substances, systemic absorption, redistribution to healthy organs and elimination is an important subject for study that will dictate the pace of translation (AHMAD *et al.*, 2015). Naturally occurring endogenous substances such as DPPC (1,2 dipalmitoyl-sn-glycero-3-phosphocholine), a phospholipid major component of lung surfactant, are promising sources of safer excipients for inhalation. It is

regarded as safe, as it presents fast metabolization, and is used to increase permeability (YE; MA; ZHU, 2022b). AIR® insulin inhalation powder and Inbrija®, the levodopa (42 mg) are examples of marketed products containing this DPPC as surfactant (YE; MA; ZHU, 2022b). Toxicity by long term use is still an potential issue even for marketed products as Afrezza®, inhaled insulin, as acute bronchospasm and wheezing are observed side effects after administration (YE; MA; ZHU, 2022b).

Regulatory Agencies such as EMA highlight the need for toxicity evaluation for inhalation not only by animal study, but also clinical safety assessment in humans (EUROPEAN MEDICINES AGENCY, 2019). The guidelines also discuss that due to the possible interaction of the API and the excipient, evaluation of the compatibility of this new combination is needed, as well as the toxicity of degradation products when applicable (FOOD AND DRUG ADMINISTRATION, 2002). Safety studies alone are expensive and demand a long period for approval, while the end product's specifications are strict regarding particle size distribution, moisture and present some particularities as amorphous content, contributing to a high cost. Therefore, these regulatory demands, the product cost and relatively small demand impair economic feasibility and make this specific market less attractive for suppliers. New research should also consider adopting fewer and better described excipients, exploring available technologies to obtain simpler and more feasible formulations.

Table 3.1. FDA-approved excipients for inhalation.

Excipient	Function	Product examples
Lactose	Stabilizing or bulking agent	UTIBRON, Armonair, Relenza®
Mannitol	Stabilizing or bulking agent	Insulin (Exubera®)
Glycine	Buffering agent	Insulin (Exubera®)
Sodium Citrate	Buffering or stabilizing agent	Insulin (Exubera®)
Sodium hydroxide	Used in manufacturing process	Insulin (Exubera®)
Polysorbate 80	Surfactant	Insulin (Technosphere Afrezza®)
Magnesium Stearate	Force control agent	Anoro, Bero® Ellipta® UTIBRON
DSPC	Surfactant	Tobi® Podhaler®
DPPC	Surfactant	AIR® insulin; Inbrija®
calcium chloride	-	Tobi® Podhaler®; Inbrija®; Dornase ALFA, (Pulmozyme®)
sodium chloride	-	Inbrija®

Source: elaborated by the author.

3.2.3 Pitfalls in current evaluation methods

The third challenge regarding formulation, besides lung physiology and excipient toxicity knowledge, is the limitation of current available methods performance evaluation, from aerosolization to efficacy evaluation.

3.2.3.1 Aerosolization performance and *in vivo* correlation

Aerosolization performance is mainly analyzed by compendial methods according to USP 601, that defines concepts as fine particle fraction (FPF), emitted dose (ED), median aerodynamic diameter (MMAD) and geometric standard deviation (GSD). These values are obtained by analysis that can be performed in different apparatus, but the most used and reliable described in US Pharmacopeia are the Andersen cascade impactor (ACI) and Next generation impactor (NGI) (THE UNITED STATES PHARMACOPEIA, 2007a). Cascade impaction test

is a common test demanded by many regulatory agencies, as ANVISA, FDA, EMA, and Japanese Pharmacopeia, and determines aerodynamic size distribution by separating aerosol particles and droplets from a moving airstream generated by a vacuum pump based on particle inertia. Although mainly described for quality control purposes, determining batch-to-batch consistency by variation of delivered doses, they are also extensively used for development, to determine if the formulation could meet desired characteristics for efficient delivery (RUZYCKI *et al.*, 2022). The main issues in this practice are the poor *in vitro-in vivo* correlation and the lack of standardization of the methodology that hamper comparison between different studies (RUZYCKI *et al.*, 2022).

As the apparatus are simplified versions of respiratory tract, they poorly replicate mouth-throat sequestration or extra-thoracic deposition, overestimating lung dose deposition (LEUNG *et al.*, 2015). A study evaluating different mouth-throat models found that flow condition and model geometry had a direct impact over deposited doses (WEI *et al.*, 2018). Although it is reported that some devices with higher resistance (Easyhaler) could be less susceptive to airflow variations and provide a more accurate in vivo correlation with conventional pharmacopeial methods (RUZYCKI *et al.*, 2022), in order to improve *in vivo* correlation, realistic throat models as Alberta Idealized Throat – Copley; Virginia Commonwealth University models; and oropharyngeal consortium (OPC) models can be adopted (WEI *et al.*, 2018). Nevertheless, Leung et. al. reported possible artifacts from cascade analysis using Alberta throats and US Pharmacopeia throat, as they favored de-agglomeration for some formulations and inhalers, and even when coated with silicon to prevent rebounding, *in vivo* correlation was not constant throughout the nine tested devices (LEUNG *et al.*, 2015).

Time interval between doses, coating and airflow can impact significantly FPF results (RUZYCKI *et al.*, 2022). Particle deposition is subjected to different forces of inertial impaction, sedimentation and diffusion (DEMOLY *et al.*, 2014). Smaller particles in the range of 1.5 μm, for example, have extremely low settling velocity by sedimentation, and can have higher variation upon lower interval times (DEMOLY *et al.*, 2014). Also, the lack of coating with silicon oil or glycerol can contribute to inaccurate plate deposition due to particle bounce and re-entrainment (COPLEY, 2018). Ohar et al. evaluated FPF and MMDA of tiotropium delivered by HandiHaler® through different breathing patterns and observed direct increase in FPF and decrease in MMDA for higher airflows (OHAR *et al.*, 2020). The apparatus variation also do not show a direct correlation, as it was reported that similarity in the results could be observed for pMDI in NGI and ACI for lower flow rates (28.3 and 30 L/min), the equivalence was not observed for higher airflows, as 60 L/min (GUO *et al.*, 2008). A comparative evaluation

published by Yoshida et. al (YOSHIDA *et al.*, 2017) between NGI and ACI for four DPI products Relenza® (GlaxoSmithKline Co.), Seebri® (Novartis Pharma Co.), Pulmicort® (Astrazeneca Co.), and Spiriva® reported significant differences in the obtained MMDA results. For Pulmicort® (Tubuhaler®), a decrease in MMDA was observed when increasing flow rate from 30 to 90 L/min for NGI, whose results were smaller than those obtained for ACI at 28.3, 45, and 60 L/min (YOSHIDA *et al.*, 2017). It is important to clarify that when standardized and validated, a fair correlation between different apparatus, as abbreviated impactors and pharmacopeial impactors (NGI or ACI) can be established, as shown in a multi-laboratory study for 5 different orally inhaled products (NICHOLS *et al.*, 2016), but there is still room for *in vitro-in vivo* correlation improvement.

3.2.3.2 *In vitro* evaluation vs tumor environment and current protocols

Lung cancer cell lines were first successfully obtained by John Minna and Adi Gazdar in 1970s and currently more than 200 lung cancer cell lines are available (POLITI; DELA CRUZ; HOMER, 2014). Since cell lines are immortalized lineages, with high purity, short period for culture and homogenous expression, they can be easily adopted in many laboratories due to the cost and reproducibility (HUO; D'ARCANGELO; TSAO, 2020). Cell lines are particularly important for types of cancer with increased difficulty to obtain patient cells through biopsy, such as small cell lung cancer (SCLC). SCLC patients rarely undergo surgical resection and the material collected in those procedures are scarce and would have limited chances to result in viable cultures (GAZDAR *et al.*, 2010). Patient derived primary cells obtained from biopsies could be an interesting guiding tool for personalized treatment decisions (HUO; D'ARCANGELO; TSAO, 2020). In vitro assessment with cell lines is effective as a screening step for new drugs and formulations but cannot accurately predict in vivo efficacy. Tumor microenvironment plays an important role in responses to treatment, and have been reverse translated to intricate approaches: 3-D cultures, co-culture systems (organoids), organ-on-a-chip and patient-derived xenografts (HUO; D'ARCANGELO; TSAO, 2020).

In 2009 the first organoid derived from a single stem cell was obtained, and presented capacity for self-proliferation and differentiation (XIA *et al.*, 2019). In the same year, tracheospheres were obtained from airway basal stem cells, capable of self-renewing and differentiating to airway mucociliary cell types (SEN; FREUND; GOMPERTS, 2022). Co-culture of multiple cell types provided ways to investigate mechanisms as angiogenesis. Kniebs et al. cultivated human umbilical vein endothelial cells, with mesenchymal stem cells and lung cancer cells A549 (KNIEBS *et al.*, 2021). Using fibrin gel as basis, although a direct interaction

between cancer cells and vascular structures was not established, the later exhibited significant elongation as responses to hypoxic conditions, which led to increased resistance to treatment with gefitinib and paclitaxel in comparison to 2-D cultures (KNIEBS *et al.*, 2021). Lung epithelial-endothelial monolayers in contact with a semipermeable membrane exposed to air and fluid were proven to serve as a model for pathologies as inflammation and pulmonary edema, useful for drug screening (SKARDAL; SHUPE; ATALA, 2016).

A comprehensive research reported the creation of a biobank composed of 80 lung cancer organoids (KIM *et al.*, 2019). Kim et al. described successful protocols of approximately 4 weeks for the establishment of the organoids, proving the feasibility of the application of an organoid culture for personalized cancer medicine. In the same year, a case report described the capacity of patient-derived tumor spheroids to mimic the outcomes of the given treatments. A 3D culture was established from the surgery of a lung adenocarcinoma, stage III patient and reflected the same drug sensitivity to cisplatin-based chemotherapy and anti-programmed death 1 drug pembrolizumab and preserved immunological and genetic profile (DI LIELLO *et al.*, 2019). Together, these studies prove the applicability of patient-derived organoids to precision medicine and as a clinical reverse translated research tool (DI LIELLO *et al.*, 2019).

Further evolution of organoids is the model that aimed for replication of integrated organs response, the organ-on-a-chip. This system combines multiple 3D tissue architectures with a microfluidic device, integrating, for example, cardiac, liver and lung, which could anticipate toxicological screenings in the future (SKARDAL *et al.*, 2017). Technologies such as 3D bioprinting can accelerate the process and add geometric complexity to mimic real tissues (MATAI *et al.*, 2020). There are different modalities for 3D bioprinting, and while the most understood one mimics would be a conventional desktop printer, with bioinks dispensing 10^4-30^4 cells per droplet, the most used one is the extrusion-based bioprinting (MATAI *et al.*, 2020). Piston or rotating screw is used to push more viscous bioinks from the plastic syringes as cylindrical filaments onto sterile substrates (MATAI *et al.*, 2020). Choi et al. fabricated vascularized lung cancer organoids by extrusion approach that enabled cancer cell-matrix and cancer cell-stromal interactions to evaluate response to gefitinib and poziotinib (CHOI *et al.*, 2023). Stromal, vascular and lung cancer cells with pulmonary fibrosis-derived lung fibroblasts composed a complex bioprinted tissue used as a fibrosis model, that exhibited increased cell proliferation and drug resistance compared with non-fibrotic lung cancer model (CHOI *et al.*, 2023).

Although those advancements in cellular *in vitro* models are promising, a challenge for inhalable dry powders is the method adopted for drug sample preparation before cell exposure.

Dry powders sample preparation often involves previous dispersion in water (TULBAH; GAMAL, 2021) and even small amounts of DMSO or solvents to the stock solution (LEE *et al.*, 2020) before cell exposure. Since these additional solubilizing agents are not present in the formulation, it can hamper analysis, overestimating the potential cytotoxicity. This methodology also precludes evaluation of particle size and shape, which are important attributes for this route of administration, as discussed earlier. Strategies that could be applied to improve these protocols were not extensively explored for cellular analysis, but rather for dissolution methods. In contrast to previously solubilizing or resuspending the formulation, an alternative method could consist in previous aerosolization of the formulation using ACI and NGI directly into modified vessels, filters or membranes, as proposed before dissolution evaluation in USP Apparatus 2 or Franz diffusion cell (VELAGA *et al.*, 2018). Dissolution of inhalable formulations is a controversial subject, since it has not been clearly demonstrated that it is a critical attribute. Given the amount of liquid in the lungs and its complex composition of endogenous surfactants, the replication and development of protocols is a difficult challenge (FORBES; RICHER; BUTTINI, 2015; NOKHODCHI; CHAVAN; GHAFOURIAN, 2023; VELAGA *et al.*, 2018).

3.2.3.3 Efficacy assessment: *in vivo* cost-benefit balance

For many administration routes as oral and intravenous, *in vivo* models can be considered gold standard for systemic evaluation of drug effect, but protocols for inhalable formulations present inherent artifacts that can result in biased interpretations. Anatomical characteristics and respiratory parameters differ considerably inter-species, from nose turbinates' structures that impact internal air turbulence; to general airway branching structure (dichotomous for humans versus monopodial for small rodents) that can alter airflow speed, direction and, thus the overall mechanism of particle deposition (GUILLON *et al.*, 2018). Small rodents are nose only compulsive breathers, with a respiration rate of 162 breaths/min for mice, while larger mammals as primates, dogs and pigs are nose and mouth breathers, presenting lower rates, as 12 for humans and 20 breaths/min for pigs (GUILLON *et al.*, 2018). Therefore, from the start, extrapolation of deposition results obtained for other species to human prediction is very challenging.

Drugs can be administered through facemasks and inhalation chambers, but exhibit expressive drug losses (WANG *et al.*, 2014) and can be challenging to determine the relation between dispensed dose, inhaled amount and final deposited fraction. One of the most reported methods for dry powder administration is intratracheal administration or instillation through the

device Aerosolizer and Dry Powder Insufflator™ (from Penn-Century Inc., US). This method is invasive, requiring administration of anesthetics and can present tolerability issues, causing inflammation and lung lesions (GUILLON *et al.*, 2018). Besides, it can overestimate deposition, since it forces particles that could not naturally reach deep respiratory tract if orally inhaled (CURBANI *et al.*, 2019). It is worth mentioning that Penn-Century's patented devices are no longer available, as the Company was closed in 2015. Alternatives have been explored, as adaptations of syringe with a 20-guage needle, published methods can involve additional steps before instillation, as suspension in saline (CHENNAKESAVULU *et al.*, 2018), possibly to avoid clogging. This type of manipulation of a DPI can also add uncertainty to the protocol, hindering the evaluation of the influence of aerodynamic properties in lung deposition and consequent efficacy conclusions. A more recent device commercialized by Aptar® is the PADA (Powder Administration Device for Animals) has the purpose to directly to the lungs of mice, supporting preclinical studies of powders for inhalation.

Protocols for lung cancer evaluation in animals can be very distinct: intravenous our subcutaneous administration of cancer cells; exposure to carcinogens as tobacco smoke; intravenous injection of chemical carcinogens as urethane; or multiple intra-tracheal injections of the carcinogen 3-methylcholanthrene (HYNDS *et al.*, 2021). Unfortunately, most of those protocols result in extra-lung tumors and are not applicable for evaluation of inhaled drugs. Genetically engineered mouse models (GEMM) can generate multiple small tumors in the lung, but the difference of lifespan translates in different disease evolution (HYNDS *et al.*, 2021). Response to treatments has already been reported to differ in some cases, as GEMMs small cell lung cancer (SCLC) demonstrate no sensitivity to platinum-etoposide chemotherapy (BUNN *et al.*, 2016).

Naturally an animal lung cancer model should meet the core question of the research, and *in vivo* experiments provide invaluable information that can be later used for *in silico* modeling and building of pharmacokinetic knowledge. But regarding efficacy evaluation of inhalable dry powders for lung tumor treatment, we believe *in vivo* evaluation should be conducted only after deep *in vitro* evaluation in distinct and more complex models. A cost-benefit analysis is required considering the number of animals required to obtain a statistical significance; the invasiveness of protocols either to establish an adequate and relevant lung cancer model and to administer multiple doses of the formulation; opposed to the numerous artifacts that follow those protocols, and the expected confirmation.

3.3 DEVICES AND PATIENTS

Since most of DPI devices are passive, relying on patients' inspiratory flow to provide energy for deagglomeration (RUZYCKI *et al.*, 2022), the breathing pattern, gender, age and training about the inhalation maneuver can influence the delivery (DELVADIA *et al.*, 2016; HICKEY, 1992; LAUBE *et al.*, 2011). DPI global market size was worth USD 19.66 billion in 2022 and is expected to grow to USD 27.98 billion in 2032 (REPORTS AND DATA, 2023). Spinhaler (Fisons Pharmaceuticals) was the first launched capsule inhaler in 1967, and since then innovative designs are patented, stimulating continuous development and launching of new devices, that sum up over 40 models that reached the market (DE BOER; HAGEDOORN; GRASMEIJER, 2022). Although the variety of devices reflect advances in performance improvement, differences in design and maneuver, it can also serve as distraction to doctors from evaluating other important characteristics, and lead patients to errors during administration when changing medications (CLARK, ANDREW R.; WEERS, JEFFRY G.; RAJIV DHAND, 2020). Conventional DPI devices consist in a chamber that receives the capsule containing the formulation and hidden needles that are activated by the patient, puncture the capsule, releasing the powder upon inhalation through a mouthpiece. They can be classified according to the number of doses in single-unit dose inhalers as Aerolizer ®, multi-unit dose inhalers as Diskus®, and multidose reservoir-inhalers as Turbuhaler® (YE; MA; ZHU, 2022b). The advantages of multi-dose inhalers are the lower number of steps to inhalation, decreasing misusage possibilities and reducing patient direct contact with the API, important for safety regarding cytotoxic drugs. Nevertheless, the use of single-use disposable devices is also interesting to ensure best device conditions such as cleanness and adequate storage from humidity and contamination.

For lung cancer patients, depending on the stage of the disease, the respiratory capacity could be an important limitation for the extent of benefit of inhaled treatment (KOSMIDIS *et al.*, 2019a). But it is a misconception that only patients with a good inspiratory capacity are able to effectively use those devices, as most of DPIs currently available in the market were intended for patients with asthma or chronic obstructive pulmonary disease (COPD) (BERKENFELD; LAMPRECHT; MCCONVILLE, 2015). Devices present a specific resistance to airflow due to the differences in internal compartments, as needle position and caliber and design of swirl chambers and grids (Clark, Andrew R. et al., 2020). Since it does not present propellant, the

only force that will promote the fluidization of the powder inside the capsule is the air turbulence generated by patient aspiration (YE; MA; ZHU, 2022b). It could be intuitive to propose that larger pressure drops (faster inhalations) and higher flow rates (inhalation of higher amount of air) would result in better deagglomeration and increased lung deposition, but it is not always right, as illustrated in Figure 3.1 (CLARK, ANDREW R.; WEERS, JEFFRY G.; RAJIV DHAND, 2020). Powder dispersion is generally benefited by pressure drop because of the turbulence generated by the airflow, but with a higher airflow the deposition in the oropharyngeal region increases due to inertial impaction (CLARK, ANDREW R.; WEERS, JEFFRY G.; RAJIV DHAND, 2020). Different studies show that many devices with high and medium airflow resistance can perform well in a range of 2 to 4 kPa pressure drop, which corresponds to an airflow achievable even for a severe COPD patient (HOPPENTOCHT *et al.*, 2014). Higher resistant devices seem to provide the necessary pressure drop easier than low resistance ones, and also provide more effective powder redispersion (CLARK, ANDREW R.; WEERS, JEFFRY G.; RAJIV DHAND, 2020). In contrast, devices with low airflow resistance are preferred by patients, and can improve compliance with the treatment (CLARK, ANDREW R.; WEERS, JEFFRY G.; RAJIV DHAND, 2020). A comparison of pressure drop and airflow with 6 different devices showed a clear division between group with marked increased FPF with increase in pressure drop for medium/high resistance (Symbicort Turbohaler, Novolizer and Easyhaler) and a group with constant FPF for low or medium/low resistance devices (Cyclohaler, Seretide Diskus and Rolenium Elpenhaler) (DEMOLY *et al.*, 2014).

Figure 3.1. Lung dose versus pressure drop for commercial DPIs. (A) In vivo data determined by gamma scintigraphy or pharmacokinetics. (B) In vitro data determined by cascade impactors or mouth/oropharyngeal models.
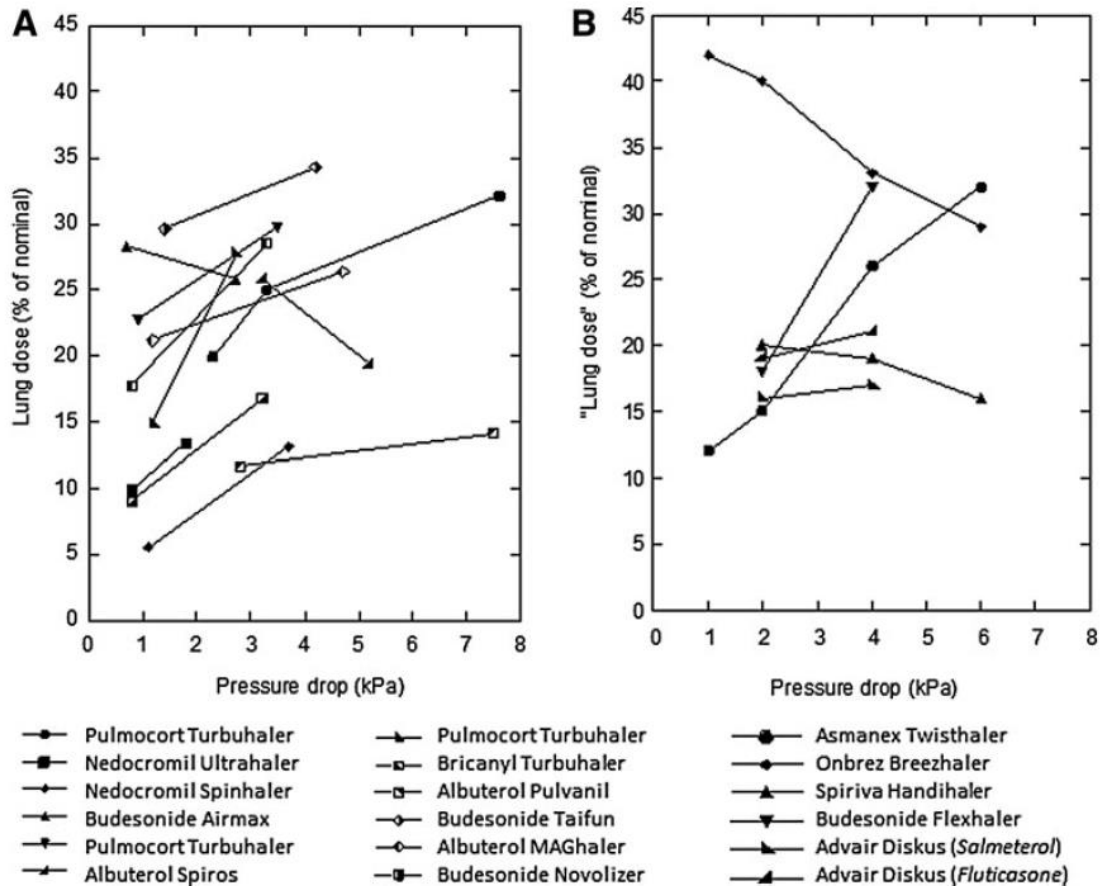
Source: reproduced with permission of (CLARK, ANDREW R.; WEERS, JEFFRY G.; RAJIV DHAND, 2020).

Device is a vital factor for effective delivery, and for the above-mentioned reasons, they are not interchangeable. Thalberg et. al. compared the performance of three reservoir type devices: Novopulmon Novolizer®, DuoResp Spiromax® and Giona Easyhaler® by opening each one and interchanging budesonide formulations (THALBERG *et al.*, 2023). The first two devices presenting cyclone-type geometries presented more favorable aerosolization capacity, in comparison to the straight outlet type (Easyhaler). The same budesonide formulation from Giona Easyhaler presented a difference in FPF of 18% to 51% when evaluated at the original device and Spiromax device, respectively (THALBERG *et al.*, 2023). At the same time, Novolizer formulation presenting 47% FPF in the original device, changed drastically to 2% FPF in the Easyhaler device (THALBERG et al., 2023). This study exemplifies the impact of design on dispersion of the formulation, as cyclone-type geometries resulted in significant improvement of FPF when compared to Easyhaler.

The deposition efficacy of current available devices is relatively low, and errors in maneuver combined with patient compliance already result in complications for COPD and asthma patients, but these challenges must be overcome to help translation of inhalable cancer treatment. Advances regarding the activation by breathing were achieved through Digihaler®, that records usage data that is relevant to clinical follow up, as date and time of usage as well as flow volume and peak inspiratory flow, and can also remind administration time to improve compliance with treatment (MOHAN *et al.*, 2022). Active devices with aerosolization independent of patients' inspiratory capacity have been developed with addition of external energy sources, like compressed air (Exubera from Pfizer), electricity (Spiros from Dura) or thermal energy (Adasuve from Alexza) (DE BOER; HAGEDOORN; GRASMEIJER, 2022). This mechanisms can help delivering medication with improved dose consistency, facilitating administration to patients with impaired lung function (YE; MA; ZHU, 2022b).

3.4 CONCLUSION

Self-administered chemotherapy through a DPI at the patient's own house, instead of hours at the hospital for infusions, with increased treatment response and reduced adverse effects. This modality of treatment would certainly contribute to patients' compliance and increase the quality of life. The potential is real, but the challenges to be faced are numerous: to deepen comprehension of fate of particles after administration, performing toxicity studies of excipients, investing in protocols for performance evaluation and *in vitro-in vivo* correlation, and in device improvement. While this knowledge is built, the rationale of formulation development of DPIs could also pivot towards the use of fewer components, aiming for optimization of particle characteristics through exploration of available technology.

3.5 REFERENCES

AHMAD, J.; AKHTER, S.; RIZWANULLAH, M.; AMIN, S.; RAHMAN, M.; AHMAD, M. Z.; RIZVI, M. A.; KAMAL, M. A.; AHMAD, F. J. Nanotechnology-Based Inhalation Treatments for Lung Cancer: State of the Art. **Nanotechnology, Science and Applications**, v. 8, p. 55–66, 2015.

AI, X.; GUO, X.; WANG, J.; STANCU, A. L.; JOSLIN, P. M. N.; ZHANG, D.; ZHU, S. Targeted Therapies for Advanced Non-Small Cell Lung Cancer. v. 9, p. 19, 2018.

ALHAJJ, N.; CHEE, C. F.; WONG, T. W.; RAHMAN, N. A.; ABU KASIM, N. H.; COLOMBO, P. Lung Cancer: Active Therapeutic Targeting and Inhalational Nanoproduct Design. **Expert Opinion on Drug Delivery**, v. 15, n. 12, p. 1223–1247, 2018.

ALLARD, B.; PANARITI, A.; MARTIN, J. G. Alveolar Macrophages in the Resolution of Inflammation, Tissue Repair, and Tolerance to Infection. **Frontiers in Immunology**, v. 9, p. 1777, 31 jul. 2018.

BARANOV, M. V.; KUMAR, M.; SACANNA, S.; THUTUPALLI, S.; VAN DEN BOGAART, G. Modulation of Immune Responses by Particle Size and Shape. **Frontiers in Immunology**, v. 11, p. 607945, 12 fev. 2021.

BERKENFELD, K.; LAMPRECHT, A.; MCCONVILLE, J. T. Devices for Dry Powder Drug Delivery to the Lung. **AAPS PharmSciTech**, v. 16, n. 3, p. 479–490, jun. 2015.

BUNN, P. A.; MINNA, J.; AUGUSTYN, A.; GAZDAR, A.; OUADAH, Y.; KRASNOW, M. A.; BERNS, A.; BRAMBILLA, E.; REKHTMAN, N.; MASSION, P. P.; NIEDERST, M.; PEIFER, M.; YOKOTA, J.; GOVINDAN, R.; POIRIER, J.; BYERS, L. A.; WYNES, M. W.; MCFADDEN, D.; MACPHERSON, D.; HANN, C. L.; FARAGO, A. F.; DIVE, C.; TEICHER, B. A.; PEACOCK, C.; JOHNSON, J. E.; COBB, M. H.; WENDEL, H.-G.; SPIGEL, D.; SAGE, J.; YANG, P.; PIETANZA, M. C.; KRUG, L. M.; HEYMACH, J.; UJHAZY, P.; ZHOU, C.; GOTO, K.; DOWLATI, A.; CHRISTENSEN, C. L.; PARK, K.; EINHORN, L. H.; EDELMAN, M. J.; GIACCONE, G.; GERBER, D. E.; SALGIA, R.; OWONIKOKO, T.; MALIK, S.; KARACHALIOU, N.; GANDARA, D. R.; SLOTMAN, B. J.; BLACKHALL, F.; GOSS, G.; THOMAS, R.; RUDIN, C. M.; HIRSCH, Fred. R. Small Cell Lung Cancer: Can recent advances in biology and molecular biology be translated into improved outcomes? **Journal of thoracic oncology : official publication of the International Association for the Study of Lung Cancer**, v. 11, n. 4, p. 453–474, abr. 2016.

CHANG, R. Y. K.; CHAN, H.-K. Advancements in Particle Engineering for Inhalation Delivery of Small Molecules and Biotherapeutics. **Pharmaceutical Research**, v. 39, n. 12, p. 3047–3061, 1 dez. 2022.

CHENNAKESAVULU, S.; MISHRA, A.; SUDHEER, A.; SOWMYA, C.; SURYAPRAKASH REDDY, C.; BHARGAV, E. Pulmonary Delivery of Liposomal Dry Powder Inhaler Formulation for Effective Treatment of Idiopathic Pulmonary Fibrosis. **Asian Journal of Pharmaceutical Sciences**, v. 13, n. 1, p. 91–100, jan. 2018.

CHOI, Y.; LEE, H.; ANN, M.; SONG, M.; RHEEY, J.; JANG, J. 3D Bioprinted Vascularized Lung Cancer Organoid Models with Underlying Disease Capable of More Precise Drug Evaluation. **Biofabrication**, v. 15, n. 3, p. 034104, 1 jul. 2023.

CLARK, ANDREW R.; WEERS, JEFFRY G.; RAJIV DHAND. **The Confusing World of Dry Powder Inhalers: It Is All About Inspiratory Pressures, Not Inspiratory Flow Rates**. Disponível em: <https://www.liebertpub.com/doi/epdf/10.1089/jamp.2019.1556>. Acesso em: 26 jul. 2023.

COPLEY. **Variability in Cascade Impaction: Sources, Impact and Strategies for Reduction**ONdrugDelivery Magazine, nov. 2018. Disponível em: <https://www.ondrugdelivery.com/variability-in-cascade-impaction-sources-impact-and-strategies-for-reduction/>. Acesso em: 11 ago. 2023.

CURBANI, F.; DE OLIVEIRA BUSATO, F.; MARCARINI DO NASCIMENTO, M.; OLIVIERI, D. N.; TADOKORO, C. E. Inhale, Exhale: Why Particulate Matter Exposure in Animal Models Are so Acute? Data and Facts behind the History. **Data in Brief**, v. 25, p. 104237, ago. 2019.

CZECHTIZKY, W.; SU, W.; RIPA, L.; SCHIESSER, S.; HÖIJER, A.; COX, R. J. Advances in the design of new types of inhaled medicines. *Em*: **Progress in Medicinal Chemistry**. [s.l.] Elsevier, 2022. p. 93–162.

72

DE BOER, A. H.; HAGEDOORN, P.; GRASMEIJER, F. Dry Powder Inhalation, Part 2: The Present and Future. **Expert Opinion on Drug Delivery**, v. 19, n. 9, p. 1045–1059, 2 set. 2022.

DELVADIA, R. R.; WEI, X.; LONGEST, P. W.; VENITZ, J.; BYRON, P. R. *In Vitro* Tests for Aerosol Deposition. IV: Simulating Variations in Human Breath Profiles for Realistic DPI Testing. **Journal of Aerosol Medicine and Pulmonary Drug Delivery**, v. 29, n. 2, p. 196–206, abr. 2016.

DEMOLY, P.; HAGEDOORN, P.; DE BOER, A. H.; FRIJLINK, H. W. The Clinical Relevance of Dry Powder Inhaler Performance for Drug Delivery. **Respiratory Medicine**, v. 108, n. 8, p. 1195–1203, 1 ago. 2014.

DI LIELLO, R.; CIARAMELLA, V.; BARRA, G.; VENDITTI, M.; DELLA CORTE, C. M.; PAPACCIO, F.; SPARANO, F.; VISCARDI, G.; IACOVINO, M. L.; MINUCCI, S.; FASANO, M.; CIARDIELLO, F.; MORGILLO, F. Ex Vivo Lung Cancer Spheroids Resemble Treatment Response of a Patient with NSCLC to Chemotherapy and Immunotherapy: Case Report and Translational Study. **ESMO Open**, v. 4, n. 4, p. e000536, 2019.

DING, L.; TANG, S.; WYATT, T. A.; KNOELL, D. L.; OUPICKÝ, D. Pulmonary SiRNA Delivery for Lung Disease: Review of Recent Progress and Challenges. **Journal of Controlled Release**, v. 330, p. 977–991, fev. 2021.

EL-SHERBINY, I. M.; EL-BAZ, N. M.; YACOUB, M. H. Inhaled Nano- and Microparticles for Drug Delivery. **Global Cardiology Science and Practice**, v. 2015, n. 1, p. 2, jan. 2015.

EUROPEAN MEDICINES AGENCY. **GUIDELINE ON THE REQUIREMENTS FOR CLINICAL DOCUMENTATION FOR ORALLY INHALED PRODUCTS (OIP) INCLUDING THE REQUIREMENTS FOR DEMONSTRATION OF THERAPEUTIC EQUIVALENCE BETWEEN TWO INHALED PRODUCTS FOR USE IN THE TREATMENT OF ASTHMA AND CHRONIC OBSTRUCTIVE PULMONARY DISEASE (COPD) IN ADULTS AND FOR USE IN THE TREATMENT OF ASTHMA IN CHILDREN AND ADOLESCENTS**jan. 2019. Disponível em: <https://www.ema.europa.eu/en/documents/scientific-guideline/guideline-requirements-clinical-documentation-orally-inhaled-products-including-requirements_en.pdf>. Acesso em: 22 ago. 2021.

FOOD AND DRUG ADMINISTRATION. **Nasal Spray and Inhalation Solution, Suspension, and Spray Drug Products — Chemistry, Manufacturing, and Controls Documentation**jul. 2002. . Acesso em: 21 ago. 2021.

FORBES, B.; RICHER, N. H.; BUTTINI, F. Dissolution: A Critical Performance Characteristic of Inhaled Products? *Em*: **Pulmonary Drug Delivery**. [s.l.] John Wiley & Sons, Ltd, 2015. p. 223–240.

GAZDAR, A. F.; GIRARD, L.; LOCKWOOD, W. W.; LAM, W. L.; MINNA, J. D. Lung Cancer Cell Lines as Tools for Biomedical Discovery and Research. **JNCI: Journal of the National Cancer Institute**, v. 102, n. 17, p. 1310–1321, 8 set. 2010.

GRONEBERG, D. A.; WITT, C.; WAGNER, U.; CHUNG, K. F.; FISCHER, A. Fundamentals of Pulmonary Drug Delivery. **Respiratory Medicine**, v. 97, n. 4, p. 382–387, abr. 2003.

GUILLON, A.; SÉCHER, T.; DAILEY, L. A.; VECELLIO, L.; DE MONTE, M.; SI-TAHAR, M.; DIOT, P.; PAGE, C. P.; HEUZÉ-VOURC'H, N. Insights on Animal Models to Investigate Inhalation Therapy: Relevance for Biotherapeutics. **International Journal of Pharmaceutics**, v. 536, n. 1, p. 116–126, jan. 2018.

GUO, C.; GILLESPIE, S. R.; KAUFFMAN, J.; DOUB, W. H. Comparison of Delivery Characteristics from a Combination Metered-Dose Inhaler Using the Andersen Cascade Impactor and the Next

Generation Pharmaceutical Impactor. **Journal of Pharmaceutical Sciences**, v. 97, n. 8, p. 3321–3334, ago. 2008.

HADIWINOTO, G. D.; LIP KWOK, P. C.; LAKERVELD, R. A Review on Recent Technologies for the Manufacture of Pulmonary Drugs. **Therapeutic Delivery**, v. 9, n. 1, p. 47–70, jan. 2018.

HAMISHEHKAR, H.; RAHIMPOUR, Y.; JAVADZADEH, Y. The Role of Carrier in Dry Powder Inhaler. *Em*: SEZER, A. D. **Recent Advances in Novel Drug Carrier Systems**. [s.l.] InTech, 2012.

HE, S.; GUI, J.; XIONG, K.; CHEN, M.; GAO, H.; FU, Y. A Roadmap to Pulmonary Delivery Strategies for the Treatment of Infectious Lung Diseases. **Journal of Nanobiotechnology**, v. 20, n. 1, p. 101, dez. 2022.

HICKEY, A. J. **Pharmaceutical Inhalation Aerosol Technology**. 2. ed. [s.l.] Marcel Dekker, Incorporated, 1992. v. 56365 p.

HOPPENTOCHT, M.; HAGEDOORN, P.; FRIJLINK, H. W.; DE BOER, A. H. Technological and Practical Challenges of Dry Powder Inhalers and Formulations. **Advanced Drug Delivery Reviews**, v. 75, p. 18–31, ago. 2014.

HUANG, G.; SHUAI, S.; ZHOU, W.; CHEN, Y.; SHEN, B.; YUE, P. To Enhance Mucus Penetration and Lung Absorption of Drug by Inhalable Nanocrystals-In-Microparticles. **Pharmaceutics**, v. 14, n. 3, p. 538, 28 fev. 2022.

HUO, K.-G.; D'ARCANGELO, E.; TSAO, M.-S. Patient-Derived Cell Line, Xenograft and Organoid Models in Lung Cancer Therapy. **Translational Lung Cancer Research**, v. 9, n. 5, p. 2214–2232, out. 2020.

HYNDS, R. E.; FRESE, K. K.; PEARCE, D. R.; GRÖNROOS, E.; DIVE, C.; SWANTON, C. Progress towards non-small-cell lung cancer models that represent clinical evolutionary trajectories. **Open Biology**, v. 11, n. 1, p. 200247, 13 jan. 2021.

KIM, I.; BYEON, H. J.; KIM, T. H.; LEE, E. S.; OH, K. T.; SHIN, B. S.; LEE, K. C.; YOUN, Y. S. Doxorubicin-Loaded Highly Porous Large PLGA Microparticles as a Sustained- Release Inhalation System for the Treatment of Metastatic Lung Cancer. **Biomaterials**, v. 33, n. 22, p. 5574–5583, ago. 2012.

KIM, M.; MUN, H.; SUNG, C. O.; CHO, E. J.; JEON, H.-J.; CHUN, S.-M.; JUNG, D. J.; SHIN, T. H.; JEONG, G. S.; KIM, D. K.; CHOI, E. K.; JEONG, S.-Y.; TAYLOR, A. M.; JAIN, S.; MEYERSON, M.; JANG, S. J. Patient-Derived Lung Cancer Organoids as in Vitro Cancer Models for Therapeutic Screening. **Nature Communications**, v. 10, n. 1, p. 3991, 5 set. 2019.

KNAP, K.; KWIECIEŃ, K.; RECZYŃSKA-KOLMAN, K.; PAMUŁA, E. Inhalable microparticles as drug delivery systems to the lungs in a dry powder formulations. **Regenerative Biomaterials**, v. 10, p. rbac099, 8 dez. 2022.

KNIEBS, C.; LUENGEN, A. E.; GUENTHER, D.; CORNELISSEN, C. G.; SCHMITZ-RODE, T.; JOCKENHOEVEL, S.; THIEBES, A. L. Establishment of a Pre-Vascularized 3D Lung Cancer Model in Fibrin Gel—Influence of Hypoxia and Cancer-Specific Therapeutics. **Frontiers in Bioengineering and Biotechnology**, v. 9, p. 761846, 14 out. 2021.

KOSMIDIS, C.; SAPALIDIS, K.; ZAROGOULIDIS, P.; SARDELI, C.; KOULOURIS, C.; GIANNAKIDIS, D.; PAVLIDIS, E.; KATSAOUNIS, A.; MICHALOPOULOS, N.; MANTALOBAS, S.; KOIMTZIS, G.; ALEXANDROU, V.; TSIOUDA, T.; AMANITI, A.; KESISOGLOU, I. Inhaled Cisplatin for NSCLC: Facts and Results. **International Journal of Molecular Sciences**, v. 20, n. 8, p. 2005, 24 abr. 2019.

KUZMOV, A.; MINKO, T. Nanotechnology Approaches for Inhalation Treatment of Lung Diseases. **Journal of Controlled Release**, v. 219, p. 500–518, dez. 2015.

LAUBE, B. L.; JANSSENS, H. M.; DE JONGH, F. H. C.; DEVADASON, S. G.; DHAND, R.; DIOT, P.; EVERARD, M. L.; HORVATH, I.; NAVALESI, P.; VOSHAAR, T.; CHRYSTYN, H. What the Pulmonary Specialist Should Know about the New Inhalation Therapies. **European Respiratory Journal**, v. 37, n. 6, p. 1308–1417, 1 jun. 2011.

LEE, W.-H.; LOO, C.-Y.; TRAINI, D.; YOUNG, P. M. Development and Evaluation of Paclitaxel and Curcumin Dry Powder for Inhalation Lung Cancer Treatment. **Pharmaceutics**, v. 13, n. 1, p. 9, 22 dez. 2020.

LEUNG, S. S. Y.; TANG, P.; ZHOU, Q.; TONG, Z.; LEUNG, C.; DECHARAKSA, J.; YANG, R.; CHAN, H.-K. De-Agglomeration Effect of the US Pharmacopeia and Alberta Throats on Carrier-Based Powders in Commercial Inhalation Products. **The AAPS Journal**, v. 17, n. 6, p. 1407–1416, nov. 2015.

LI, L. Investigation of L-Leucine in Reducing the Moisture-Induced Deterioration of Spray-Dried Salbutamol Sulfate Power for Inhalation. **International Journal of Pharmaceutics**, 2017.

LOIRA-PASTORIZA, C.; TODOROFF, J.; VANBEVER, R. Delivery Strategies for Sustained Drug Release in the Lungs. **Advanced Drug Delivery Reviews**, v. 75, p. 81–91, ago. 2014.

MATAI, I.; KAUR, G.; SEYEDSALEHI, A.; MCCLINTON, A.; LAURENCIN, C. T. Progress in 3D Bioprinting Technology for Tissue/Organ Regenerative Engineering. **Biomaterials**, v. 226, p. 119536, jan. 2020.

MOHAN, A. R.; WANG, Q.; DHAPARE, S.; BIELSKI, E.; KAVIRATNA, A.; HAN, L.; BOC, S.; NEWMAN, B. Advancements in the Design and Development of Dry Powder Inhalers and Potential Implications for Generic Development. **Pharmaceutics**, v. 14, n. 11, p. 2495, 17 nov. 2022.

NEWMAN, S. P. Delivering Drugs to the Lungs: The History of Repurposing in the Treatment of Respiratory Diseases. **Advanced Drug Delivery Reviews**, v. 133, p. 5–18, ago. 2018.

NICHOLS, S. C.; MITCHELL, J. P.; SANDELL, D.; ANDERSSON, P. U.; FISCHER, M.; HOWALD, M.; PENGILLEY, R.; KRÜGER, P. A Multi-Laboratory in Vitro Study to Compare Data from Abbreviated and Pharmacopeial Impactor Measurements for Orally Inhaled Products: A Report of the European Aerosol Group (EPAG). **AAPS PharmSciTech**, v. 17, n. 6, p. 1383–1392, dez. 2016.

NOKHODCHI, A.; CHAVAN, S.; GHAFOURIAN, T. In Vitro Dissolution and Permeability Testing of Inhalation Products: Challenges and Advances. **Pharmaceutics**, v. 15, n. 3, p. 983, 18 mar. 2023.

OHAR, J. A.; BAUER, A.; SHARMA, S.; SANJAR, S. In Vitro Effect of Different Airflow Rates on the Aerosol Properties of Nebulized Glycopyrrolate in the EFlow® Closed System and Tiotropium Delivered in the HandiHaler®. **Pulmonary Therapy**, v. 6, n. 2, p. 289–301, 1 dez. 2020.

OKUDA, T.; OKAMOTO, H. Present Situation and Future Progress of Inhaled Lung Cancer Therapy: Necessity of Inhaled Formulations with Drug Delivery Functions. **Chemical and Pharmaceutical Bulletin**, v. 68, n. 7, p. 589–602, 1 jul. 2020.

PINTO, J. T.; ZELLNITZ, S.; GUIDI, T.; SCHIARETTI, F.; SCHROETTNER, H.; PAUDEL, A. Spray-Congealing and Wet-Sieving as Alternative Processes for Engineering of Inhalation Carrier Particles: Comparison of Surface Properties, Blending and In Vitro Performance. **Pharmaceutical Research**, v. 38, n. 6, p. 1107–1123, 2021.

POLITI, K.; DELA CRUZ, C. S.; HOMER, R. Thoracic Neoplasia: Carcinoma. *Em*: **Pathobiology of Human Disease**. [s.l.] Elsevier, 2014. p. 2677–2689.

PRAPHAWATVET, T.; PETERS, J. I.; WILLIAMS, R. O. Inhaled Nanoparticles–An Updated Review. **International Journal of Pharmaceutics**, v. 587, p. 119671, set. 2020.

REPORTS AND DATA. **Pharma and Healthcare - Dry Powder Inhaler Device Market**mar. 2023. Disponível em: <https://www.reportsanddata.com/report-detail/dry-powder-inhaler-device-market#:~:text=Market%20Synopsis,4%25%20during%20the%20forecast%20period>. Acesso em: 31 jul. 2023.

ROA, W. H.; AZARMI, S.; AL-HALLAK, M. H. D. K.; FINLAY, W. H.; MAGLIOCCO, A. M.; LÖBENBERG, R. Inhalable Nanoparticles, a Non-Invasive Approach to Treat Lung Cancer in a Mouse Model. **Journal of Controlled Release**, v. 150, n. 1, p. 49–55, 28 fev. 2011.

ROSIÈRE, R.; BERGHMANS, T.; DE VUYST, P.; AMIGHI, K.; WAUTHOZ, N. The Position of Inhaled Chemotherapy in the Care of Patients with Lung Tumors: Clinical Feasibility and Indications According to Recent Pharmaceutical Progresses. **Cancers**, v. 11, n. 3, p. 329, 7 mar. 2019a.

ROSIÈRE, R.; BERGHMANS, T.; DE VUYST, P.; AMIGHI, K.; WAUTHOZ, N. The Position of Inhaled Chemotherapy in the Care of Patients with Lung Tumors: Clinical Feasibility and Indications According to Recent Pharmaceutical Progresses. **Cancers**, v. 11, n. 3, p. 329, 7 mar. 2019b.

RUZYCKI, C. A.; TAVERNINI, S.; MARTIN, A. R.; FINLAY, W. H. Characterization of Dry Powder Inhaler Performance through Experimental Methods. **Advanced Drug Delivery Reviews**, v. 189, p. 114518, out. 2022.

SANDERS, M. Inhalation Therapy: An Historical Review. **Primary Care Respiratory Journal**, v. 16, n. 2, p. 71–81, 13 mar. 2007.

SEN, C.; FREUND, D.; GOMPERTS, B. N. Three-Dimensional Models of the Lung: Past, Present and Future: A Mini Review. **Biochemical Society Transactions**, v. 50, n. 2, p. 1045–1056, 29 abr. 2022.

SHAH, S. R.; PRAJAPATI, H. R.; SHETH, D. B.; GONDALIYA, E. M.; VYAS, A. J.; SONIWALA, M. M.; CHAVDA, J. R. Pharmacokinetics and *in Vivo* Distribution of Optimized PLGA Nanoparticles for Pulmonary Delivery of Levofloxacin. **Journal of Pharmacy and Pharmacology**, v. 72, n. 8, p. 1026–1037, 9 jul. 2020.

SKARDAL, A.; MURPHY, S. V.; DEVARASETTY, M.; MEAD, I.; KANG, H.-W.; SEOL, Y.-J.; SHRIKE ZHANG, Y.; SHIN, S.-R.; ZHAO, L.; ALEMAN, J.; HALL, A. R.; SHUPE, T. D.; KLEENSANG, A.; DOKMECI, M. R.; JIN LEE, S.; JACKSON, J. D.; YOO, J. J.; HARTUNG, T.; KHADEMHOSSEINI, A.; SOKER, S.; BISHOP, C. E.; ATALA, A. Multi-Tissue Interactions in an Integrated Three-Tissue Organ-on-a-Chip Platform. **Scientific Reports**, v. 7, n. 1, p. 8837, 18 ago. 2017.

SKARDAL, A.; SHUPE, T.; ATALA, A. Organoid-on-a-Chip and Body-on-a-Chip Systems for Drug Screening and Disease Modeling. **Drug Discovery Today**, v. 21, n. 9, p. 1399–1411, set. 2016.

STEIN, S. W.; THIEL, C. G. The History of Therapeutic Aerosols: A Chronological Review. **Journal of Aerosol Medicine and Pulmonary Drug Delivery**, v. 30, n. 1, p. 20–41, fev. 2017.

SUNG, H.; FERLAY, J.; SIEGEL, R. L.; LAVERSANNE, M.; SOERJOMATARAM, I.; JEMAL, A.; BRAY, F. Global Cancer Statistics 2020: GLOBOCAN Estimates of Incidence and Mortality Worldwide for 36 Cancers in 185 Countries. **CA: A Cancer Journal for Clinicians**, v. 71, n. 3, p. 209–249, 2021a.

SUNG, H.; FERLAY, J.; SIEGEL, R. L.; LAVERSANNE, M.; SOERJOMATARAM, I.; JEMAL, A.; BRAY, F. Global Cancer Statistics 2020: GLOBOCAN Estimates of Incidence and Mortality Worldwide for 36 Cancers in 185 Countries. **CA: A Cancer Journal for Clinicians**, v. 71, n. 3, p. 209–249, maio 2021b.

THALBERG, K.; AHMADI, R.; STUCKEL, J.; ELFMAN, P.; SVENSSON, M. The Match between Adhesive Mixture Powder Formulations for Inhalation and the Inhaler Device. **European Journal of Pharmaceutical Sciences**, v. 186, p. 106457, jul. 2023.

THE UNITED STATES PHARMACOPEIA. **General Chapters: <601> AEROSOLS, NASAL SPRAYS, METERED-DOSE INHALERS, AND DRY POWDER INHALERS; USP 31 NF26**2007. Disponível em: <http://www.uspbpep.com/usp31/v31261/usp31nf26s1_c601.asp>. Acesso em: 9 out. 2020.

TULBAH, A. S.; GAMAL, A. Design and Characterization of Atorvastatin Dry Powder Formulation as a potential Lung Cancer Treatment. **Saudi Pharmaceutical Journal : SPJ**, v. 29, n. 12, p. 1449–1457, dez. 2021.

VELAGA, S. P.; DJURIS, J.; CVIJIC, S.; ROZOU, S.; RUSSO, P.; COLOMBO, G.; ROSSI, A. Dry Powder Inhalers: An Overview of the in Vitro Dissolution Methodologies and Their Correlation with the Biopharmaceutical Aspects of the Drug Products. **European Journal of Pharmaceutical Sciences**, v. 113, p. 18–28, fev. 2018.

WANG, W.; HUANG, Z.; HUANG, Y.; ZHANG, X.; HUANG, J.; CUI, Y.; YUE, X.; MA, C.; FU, F.; WANG, W.; WU, C.; PAN, X. Pulmonary Delivery Nanomedicines towards Circumventing Physiological Barriers: Strategies and Characterization Approaches. **Advanced Drug Delivery Reviews**, v. 185, p. 114309, jun. 2022.

WANG, Y.-B.; WATTS, A. B.; PETERS, J. I.; LIU, S.; BATRA, A.; WILLIAMS, R. O. In Vitro and In Vivo Performance of Dry Powder Inhalation Formulations: Comparison of Particles Prepared by Thin Film Freezing and Micronization. **AAPS PharmSciTech**, v. 15, n. 4, p. 981–993, 14 maio 2014.

WEBER, S.; ZIMMER, A.; PARDEIKE, J. Solid Lipid Nanoparticles (SLN) and Nanostructured Lipid Carriers (NLC) for Pulmonary Application: A Review of the State of the Art. **European Journal of Pharmaceutics and Biopharmaceutics**, v. 86, n. 1, p. 7–22, jan. 2014.

WEI, X.; HINDLE, M.; KAVIRATNA, A.; HUYNH, B. K.; DELVADIA, R. R.; SANDELL, D.; BYRON, P. R. *In Vitro* Tests for Aerosol Deposition. VI: Realistic Testing with Different Mouth–Throat Models and *In Vitro—In Vivo* Correlations for a Dry Powder Inhaler, Metered Dose Inhaler, and Soft Mist Inhaler. **Journal of Aerosol Medicine and Pulmonary Drug Delivery**, v. 31, n. 6, p. 358–371, dez. 2018.

XIA, X.; LI, F.; HE, J.; AJI, R.; GAO, D. Organoid Technology in Cancer Precision Medicine. **Cancer Letters**, v. 457, p. 20–27, ago. 2019.

XIE, Y.; AILLON, K. L.; CAI, S.; CHRISTIAN, J. M.; DAVIES, N. M.; BERKLAND, C. J.; FORREST, M. L. Pulmonary Delivery of Cisplatin–Hyaluronan Conjugates via Endotracheal Instillation for the Treatment of Lung Cancer. **International Journal of Pharmaceutics**, v. 392, n. 1–2, p. 156–163, 15 jun. 2010.

YE, Y.; MA, Y.; ZHU, J. The future of dry powder inhaled therapy: Promising or discouraging for systemic disorders? **International Journal of Pharmaceutics**, v. 614, p. 121457, 25 fev. 2022.

YOSHIDA, H.; KUWANA, A.; SHIBATA, H.; IZUTSU, K.; GODA, Y. Comparison of Aerodynamic Particle Size Distribution Between a Next Generation Impactor and a Cascade Impactor at a Range of Flow Rates. **AAPS PharmSciTech**, v. 18, n. 3, p. 646–653, abr. 2017.

YUE, P.; ZHOU, W.; HUANG, G.; LEI, F.; CHEN, Y.; MA, Z.; CHEN, L.; YANG, M. Nanocrystals Based Pulmonary Inhalation Delivery System: Advance and Challenge. **Drug Delivery**, v. 29, n. 1, p. 637–651, 31 dez. 2022.

ZHU, X.; KONG, Y.; LIU, Q.; LU, Y.; XING, H.; LU, X.; YANG, Y.; XU, J.; LI, N.; ZHAO, D.; CHEN, X.; LU, Y. Inhalable Dry Powder Prepared from Folic Acid-Conjugated Docetaxel Liposomes Alters Pharmacodynamic and Pharmacokinetic Properties Relevant to Lung Cancer Chemotherapy. **Pulmonary Pharmacology & Therapeutics**, v. 55, p. 50–61, abr. 2019.

ZILLEN, D.; BEUGELING, M.; HINRICHS, W. L. J.; FRIJLINK, H. W.; GRASMEIJER, F. Natural and Bioinspired Excipients for Dry Powder Inhalation **Formulations. Current Opinion in Colloid & Interface Science**, v. 56, p. 101497, 1 dez. 2021.

CHAPTER 4 EXPLORATORY TESTING FOR FLUBENDAZOLE NANOPARTICLES OBTENTION

4.1 FLUBENDAZOLE PHYSICOCHEMICAL CHARACTERISTICS

Flubendazole is usually administered orally in doses of approximately 5 mg/kg, 3 times a day, reaching a maximum plasma concentration of less than 5 ng/ml, even after ingestion of 2 g, which is considered very limited (ČÁŇOVÁ; ROZKYDALOVÁ; RUDOLF, 2017). Since poor solubility (0.005 mg/mL) (GABRIEL L. B. DE ARAUJO *et al.*, 2018; VIALPANDO *et al.*, 2016) is the limitation for bioavailability (VIALPANDO *et al.*, 2016), new solubilization approaches should be applied for the development of alternative formulations that turn feasible the use of flubendazole for cancer treatment.

Flubendazole physicochemical properties (Table 4.1) show an intermediary logP, and relatively high Tm, which can be considered a 'brick-dust' (DITZINGER *et al.*, 2019). This type of substance presents a solid-state limited solubility, and high crystal lattice energy, which means that the breakdown of the crystal is the most difficult step (DITZINGER *et al.*, 2019). In contrast, substances with low Tm and high logP are known as 'grease balls', and would have the solvation step in water as most difficult step for dissolution (DITZINGER *et al.*, 2019).

Table 4.1.FBZ Physicochemical characteristics.

Characteristic	Value
Molecular weight (g/mol)	313.1
Tm (°C)	238
Tg (°C)	156
pKa	3.6 and 9.6
LogP	3
Solubility (mg/mL) in ambient conditions	
Water	0.005
Methanol	0.110
Acetone	0.180
Dichloromethane	0.140
Formic acid	340.0
DMSO*	1.0
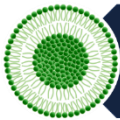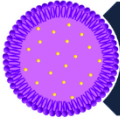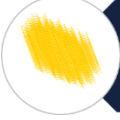
Source: adapted from (VIALPANDO *et al.*, 2016);*(CAYMAN CHEMICAL, 2022)

One approach to improve the solubility of the drug is the particle size reduction. At the nanometric scale, the increase in the ratio of surface area per volume of particle is more significant than for sizes above 1 μm (SHEGOKAR; MÜLLER, 2010). This larger surface area translates into higher interaction of solvent molecules and smaller diffusion distance, which in

addition to a decrease in intermolecular forces by rearrangement in the crystalline state, results in increased saturation solubility (MIRZA; AHIRRAO; KSHIRSAGAR, 2017). The dissolution rate is also enhanced by two factors, as explained by the Noyes-Whitney equation: surface area and saturation solubility (BUCKTON; BEEZER, 1992). The consequent increase in bioavailability could reduce the dose required for the therapeutic effect (BHATIA, 2016).

In order to increase permeation, solubility, prolong release time or protect from degradation, drugs can be encapsulated, wrapped in a matrix or linked to other molecules, originating different types of nanoparticles, such as liposomes, lipid nanocarriers, nanoemulsions, and nanocrystals (MÜLLER; GOHLA; KECK, 2011a). Thus, the development of inhaled formulations containing nanoparticles has great potential to improve antitumor therapies. Considering FBZ physicochemical properties, the intended pharmaceutical form and available methods, liposome, solid lipid nanoparticles and nanocrystals were selected as possible strategies (Figure 4.1). In this chapter, we describe the screening tests applied for the selection of the most suitable nanoparticle for FBZ, aiming a final dry powder product for inhalation.

Figure 4.1. Rationale for selection of the most suitable nanoparticle type for the delivery of flubendazole in a dry powder for inhalation.

Source: elaborated by the author.

4.2 MATERIAL AND METHODS

4.2.1 Materials

FBZ was obtained from Changzhou Yabang – QH Pharmachem CO., LTD (China). Poloxamers were kindly donated by BASF Japan (Tokyo, Japan). Mannitol, L-leucine, formic

acid, acetonitrile, polyvinylpyrrolidone (PVP K30), polyvinyl alcohol (PVA), and dimethyl sulfoxide (DMSO) were purchased from Wako Pure Chemical (Osaka, Japan). 1,2-Dipalmitoyl-sn-glycero-3-phosphocholine (DPPC) was supplied by TCI (Tokyo Chemical Industry).

4.2.2 Methods

4.2.2.1 Liposome preparation

Liposomes were prepared by thin film hydration method, the most common preparation procedure, also known as the Bangham method (WANG *et al.*, 2022a). Cholesterol and DPPC were dissolved in a volatile solvent such as dichloromethane, ethanol, methanol, or chloroform, in a round bottom flask and the solution was evaporated, forming a thin film on the flask wall. The liposomal formation was obtained by hydrating the thin film with aqueous medium. The obtained solution was extruded by a membrane to reduce liposome size (WANG *et al.*, 2022a).

4.2.2.2 Solid lipid nanoparticle preparation

Solid lipid nanoparticles were prepared through hot self-nano-emulsification method as previously described, with modifications (NEGI *et al.*, 2013). Briefly, lipid and surfactant were mixed and melted before FBZ addition. Hot distilled water (80 °C) was added into the mixture, with gentle shaking. Cold distilled water was then added to the nanoemulsion to promote rapid solidification of lipid nanoparticles. SLNs dispersion was centrifuged at 14,000 rpm for 30 min, and supernatant was recovered and analyzed by DLS.

Figure 4.2. Solid lipid nanoparticle preparation by hot self-nano-emulsification method.
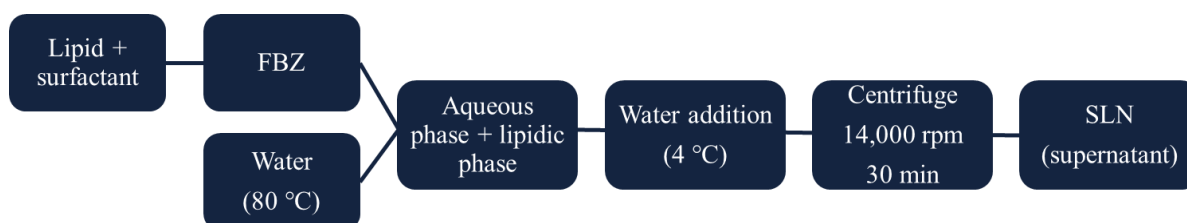
Source: elaborated by the author.

4.2.2.3 Nanocrystal obtention through spray drying with two-solution mixing-type spray nozzle

One-step nanoparticle obtention was performed as previously reported, with modifications (TAKI *et al.*, 2016). FBZ was dissolved in formic acid and diluted in acetone in the proportion 1:9 to 0.2 or 0.3% to make spraying viable, and separately, the mannitol carrier was solubilized in water. Flubendazole nanocrystals were obtained by spray drying using a twin

Jet Nozzle RJ10 TLM1 atomizer connected to a two-solution mixer spray nozzle (Ohkawara Kakohki Co. Ltd.; Yokohama, Japan).

4.2.2.4 Nanocrystal preparation by nanoprecipitation

FBZ nanoparticles were prepared by the nanoprecipitation method, as previously reported (TANEJA; SHILPI; KHATRI, 2016) with adaptations. Briefly, FBZ was solubilized in formic acid (125 mg/ml) and added to 15 ml of a stabilizer solution (0.5% w/w of PVA, PVP or poloxamer 188 in water) under magnetic stirring and probe ultrasonication (Ultrasonic Disperser, UH-10, SMT Co. LTD.). Ultrasonication continued after addition for 10 minutes. The starting stabilizer solution temperature was 4 °C, and experiments were conducted at room temperature without further cooling. The FBZ concentration in formic acid was fixed, aiming for a high concentration to avoid precipitation issues, and ultrasonication was fixed at 70%.

4.2.2.5 Thermal analysis

The assessment of solubility of FBZ in the lipids was evaluated by differential scanning calorimetry (DSC). Approximately 2 mg of FBZ was weighed in aluminum crucibles and analyzed alone or as a mixture with glyceryl palmitostearate, glyceryl dibehenate or stearic acid in different ratios: 1 FBZ: 1 lipid; 2 FBZ: 1 lipid; 3 FBZ: 1 lipid. The crucibles were crimped and analyzed from 25 °C to 300 °C, at a heating rate of 10 °C/min under an inert atmosphere of N_2 (20 mL/min), in the Shimadzu equipment DSC-60 (Shimadzu).

4.2.2.6 Particle size evaluation

Particle size, before and after spray drying, was determined using a dynamic light scattering instrument (ZetaSizer Nano-ZS; Malvern Instrument Ltd., Malvern, U.K.). Samples were diluted or resuspended in distilled water, and measurements were conducted in triplicate with 15 s intervals at 25 °C.

4.2.2.7 Scanning electron microscopy (SEM)

Sample was deposited in an adhesive carbon tape and covered with a Pt–Pd film (E-102 ion sputter; Hitachi, Tokyo, Japan). Morphology of inhalable particles was evaluated using a scanning electron microscope (SEM, S-4300; Hitachi, Tokyo, Japan).

4.2.2.8 *In vitro* evaluation of aerosolization performance

The aerosol performances of FBZ inhalable particles were evaluated using an 8-stage Andersen cascade impactor (Andersen nonviable sampler, AN-200; Tokyo Direc Co., Tokyo, Japan) as previously described with minor modifications (TAKI *et al.*, 2016). The impactor is composed of a throat, an adaptor, and a preseparator, followed by eight stages (0 to 7) with cutoff aerodynamic size ranges of >11.0 μm, 7.0-11.0 μm, 4.7-7.0 μm, 3.3-4.7 μm, 2.1-3.3 μm, 1.1-2.1 μm, 0.65-1.1 μm, and 0.65-0.43 μm (FUKUSHIGE *et al.*, 2020). Briefly, 25 mg of the sample was loaded into a gelatin capsule (size 2, Qualicaps Co. Ltd., Nara, Japan) and assembled in a reverse Jethaler® dry powder inhaler (Tokico System Solutions, Ltd., Kanagawa, Japan). The surface of the collection plates was coated with a silicon spray to minimize particle re-entrainment. The vacuum pump was activated, and the airflow was equilibrated at 28.3 ml/min. After stabilization, the inhaler was connected to the mouthpiece and actuated, and after 10 s, the vacuum pump was turned off. Three actuations were performed to ensure proper recovery. Samples deposited in each stage of the cascade impactor and in the device, capsule, mouthpiece, throat, and preseparator were collected with 5 ml of an acetonitrile/water mixture (60:40 v/v). The FBZ concentration was determined by measuring the absorbance of the sample solution from 300 to 400 nm using a UV–Vis spectrophotometer (Nivo 3S plate reader (PerkinElmer Inc.; Waltham, MA, USA)) and calculating through partial least squares regression using Minitab® 17 software. The fine particle fraction (FPF) was calculated as detailed (THE UNITED STATES PHARMACOPEIA, 2007b).

(1) *FPF* = Sum of recovered mass from stage 3 to 7/Total mass of delivered drug (from the mouthpiece to stage 7).

4.3   RESULTS AND DISCUSSION

4.3.1   Liposome

From known nanoparticles (Figure 2.6), liposomes, solid lipid nanoparticles (SLN) and nanocrystals were selected as candidates for FBZ nanoparticles. Liposomes, the self-assembling vesicular structures containing aqueous solution encapsulated by one or multiple concentric phospholipid membranes, can deliver lipophilic drugs entrapped within the membrane, and a hydrophilic compound in the aqueous solution (Laouini et al., 2012; Mehta, 2016). Simple FBZ solubilization tests were performed in dichloromethane, ethanol, methanol,

and chloroform to confirm the information obtained in the literature, but the amount of solvent necessary would become a prohibitive factor for scale-up, and thus eliminated.

4.3.2   Solid lipid nanocarriers

Since the solubility of flubendazole in organic solvents is reduced, direct solubilization in a lipid, favored by increasing the temperature with the aid of surfactants, was explored as alternative approach. In order to obtain SLN by hot self-nano-emulsification, an adequate ratio of lipid, surfactant and API must be determined. But as a screening step, the feasibility of the method could be determined by determining best lipid and the extent of FBZ solubilization in a proposed mixture. For this purpose, solubility evaluations were initially carried out through DSC, comparing FBZ alone (Figure 4.3) to physical mixtures with glyceryl palmitostearate (Figure 4.4), glyceryl dibehenate (Figure 4.5), and stearic acid (Figure 4.6) in different proportions. The lipid that promoted the greatest reduction of the peak corresponding to flubendazole fusion would indicate a greater ability to solubilize the drug. Comparing DSC results, it is possible to observe that flubendazole presents greater solubility in stearic acid.

Figure 4.3. DSC curve of pure flubendazole, at 10 °C/min, under dynamic atmosphere of N_2.
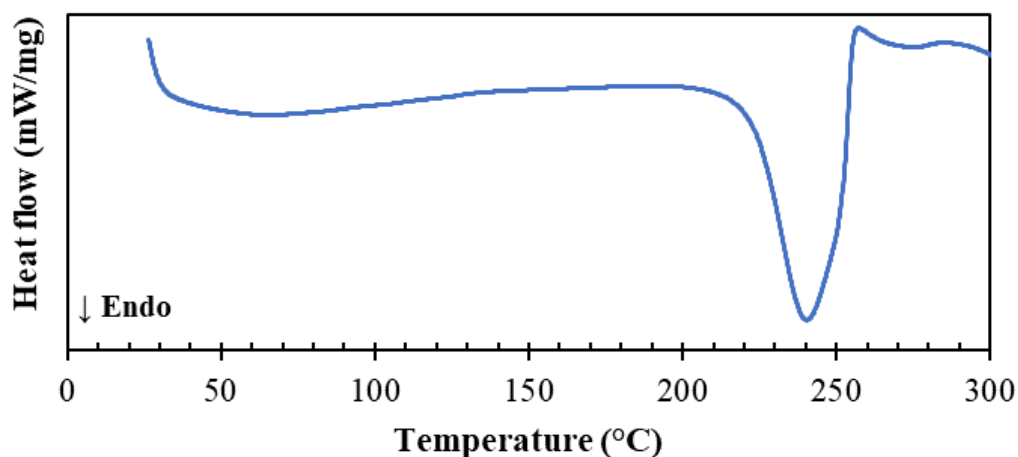
Source: elaborated by the author.

Figure 4.4. DSC curve of glyceryl palmitostearate at 10 °C/min, under dynamic atmosphere of N_2.
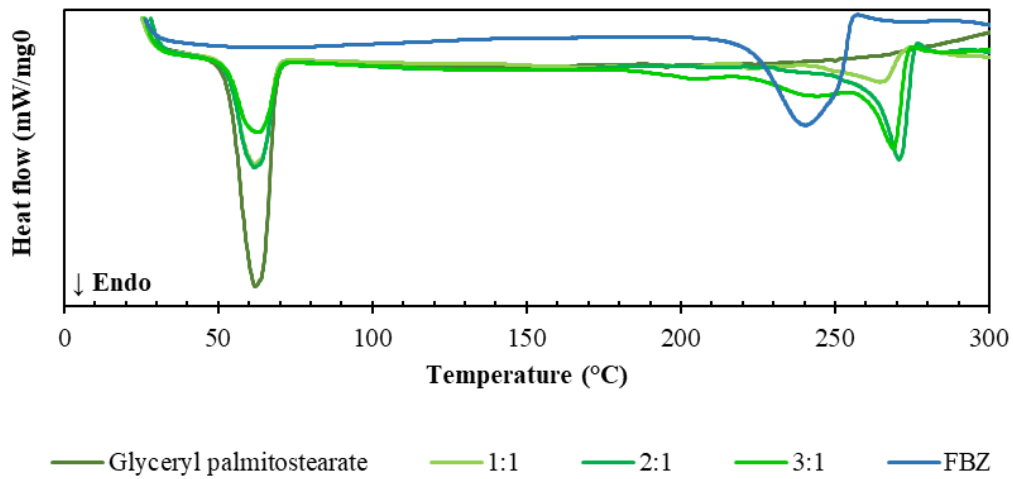
Source: elaborated by the author.

Figure 4.5. DSC curve of glyceryl dibehenate at 10 °C/min, under dynamic atmosphere of N_2.
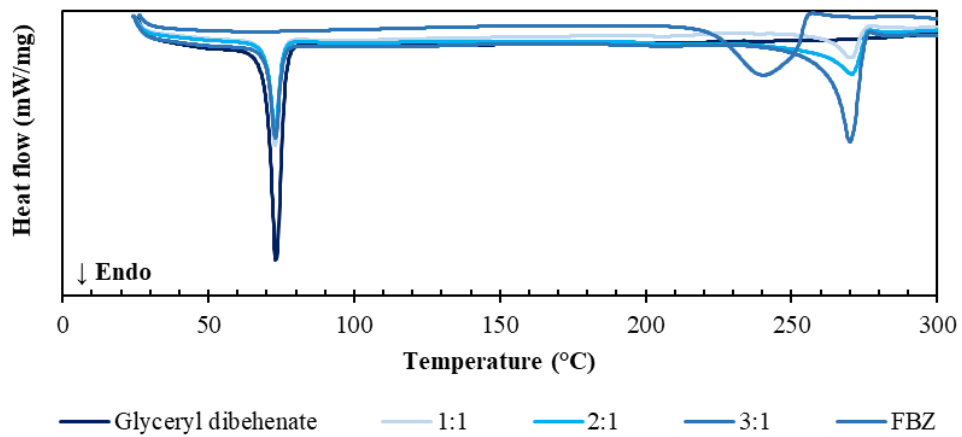
Source: elaborated by the author.

Figure 4.6. DSC curve of stearic acid at 10 °C/min, under dynamic atmosphere of N_2.
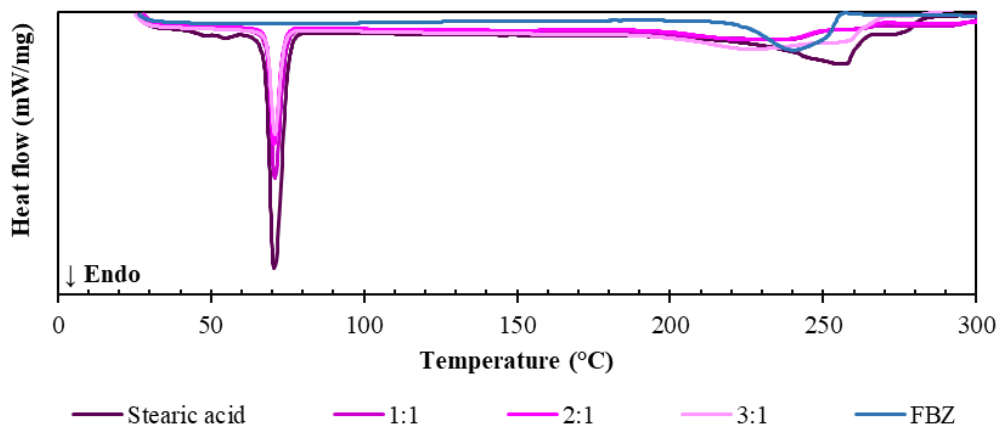
Source: elaborated by the author.

After selection of stearic acid, the next step was to select the best surfactant. Hot self-emulsification method was performed with different poloxamers to identify which would favor obtaining the smallest particle size to be added to the formulation. The obtained results were organized in Table 4.2.

Table 4.2. DLS results of solid lipid nanoparticles prepared with different poloxamers as stabilizers.

Poloxamer	388	237	188	407
Z-ave (nm)	201.1 ± 4.3	242.2 ± 8.8	345.5 ± 15.8	436.9 ± 26.6
PDI	0.133 ± 0.02	0.166 ± 0.02	0.140 ± 0.03	0.279 ± 0.03

Promising particle size results are obtained with poloxamer 388 (Z-ave 201.1 and PDI 0.133), and it was selected to preliminary tests for mixture design. Unfortunately, mixtures of different ratios of stearic acid and poloxamer 388 did not result in increase of FBZ solubility beyond the solubility in pure stearic acid (1.4 mg/g). Given such a low initial concentration (0.14%), the solid lipid nanoparticle was also discarded as an alternative for obtaining flubendazole nanoparticles.

4.3.3 Nanocrystal obtention through spray drying with two-solution mixing-type spray nozzle

The spray drying technique basically promotes the drying of a solution or suspension by atomization in a chamber with a heated gas, where the solvent is immediately removed and the powder collected in a container (HADIWINOTO; LIP KWOK; LAKERVELD, 2018a). There are different types of spray guns, and the conventional one is designed with parallel flow of air and liquid, as illustrated in the Figure 4.7.

Figure 4.7. Conventional spray gun, with parallel flow of air and liquid.
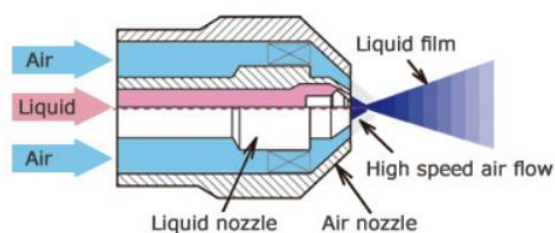
Source: (OHKAWARA KAKOHKI, 2007).

Another type of spray gun, illustrated in Figure 4.8, allows the entry of two distinct liquid phases, promoting their combination inside the gun. This configuration allows

nanoprecipitation and drying as a one-step process, as previously demonstrated by Ozeki, T. and colleagues (OZEKI et al., 2012). Inside the gun, the organic phase containing the drug is mixed with the aqueous solution of the carrier (TAKI et al., 2016). As the composition of the solvent is changed, drug nanocrystals can be formed and drying can occur before the crystals grow, allowing their deposition on the carrier (TAKI et al., 2016).

Figure 4.8. Two-solution mixing type nozzle.
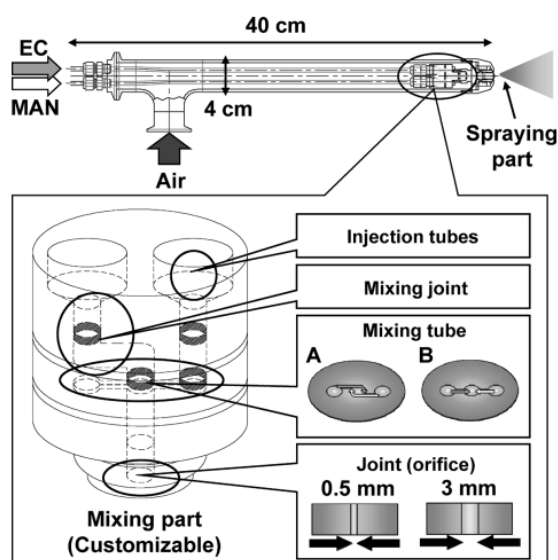
Source: (OZEKI *et al.*, 2012).

For this process, the following critical process and formulation parameters can be identified:

- Inlet air temperature: it should be as low as possible in order to minimize exposure of the drug to high temperatures and reduce the cost of the process, but sufficient to promote solvent evaporation (ARPAGAUS, 2018). It has a direct impact on product moisture and particle morphology.

- Atomization pressure: influences the size of the droplet formed by the spray, and consequent final particle size (AL-KHATTAWI *et al.*, 2018).

- Feed flow rate: corresponds to the amount of solution pumped per time to the equipment. It has a direct correlation with the final moisture of the product and the drying capacity of the equipment, which can impact the morphology of the particle.

- As two solutions are simultaneously atomized, each flow rate would correspond to the ratio of solvent and anti-solvent, which could directly impact on FBZ particle size.

- Concentration of solutions: the concentration of solids in the solutions can impact the morphology of particles (VICENTE *et al.*, 2013). In the case of FBZ, as its solubility is very low, the concentration adopted for the process was the highest possible for which no precipitation was observed during the process time.

Based on theoretical knowledge, and brief risk assessment, a screening step was carried out, with multiple variations regarding feeding rate, FBZ concentration in the product, and inlet air temperature. Loading, yield, drug particle size, polydispersity index and fine particle fraction (FPF), and outlet air temperature were evaluated (Table 4.3).

Table 4.3. List of screening batches produced by spray drying with aspersion through a two-fluid nozzle. Mannitol conc.: concentration of mannitol mass/volume of water; FBZ conc.: concentration of flubendazole mass/volume of acetone and formic acid (9:1); T. inlet air: Inlet air temperature; PDI: polydispersion index; FPF: fine particle fraction; T. outlet: Outlet air temperature.

Batch	Manitol conc. (%)	Mannitol Flow rate (kg/h)	FBZ conc (%)	FBZ Flow rate (kg/h)	T. inlet air (ºC)	FBZ Theoretical loading (%)	FBZ loading real (%)	Yield (%)	Z-ave (nm)	PDI	FPF (%)	T. outlet (ºC)
1	1.50	0.57	0.20	0.16	150	4.3	2.1	53	417.8	0.299	40.0	30.7
2	1.50	0.71	0.30	0.34	175	10.4	5.3	52	624.7	0.320	-	74.3
3	5.00	0.56	0.00	0.00	175	0.0	0.0	58	-	-	33.0	65.6
4	0.75	0.65	0.20	0.23	125	10.0	5.5	32	1728.7	0.320	30.0	48.7
7	5.40	0.52	0.20	0.47	150	3.4	4.4	56	509.3	0.440	28.1	67.0
14	1.69	0.48	0.20	0.25	150	5.8	4.8	56	2336.0	0.535	0.6	59.5

Figure 4.9. SEM of screening batches produced by spray drying with aspersion through a two-fluid nozzle.
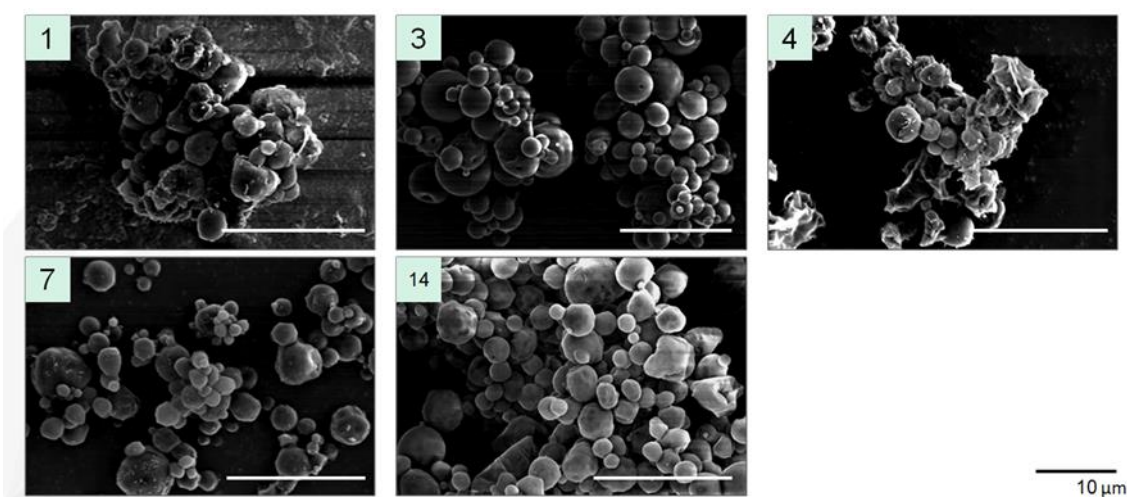
Source: elaborated by the author.

Based on the results, loss of active was observed at some stage of the process, probably due to precipitation at the end of the atomizing nozzle. The yield found was in line with

expectations, considering laboratory-scale equipment and a very small batch size, in addition to a large loss of heat from the process, with low outlet air temperature despite the high inlet air temperature adopted for the process. Regarding the morphology (Figure 4.9), it can be observed that most of the batches presented smooth and spherical particles, with the presence of collapsed particles, in batch 4. This batch represents the sample with the lowest concentration of mannitol, and may indicate that the drying surface was not rigid enough to preserve the structure with the during solvent elimination (VEHRING, 2008).

Although the characteristics could be optimized with a more comprehensive study with an experimental design, the sample resuspension was very difficult even after spray drying, and the process demanded a large volume of organic solvent. As mentioned previously, the high Tm of FBZ (238 °C) might indicate high crystal lattice energy, and consequent need of higher energy to breakdown the crystals (DITZINGER *et al.*, 2019). Therefore, a more efficient process to prepare FBZ nanocrystals should be explored.

4.3.4 Nanocrystal preparation by nanoprecipitation

One of the alternatives for increasing the concentration of the active in the final formulation, eliminating the need for solvents and ensuring the smallest particle size would be in the form of a nanosuspension. Adopting different polymers as stabilizers, nanoprecipitation tests under ultrasound were performed, as detailed in Figure 4.10.

The last nanoparticle alternative for FBZ that would increase the concentration of the active in the final formulation, reducing the use of solvents, and ensuring the smallest particle size would be in the form of a nanosuspension. Adopting different polymers as stabilizers, nanoprecipitation tests were carried out under ultrasound, as detailed in Figure 4.10.

Figure 4.10. Scheme of nanosuspension preparation through nanoprecipitation method.
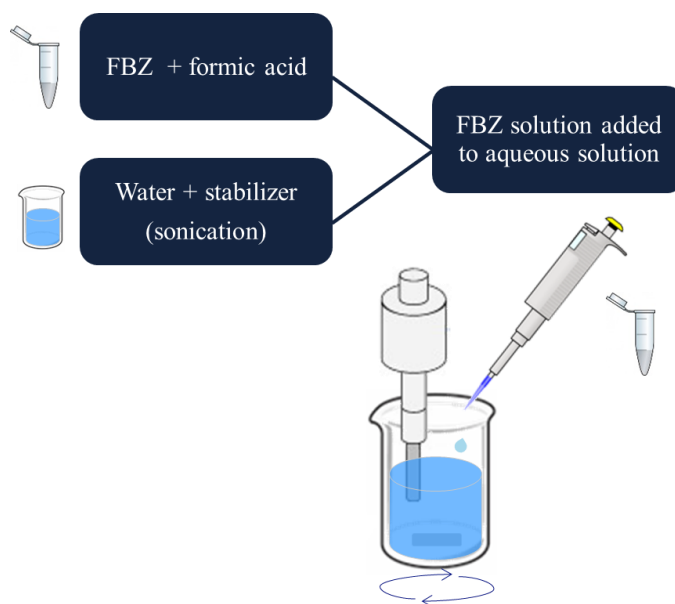
Source: elaborated by the author.

The results organized in Table 4.4 were satisfactory, and poloxamer 188 granted the smaller particle size (167.8 nm) and more uniform distribution (PDI 0.2). PVP and PVA also act as steric stabilizers, but the structure of poloxamer 188, as an amphiphilic polymer, allows the adsorption of nanocrystals on its surface by interactions with polypropylene oxide chains (TUOMELA; HIRVONEN; PELTONEN, 2016a).

Table 4.4. Influence of different stabilizers on FBZ particle size prepared by nanoprecipitation method. Stabilizer concentrations were fixed at 0.5%.

Stabilizer	Z-ave (nm)	PDI
PVA	251.3	0.220
PVP	208.2	0.247
Poloxamer 188	167.8	0.200

Poloxamer 188 has already been used as a stabilizer in the preparation of different nanosuspensions, such as glimepiride, itraconazole and paclitaxel (LIU, 2013), also for DPI formulations (SON; WORTH LONGEST; HINDLE, 2013). It also showed better toxicity results when compared to polysorbate 80, an FDA-approved surfactant for pulmonary delivery (METZ, 2020), without detection of toxicity (LINDENBERG *et al.*, 2019).

FBZ has low solubility not only in water, but also in organic solvents and in the evaluated lipids, which impairing the preparation of nanocarriers without compromising the final dose of the product (VIALPANDO *et al.*, 2016). Nanocrystals, on the other hand, since

they are composed 100% of drug, and can be produced by a controlled precipitation process, as long as it can be solubilized in a solvent miscible with the antisolvent (MÜLLER; GOHLA; KECK, 2011b). DMSO is widely used in the preparation of FBZ for intravenous administration (MORENO *et al.*, 2004), *in vitro* experiments (ZHOU, 2018) and quantification methods (LAURA *et al.*, 2015), but its extremely high boiling point of 189 °C (PUBCHEM,) prevents its elimination by spray drying. The high solubility of FBZ in formic acid (340 mg/ml) has already been explored by Vialpando and colleagues to obtain an amorphous form through spray drying (VIALPANDO *et al.*, 2016). In order to achieve a high concentration of 9.8 to 18.2%, a solution of FBZ in dichloromethane containing 10% formic acid was used, resulting in residual formic acid levels greater than 5000 ppm (VIALPANDO *et al.*, 2016). Although this solvent is classified as class 3, and considered of low toxic risk to health (THE UNITED STATES PHARMACOPEIA, 2020), these residual levels would require regulatory justifications and could impact processability (VIALPANDO *et al.*, 2016). Using the nanoprecipitation method prior to spray drying, the concentration of formic acid required for the process can be reduced to less than 1%.

4.4 CONCLUSION

Based on physicochemical characteristics, and preliminary tests, nanocrystals were determined to be the most suitable nanoparticle for FBZ aiming an inhalable dry powder product. The limiting factor that eliminated other nanocarrier options were FBZ solubility and thus the concentration that it would provide in the final product. Also, a feasible process with minimum use of organic solvents could be adopted when nanoprecipitation with assisted sonication was explored.

4.5 REFERENCES

AL-KHATTAWI, A.; BAYLY, A.; PHILLIPS, A.; WILSON, D. The Design and Scale-up of Spray Dried Particle Delivery Systems. **Expert Opinion on Drug Delivery**, v. 15, n. 1, p. 47–63, 2 jan. 2018.

ARPAGAUS, C. Pharmaceutical Particle Engineering via Nano Spray Drying - Process Parameters and Application Examples on the Laboratory-Scale. **International Journal of Medical Nano Research**, v. 5, n. 1, 31 dez. 2018. Disponível em: <https://www.clinmedjournals.org/articles/ijmnr/international-journal-of-medical-nano-research-ijmnr-5-026.php?jid=ijmnr>. Acesso em: 8 set. 2019.

BHATIA, S. Nanoparticles Types, Classification, Characterization, Fabrication Methods and Drug Delivery Applications. *Em*: BHATIA, S. **Natural Polymer Drug Delivery Systems**. Cham: Springer International Publishing, 2016. p. 33–93.

BUCKTON, G.; BEEZER, A. E. The Relationship between Particle Size and Solubility. **International Journal of Pharmaceutics**, v. 82, n. 3, p. R7–R10, maio 1992.

ČÁŇOVÁ, K.; ROZKYDALOVÁ, L.; RUDOLF, E. Anthelmintic Flubendazole and Its Potential Use in Anticancer Therapy. **Acta Medica (Hradec Kralove, Czech Republic)**, v. 60, n. 1, p. 5–11, 2017.

CAYMAN CHEMICAL. **Flubendazole Product information**2022. Disponível em: <https://cdn.caymanchem.com/cdn/insert/26064.pdf>. Acesso em: 2 set. 2023.

DITZINGER, F.; PRICE, D. J.; ILIE, A.-R.; KÖHL, N. J.; JANKOVIC, S.; TSAKIRIDOU, G.; ALEANDRI, S.; KALANTZI, L.; HOLM, R.; NAIR, A.; SAAL, C.; GRIFFIN, B.; KUENTZ, M. Lipophilicity and Hydrophobicity Considerations in Bio-Enabling Oral Formulations Approaches – a PEARRL Review. **Journal of Pharmacy and Pharmacology**, v. 71, n. 4, p. 464–482, 3 mar. 2019.

FUKUSHIGE, K.; TAGAMI, T.; NAITO, M.; GOTO, E.; HIRAI, S.; HATAYAMA, N.; YOKOTA, H.; YASUI, T.; BABA, Y.; OZEKI, T. Developing Spray-Freeze-Dried Particles Containing a Hyaluronic Acid-Coated Liposome–Protamine–DNA Complex for Pulmonary Inhalation. **International Journal of Pharmaceutics**, v. 583, p. 119338, 15 jun. 2020.

GABRIEL L. B. DE ARAUJO; FABIO FURLAN FERREIRA; CARLOS E. S. BERNARDES; JULIANA A. P. SATO; OTÁVIO M. GIL; DALVA L. A. DE FARIA; RAIMAR LOEBENBERG; STEPHEN R. BYRN; DANIELA D. M. GHISLENI; NADIA A. BOU-CHACRA; TEREZINHA J. A. PINTO; SELMA G. ANTONIO; HUMBERTO G. FERRAZ; DMITRY ZEMLYANOV; DÉBORA S. GONÇALVES; MANUEL E. MINAS DA PIEDADE. A New Thermodynamically Favored Flubendazole/Maleic Acid Binary Crystal Form: Structure, Energetics, and in Silico PBPK Model-Based Investigation. **A New Thermodynamically Favored Flubendazole/Maleic Acid Binary Crystal Form: Structure, Energetics, and in Silico PBPK Model-Based Investigation**, v. 18, n. 9, p. 2377–2386, 2018.

HADIWINOTO, G. D.; LIP KWOK, P. C.; LAKERVELD, R. A Review on Recent Technologies for the Manufacture of Pulmonary Drugs. **Therapeutic Delivery**, v. 9, n. 1, p. 47–70, jan. 2018.

KAKRAN, M.; SHEGOKAR, R.; SAHOO, N. G.; AL SHAAL, L.; LI, L.; MÜLLER, R. H. Fabrication of Quercetin Nanocrystals: Comparison of Different Methods. **European Journal of Pharmaceutics and Biopharmaceutics**, v. 80, n. 1, p. 113–121, jan. 2012.

LAURA, C.; CELINA, E.; SERGIO, S. B.; GUILLERMO, D.; CARLOS, L.; LUIS, A. Combined Flubendazole-Nitazoxanide Treatment of Cystic Echinococcosis: Pharmacokinetic and Efficacy Assessment in Mice. **Acta Tropica**, v. 148, p. 89–96, ago. 2015.

LINDENBERG, F.; SICHEL, F.; LECHEVREL, M.; RESPAUD, R.; SAINT-LORANT, G. Evaluation of Lung Cell Toxicity of Surfactants for Inhalation Route. **Journal of Toxicology and Risk Assessment**, v. 5, n. 2, 15 maio 2019. Disponível em:

<https://www.clinmedjournals.org/articles/ijtra/international-journal-of-toxicology-and-risk-assessment-ijtra-5-022.php?jid=ijtra>. Acesso em: 28 out. 2020.

LIU, P. **Nanocrystal formulation for poorly soluble drugs**. [s.l: s.n.]

METZ, J. Safety Assessment of Excipients (SAFE) for Orally Inhaled Drug Products. **ALTEX**, 2020. Disponível em: <https://www.altex.org/index.php/altex/article/view/1474>. Acesso em: 16 out. 2020.

MIRZA, R. M.; AHIRRAO, S. P.; KSHIRSAGAR, S. J. A Nanocrystal Technology: To Enhance Solubility of Poorly Water Soluble Drugs. v. 5, n. 1, 2017.

MORENO, L.; ALVAREZ, L.; MOTTIER, L.; VIRKEL, G.; SANCHEZ BRUNI, S.; LANUSSE, C. Integrated Pharmacological Assessment of Flubendazole Potential for Use in Sheep: Disposition Kinetics, Liver Metabolism and Parasite Diffusion Ability1. **Journal of Veterinary Pharmacology and Therapeutics**, v. 27, n. 5, p. 299–308, out. 2004.

MÜLLER, R. H.; GOHLA, S.; KECK, C. M. State of the Art of Nanocrystals – Special Features, Production, Nanotoxicology Aspects and Intracellular Delivery. **European Journal of Pharmaceutics and Biopharmaceutics**, v. 78, n. 1, p. 1–9, maio 2011a.

MÜLLER, R. H.; GOHLA, S.; KECK, C. M. State of the Art of Nanocrystals – Special Features, Production, Nanotoxicology Aspects and Intracellular Delivery. **European Journal of Pharmaceutics and Biopharmaceutics**, v. 78, n. 1, p. 1–9, maio 2011b.

NEGI, J. S.; CHATTOPADHYAY, P.; SHARMA, A. K.; RAM, V. Development of Solid Lipid Nanoparticles (SLNs) of Lopinavir Using Hot Self Nano-Emulsification (SNE) Technique. **European Journal of Pharmaceutical Sciences**, v. 48, n. 1–2, p. 231–239, jan. 2013.

OHKAWARA KAKOHKI. **Pressurized two-fluid nozzle**2007. Disponível em: <https://oc-sd.co.jp/english/product/?url=spraydry01.html&JOKEN=%27CODE=17%27>. Acesso em: 30 out. 2021.

OZEKI, T.; AKIYAMA, Y.; TAKAHASHI, N.; TAGAMI, T.; TANAKA, T.; FUJII, M.; OKADA, H. Development of a Novel and Customizable Two-Solution Mixing Type Spray Nozzle for One-Step Preparation of Nanoparticle-Containing Microparticles. **Biological and Pharmaceutical Bulletin**, v. 35, n. 11, p. 1926–1931, 2012.

PUBCHEM. **Dimethyl sulfoxide**. Disponível em: <https://pubchem.ncbi.nlm.nih.gov/compound/679>. Acesso em: 26 out. 2020.

SHEGOKAR, R.; MÜLLER, R. H. Nanocrystals: Industrially Feasible Multifunctional Formulation Technology for Poorly Soluble Actives. **International Journal of Pharmaceutics**, v. 399, n. 1–2, p. 129–139, 31 out. 2010.

SON, Y.-J.; WORTH LONGEST, P.; HINDLE, M. Aerosolization Characteristics of Dry Powder Inhaler Formulations for the Excipient Enhanced Growth (EEG) Application: Effect of Spray Drying Process Conditions on Aerosol Performance. **International Journal of Pharmaceutics**, v. 443, n. 1–2, p. 137–145, 25 fev. 2013.

TAKI, M.; TAGAMI, T.; FUKUSHIGE, K.; OZEKI, T. Fabrication of Nanocomposite Particles Using a Two-Solution Mixing-Type Spray Nozzle for Use in an Inhaled Curcumin Formulation. **International Journal of Pharmaceutics**, v. 511, n. 1, p. 104–110, set. 2016.

TANEJA, S.; SHILPI, S.; KHATRI, K. Formulation and Optimization of Efavirenz Nanosuspensions Using the Precipitation-Ultrasonication Technique for Solubility Enhancement. **Artificial cells, nanomedicine, and biotechnology**, v. 44, n. 3, p. 978–984, maio 2016.

THE UNITED STATES PHARMACOPEIA. **USP 31 NF26s1_c601, General Chapters: <601> AEROSOLS, NASAL SPRAYS, METERED-DOSE INHALERS, AND DRY POWDER INHALERS,**. Disponível em: <http://www.uspbpep.com/usp31/v31261/usp31nf26s1_c601.asp>. Acesso em: 10 set. 2020.

THE UNITED STATES PHARMACOPEIA. <467> RESIDUAL SOLVENTS. v. 42, p. 23, 2020.

TUOMELA, A.; HIRVONEN, J.; PELTONEN, L. Stabilizing Agents for Drug Nanocrystals: Effect on Bioavailability. **Pharmaceutics**, v. 8, n. 2, p. 16, 20 maio 2016.

VEHRING, R. Pharmaceutical Particle Engineering via Spray Drying. **Pharmaceutical Research**, v. 25, n. 5, p. 999–1022, maio 2008.

VIALPANDO, M.; SMULDERS, S.; BONE, S.; JAGER, C.; VODAK, D.; VAN SPEYBROECK, M.; VERHEYEN, L.; BACKX, K.; BOEYKENS, P.; BREWSTER, M. E.; CEULEMANS, J.; NOVOA DE ARMAS, H.; VAN GEEL, K.; KESSELAERS, E.; HILLEWAERT, V.; LACHAU-DURAND, S.; MEURS, G.; PSATHAS, P.; VAN HOVE, B.; VERRECK, G.; VOETS, M.; WEUTS, I.; MACKIE, C. Evaluation of Three Amorphous Drug Delivery Technologies to Improve the Oral Absorption of Flubendazole. **Journal of Pharmaceutical Sciences**, v. 105, n. 9, p. 2782–2793, set. 2016.

VICENTE, J.; PINTO, J.; MENEZES, J.; GASPAR, F. Fundamental Analysis of Particle Formation in Spray Drying. **Powder Technology**, v. 247, p. 1–7, out. 2013.

WANG, J.; HE, W.; CHENG, L.; ZHANG, H.; WANG, Y.; LIU, C.; DONG, S.; ZHA, W.; KONG, X.; YAO, C.; LI, X. A modified thin film method for large scale production of dimeric artesunate phospholipid liposomes and comparison with conventional approaches. **International Journal of Pharmaceutics**, v. 619, p. 121714, 10 maio 2022.

ZHOU, X. Flubendazole Inhibits Glioma Proliferation by G2/M Cell Cycle Arrest and pro-Apoptosis. p. 10, 2018.

CHAPTER 5   OPTIMIZING ADJUVANT INHALED CHEMOTHERAPY: SYNERGISTIC ENHANCEMENT IN PACLITAXEL CYTOTOXICITY BY FLUBENDAZOLE NANOCRYSTALS IN A CYCLE MODEL APPROACH

As the first author, I was responsible for conceptualization, investigation, formal analysis, visualization, writing, project administration and review and editing.

This manuscript is available at:

https://www.sciencedirect.com/science/article/pii/S0378517323007445

5.1 INTRODUCTION

Lung cancer is the second most diagnosed cancer and the leading cause of cancer-related death in 2020 (SUNG *et al.*, 2021b). Lung cancer is divided into the following major subgroups: small cell lung cancer (SCLC) and non-small cell lung cancer (NSCLC), the latter representing approximately 85% of diagnoses (DUMA; SANTANA-DAVILA; MOLINA, 2019). The primary cause is smoking (85 to 90%) (DUMA; SANTANA-DAVILA; MOLINA, 2019), but other risk factors include exposure to environmental asbestos (5 to 10% in the US), air pollution, and genetic factors (DE GROOT *et al.*, 2018). The mortality rate has gradually improved in the last few years due to advances in diagnosis, reductions in smoking, and improvements in treatments involving immunotherapy with tyrosine kinase inhibitors and monoclonal antibodies; as a result, the treatment approach has gradually shifted from palliative to curative (CHAFT *et al.*, 2021). Since platinum-based treatment remains the therapy of choice for patients with nonmetastatic NSCLC and chemotherapy still plays an important role in different stages of the disease (CHAFT *et al.*, 2021; TANG *et al.*, 2022), new strategies that improve the efficacy of available drugs and contribute to increasing patients' quality of life are essential to attain the best new immunotherapy and targeted therapy combined regimens.

Flubendazole (FBZ) is an anthelmintic drug approved for human use with known safety, and its mechanism of action, similar to taxanes, is based on interrupting the cell cycle by specific binding to the β-tubulin subunit of microtubules (ČÁŇOVÁ; ROZKYDALOVÁ; RUDOLF, 2017). The microtubule cytoskeleton is a highly dynamic structure that contains combinations of αβ-tubulin isotypes, which are important to many vital cell functions, such as mitosis; thus, failure in this process initiates the apoptosis cascade, leading to cell death (PARKER *et al.*, 2017). In a wide range of cancers, altered expression in tubulin composition is observed, which may be involved in tumor metastasis and correlated with aggressive and resistant types of the disease (PARKER *et al.*, 2017). NSCLC with high βIII-tubulin expression conferred resistance to vinca alkaloids, a chemotherapeutic class of tubulin-binding agents, resulting in impaired patient recovery from surgical resection and poor survival (PARKER *et al.*, 2017). Many studies have reported efficacy against leukemia, NSCLC, and resistant breast cancer (KIM *et al.*, 2018; MICHAELIS *et al.*, 2015a), but FBZ clinical application is compromised due to poor solubility and consequent poor bioavailability (VIALPANDO *et al.*, 2016).

Our research group has already explored different approaches to overcome this limitation by obtaining a new FBZ maleic acid salt (DE ARAUJO *et al.*, 2018) through hot melt extrusion

via oral administration (DE ASSIS *et al.*, 2022) and intravenous routes (DE SOUZA GONÇALVES *et al.*, 2023), but to repurpose FBZ for lung cancer treatment, delivery through the pulmonary route might be a promising strategy. Pulmonary drug delivery is a noninvasive and convenient route of administration that, in addition to the absence of first-pass metabolism, also presents advantages due to the physiological structure of alveoli, which exhibit a large surface area, thin epithelial barrier, and high vascularization (HAMISHEHKAR; RAHIMPOUR; JAVADZADEH, 2012). Compared to intravenous administration, pulmonary drug delivery results in a higher concentration of drugs in the lungs, which is the most important advantage of this route (KOSMIDIS *et al.*, 2019b). The lower systemic circulation detection of inhaled drugs in clinical trials reduces systemic adverse effects. Additionally, many researchers have observed accumulation in lymph nodes, which might redistribute into the lung; thus, this strategy shows great potential for metastasized cancer (MANGAL *et al.*, 2017b). The main pharmaceutical forms of inhalable formulations are solutions and suspensions, which are delivered as nasal sprays and nebulizers, and dry powders (HADIWINOTO; LIP KWOK; LAKERVELD, 2018b) and are administered through pressurized metered-dose inhalers (pMDI) and dry powder inhalers (DPI) (HAMISHEHKAR; RAHIMPOUR; JAVADZADEH, 2012). DPIs are particularly interesting due to their superior stability and reduced moisture content, capacity to deliver high doses quickly, negligible exposure of health care professionals to environmental contamination, and lack of need for propellants (ROSIÈRE *et al.*, 2019b). This local delivery approach is well established for asthma and other respiratory diseases, and despite being a relatively intuitive strategy for lung cancer, only a few nebulized chemotherapeutic formulations have been tested in clinical trials (ROSIÈRE *et al.*, 2019b). We addressed the low solubility issue by developing FBZ nanocrystals through a nanoprecipitation process and engineered the final dry powder of nanoparticles in microparticles by spray drying the suspension with a carrier, stabilizer, and aerosolization adjuvant. To the best of our knowledge, this research is the first to develop a dry powder formulation of FBZ suitable for oral inhalation and to report the potential benefit of its combination with paclitaxel for lung cancer in vitro.

5.2   MATERIALS AND METHODS

5.2.1   Materials

FBZ was obtained from Changzhou Yabang – QH Pharmachem CO., LTD (China). Poloxamer 188 was kindly donated by BASF Japan (Tokyo, Japan). Mannitol, L-leucine, formic acid, acetonitrile, polyvinylpyrrolidone (PVP K30), polyvinyl alcohol (PVA), and dimethyl sulfoxide (DMSO) were purchased from Wako Pure Chemical (Osaka, Japan). 1,2-Dipalmitoyl-sn-glycero-3-phosphocholine (DPPC) was supplied by TCI (Tokyo Chemical Industry), and PBS tablets were obtained from Takara Bio Inc. (Shiga, Japan). Gibco™ A549 lung cancer cells, RPMI 1640 medium, fetal calf serum, antibiotics (penicillin and streptomycin), and alamarBlue™ reagent were obtained from Thermo Fischer Scientific Inc. Sigma–Aldrich® trypsin and 1X PBS were purchased from Merck Group. Paclitaxel was kindly donated by Eurofarma Laboratórios S.A.

5.2.2   Quality Target Product Profile (QTPP) definition

Quality by design is defined as a systematic approach to product development that starts with the definition of the desired product quality attributes and is based on material and process knowledge to identify critical parameters and attributes that enable risk assessment to ensure product quality ("Guidance for industry. Q8(R2) Pharmaceutical development.," 2009). Considering FBZ physicochemical characteristics, administration route, treatment focus, and knowledge obtained from preliminary tests, QTTP was defined for the intended FBZ inhalable dry powder (Figure 5.1).

Figure 5.1. Quality Target Product Profile (QTPP) for flubendazole (FBZ) inhalable formulation.

Mass median aerodynamic diameter: 1-5 μm

Particles in the range of 1-5 μm mostly settle in central and distant tracts (Loira-Pastoriza et al., 2014), but the majority of the particles larger than 6 μm are retained in the upper respiratory tract (El-Sherbiny et al., 2015), and smaller than 1.0 μm are mostly exhaled by normal breathing (Hadiwinoto et al., 2018).

FBZ particle size: 100 - 500 nm

Aiming increase in solubility ratio and bioavailability once the particle reaches the lung. The average size range was adopted based on commercialized products (Peltonen and Strachan, 2020).

Emitted dose: >40 - 60%

Fraction of formulation that is atomized and leave the device. Although higher ED would be related to higher efficiency, target was defined based on commercially available products (Zarogoulidis et al., 2012).

Dry powder for inhalation

Noninvasive route, with no need of specialized professional for continuous administration, higher stability, and less exposure to the environment (Rosière et al., 2019).

Flubendazole content: 15%

Increase concentration in the site of action, minimizing dose frequency and avoiding unnecessary exposure of excipients to patients. The range for DOE study was determined by preliminary tests.

Fine Particle Fraction: 40%

Target based on commercially available products (de Boer et al., 2017; Zarogoulidis et al., 2012). Fine particle fraction represents the smaller fraction of formulation that could reach the deep respiratory tract and promote the expected local clinical effect.

Source: elaborated by the author.

5.2.3 Risk assessment

The Ishikawa or fishbone diagram (Figure 5.2) shows the process parameters and material attributes involved in the production of the inhalable FBZ dry powder formulation. As the processes for nanoparticle and powder obtention were defined as nanoprecipitation and spray drying, respectively, the process parameters were evaluated to better select the higher-ranked variables that could most impact the final product.

Figure 5.2. Ishikawa diagram for the risk assessment of obtaining flubendazole nanocrystals (FBZ SD NC) with suitable characteristics for administration as inhalable dry powder. Inlet T: inlet temperature.
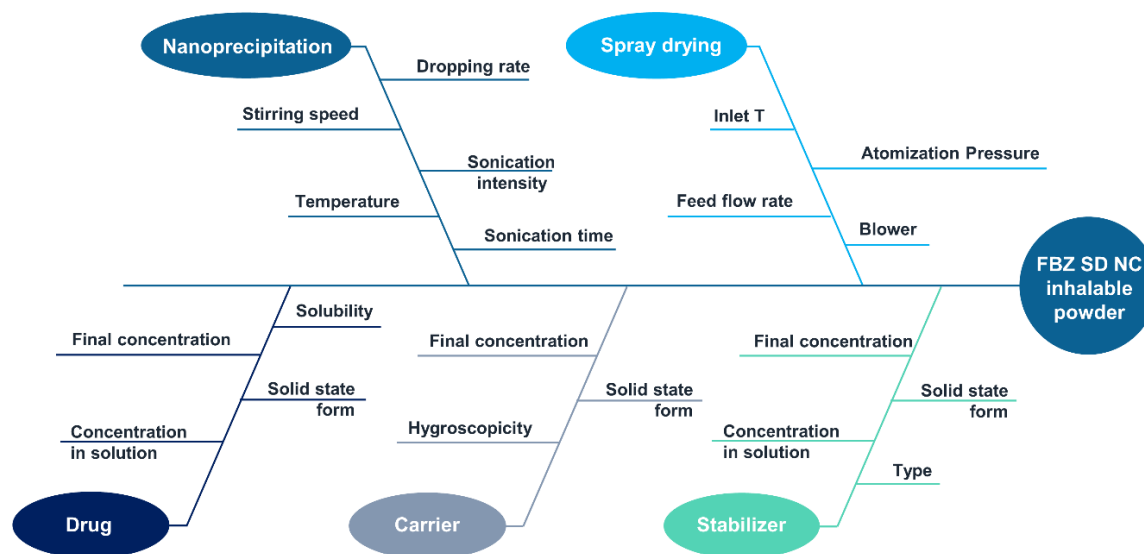
Source: elaborated by the author.

5.2.4 FBZ nanoparticle preparation

FBZ nanoparticles were obtained by the nanoprecipitation method, as previously reported (TANEJA; SHILPI; KHATRI, 2016) with adaptations. Briefly, FBZ was solubilized in formic acid (125 mg/ml) and added to 15 ml of a stabilizer solution (0.5% w/w of PVA, PVP or poloxamer 188 in water) under magnetic stirring and probe ultrasonication (Ultrasonic Disperser, UH-10, SMT Co. LTD.). Ultrasonication continued after addition for 10 minutes. Determination of the nanoprecipitation process parameters and stabilizer type was performed through a univariate study aiming for particle size reduction. The studied variables are organized in Table 5.1. The starting stabilizer solution temperature was 4 °C, and experiments were conducted at room temperature without further cooling. The FBZ concentration in formic acid was fixed, aiming for a high concentration to avoid precipitation issues, and ultrasonication was fixed at 70%. FBZ and chosen stabilizer concentrations were evaluated by a design of experiments.

Table 5.1. Stabilizer and process variables evaluated for nanoprecipitation.

Variable	Parameter
Stabilizer type (at 0.5% w/w)	PVA, PVP and poloxamer 188
Dropping rate	One shot vs dropwise
Time of sonication (min)	5 – 10
Stirring speed (rpm)	400, 600, 800

5.2.5 Formation of dry inhalable particles

Mannitol, with or without L-leucine, was previously solubilized in purified water and added to the obtained FBZ nanosuspension, which was subsequently spray-dried using an NL-3 spray dryer (Ohkawara Kakohki Co. Ltd.; Yokohama, Japan). The investigated process parameters were inlet temperature (120-150 °C), atomization pressure (0.1-0.2 MPa), and feed flow rate (6.6-13.3 g/min). The circulation blower (30 Hz) and solids concentration (0.5% w/w) were maintained constant for all tested formulations. The spray-dried product was recovered and stored at room temperature in a vacuum chamber. Yield, particle size, aerodynamic properties, and polymorphic changes were evaluated.

5.2.6 Design of experiments

To better understand the influences of formulation and process parameters on particle size and aerodynamic properties, a 2^{5-2} (5 factors at 2 levels) fractional factorial design was utilized. Two central points were added to the design, and experiments were conducted randomly. Design Expert 11 (Stat-ease®) software was used for data analysis.

Based on the fractional factorial design results, the process parameters were fixed, and a response surface methodology was employed to further clarify the formulation variables. A central composite design with 2 levels and 3 central points was performed, and the data were combined with previous results from a fractional factorial study to obtain an optimized formulation. The parameters, factor levels, and justification of each choice are detailed in Table 5.2 and Table 5.3.

Table 5.2. Formulation and process parameters studied in the design of experiments for fractional factorial design. The studied range for flubendazole and poloxamer 188 corresponded to the concentration at the final dried product (% w/w).

Parameter	Factor level		Justification
	Low	High	
Flubendazole (%)	5.0	15.0	Range was based on preliminary studies. It was evaluated to maximize loading and to study possible interactions with other process parameters and formulation variables.
Poloxamer 188 (%)	5.0	10.5	Range was based on preliminary studies. Higher concentrations could decrease particle size in nanoprecipitation step, but previous studies reported frequently impaired aerodynamic properties (Buttini et al., 2018).
Inlet air temperature (ºC)	120	150	Inlet air temperature has a direct impact on microparticle formation, regarding shape, moisture, and consequent microparticle size (Vehring, 2008).
Atomization pressure (MPa)	0.1	0.2	Atomization pressure directly influences droplets' size, and consequently, final microparticle size. It is also expected to have a great impact on yield.
Feed flow rate (g/min)	6.6	13.3	The range was defined as 40 to 80% of the equipment drying capacity (1 kg/h). Feed flow rate is related to process efficiency but was included in the study since it determines the amount of suspension that will be atomized, and therefore has an impact on microparticle size and final product moisture.

Table 5.3. Formulation and process parameters studied in the design of experiments for central composite design. The studied range for flubendazole and poloxamer 188 corresponded to the concentration at the final dried product (% w/w).

Parameter	Factor level		Justification
	Low	High	
Flubendazole	5.0	15.0	The range was maintained based on the results of a fractional factorial study focusing on higher drug concentration.
Poloxamer 188	5.0	10.5	The range was maintained based on the results of fractional factorial study given the significant impact on flubendazole particle size after spray drying, fine particle fraction, and MMAD. A more comprehensive study was necessary since it contributed to particle size reduction but impaired aerodynamic properties.

5.2.7 Particle size evaluation

Particle size, before and after spray drying, was determined using a dynamic light scattering instrument (ZetaSizer Nano-ZS; Malvern Instrument Ltd., Malvern, U.K.). Samples were diluted or resuspended in distilled water, and measurements were conducted in triplicate with 15 s intervals at 25 °C.

5.2.8 *In vitro* evaluation of aerosolization performance

The aerosol performances of FBZ inhalable particles were evaluated using an 8-stage Andersen cascade impactor (Andersen nonviable sampler, AN-200; Tokyo Direc Co., Tokyo,

Japan) as previously described with minor modifications (TAKI *et al.*, 2016). The impactor is composed of a throat, an adaptor, and a preseparator, followed by eight stages (0 to 7) with cutoff aerodynamic size ranges of >11.0 μm, 7.0-11.0 μm, 4.7-7.0 μm, 3.3-4.7 μm, 2.1-3.3 μm, 1.1-2.1 μm, 0.65-1.1 μm, and 0.65-0.43 μm (FUKUSHIGE *et al.*, 2020). Briefly, 25 mg of the sample was loaded into a gelatin capsule (size 2, Qualicaps Co. Ltd., Nara, Japan) and assembled in a reverse Jethaler® dry powder inhaler (Tokico System Solutions, Ltd., Kanagawa, Japan). The surface of the collection plates was coated with a silicon spray to minimize particle re-entrainment. The vacuum pump was activated, and the airflow was equilibrated at 28.3 ml/min. After stabilization, the inhaler was connected to the mouthpiece and actuated, and after 10 s, the vacuum pump was turned off. Three actuations were performed to ensure proper recovery. Samples deposited in each stage of the cascade impactor and in the device, capsule, mouthpiece, throat, and preseparator were collected with 5 ml of an acetonitrile/water mixture (60:40 v/v). The FBZ concentration was determined by measuring the absorbance of the sample solution from 300 to 400 nm using a UV–Vis spectrophotometer (Nivo 3S plate reader (PerkinElmer Inc.; Waltham, MA, USA)) and calculating through partial least squares regression using Minitab® 17 software. The fine particle fraction (FPF), emitted dose (ED), median mass aerodynamic diameter (MMAD), and geometric standard deviation were calculated as detailed (THE UNITED STATES PHARMACOPEIA, 2007b).

(2) *FPF* = Sum of recovered mass from stage 3 to 7/Total mass of delivered drug (from the mouthpiece to stage 7)

(3) *ED* = Sum of recovered mass from mouthpiece to stage 7/Total recovered mass (from device to stage 7)

(4) *MMAD* = Size at 50% (cumulated from stage 0 – filter)

(5) $GSD = \sqrt{\text{Size at cum 84.13\%/Size at cum15.87\%}}$

5.2.9 Powder X-ray diffraction (PXRD) and Rietveld refinement

The crystallinity of the spray-dried samples was evaluated by powder X-ray diffraction using a Rigaku Miniflex 600 equipped with Ni-filtered CuKα radiation (λ = 1.5418 Å) and a Lynxeye linear position-sensitive detector and scanned from 3 to 40° 2θ at 4°/min with a voltage of 40 kV and a current of 40 mA. The Rietveld refinement (BEZZON *et al.*, 2021) and the quantitative phase analysis were performed using TOPAS Academic V5 software through the

Fundamental Parameters feature implemented in this software. The crystal structures used in the refinement were obtained from the Cambridge Structural Database® under the reference codes DMANTL (mannitol), PEZLUE (flubendazole) (DE ARAUJO *et al.*, 2018), and LEUCIN02 (L-leucine).

5.2.10 Scanning electron microscopy (SEM)

The sample was deposited on adhesive carbon tape and covered with a Pt-Pd film (E-102 ion sputter; Hitachi, Tokyo, Japan). The morphology of inhalable particles was evaluated using a scanning electron microscope (SEM, S-4300; Hitachi, Tokyo, Japan).

5.2.11 Dynamic vapor sorption (DVS)

Approximately 5 mg of spray-dried formulation was placed in an open platinum plate and added to a platinum plate. Water sorption and desorption were analyzed through a dynamic vapor sorption analyzer (TA Instruments).

5.2.12 Saturation solubility

Saturation solubility was determined by the saturation small-scale shake-flask method at pH 7.4 DPPC 0.02% w/w (MAY *et al.*, 2014). Briefly, an excess of sample was added to 1 ml of medium in 2 ml Eppendorf tubes, closed, and shaken at 200 rpm at 37 °C for 48 h using a Thermo Shaker Incubator MS-100. After centrifugation at 2,000 rpm for 60 min, the supernatant was collected, and the absorbance was measured from 300-400 nm by a UV–Vis spectrophotometer (Nivo 3S plate reader (PerkinElmer Inc.; Waltham, MA, USA)).

5.2.13 Cytotoxicity evaluation

Cytotoxicity was evaluated as previously described with some adaptations (ARNAUD-SAMPAIO *et al.*, 2022). A549 cells were maintained in RPMI 1640 medium supplemented with 10% fetal calf serum and 1% antibiotics (penicillin and streptomycin) at 37 °C in a 5% CO_2 atmosphere. When 90% confluent, cells were seeded into 96-well plates at a density of 1.0 x 10^4 cells/well. After 24 h of incubation at 37 °C, the cells were washed with 1X PBS, RPMI medium without serum or antibiotics was added, and the cells were treated in triplicate according to the concentrations below to evaluate the cytotoxicity of the spray-dried optimized formulation of flubendazole spray-dried nanocrystals (FBZ SD NC). Spray-dried placebo and paclitaxel were used as negative and positive controls, respectively. Paclitaxel was dissolved first in DMSO, and placebo and FBZ SD NC were dissolved in media.

- Paclitaxel treatment after 48 h exposure: 0.3 nM, 1 nM, 3 nM, 10 nM, 30 nM, 100 nM, 300 nM, 1000 nM, and 3000 nM;

- FBZ SD NC treatment: 300 nM, 1000 nM, 3000 nM, 10000 nM, and 30000 nM;

- Placebo 48 h after exposure (mass corresponding to flubendazole concentration in spray-dried formulation): 300 nM, 1000 nM, 3000 nM, 10000 nM, and 30000 nM.

After 48 h of treatment, the medium was removed, and the cells were washed with 1X PBS and incubated for 2 h with a 1:10 (v/v) Alamar Blue® solution in medium without serum in a 5% CO_2 atmosphere at 37 °C. For the blank control, Alamar Blue® solution in the medium was applied directly to empty wells. Fluorescence measurements were performed at 560/590 nm with FlexStation® III, Molecular Devices equipment. Viability data are expressed as a percentage in comparison with the control group.

5.2.14 Combined treatment evaluation

A cycle treatment approach was proposed to compare paclitaxel treatment alone and previous treatment with FBZ SD NC. A549 cells were exposed to paclitaxel for 48 h at the following concentrations: 0.3 nM, 1 nM, 3 nM, 10 nM, 30 nM, 100 nM, 300 nM, 1000 nM, and 3000 nM. For the combined treatment, A549 cells were exposed to FBZ SD NC at 1000 nM for 24 h followed by paclitaxel exposure for 48 h at the same mentioned concentrations. The evaluation was performed in triplicate, and fluorescence measurement was performed using the same method detailed above.

Statistical evaluation was performed employing GraphPad Prism Software Version 8.0. FBZ SD NC versus placebo and paclitaxel (1x) versus FBZ SD NC + paclitaxel (1x) -using two-way ANOVA was followed by Sidak's posttest for multiple comparisons. The synergistic effect was evaluated by two-way ANOVA followed by Dunnett's posttest for multiple comparisons. Differences were considered statistically significant when p values were lower than 0.05.

The combination index (CI) was calculated using the highest single agent (HSA) model, as described in Equation 5, where $CI > 0$ indicates a synergistic effect and $CI < 0$ indicates an antagonistic effect (DUARTE; VALE, 2022). The adopted maximum effect corresponds to the effect of the drug with the highest value.

(6) Combination index (CI) = Maximum effect (paclitaxel or FBZ SD NC)/ Combined effect (paclitaxel + FBZ SD NC)

5.3 RESULTS AND DISCUSSION

5.3.1 FBZ nanoparticle obtention

FBZ exhibits poor solubility in water as well as many organic solvents and lipids; thus, with many types of nanocarriers, such as liposomes and solid lipid nanoparticles, promoting viable drug loading is challenging (VIALPANDO *et al.*, 2016). Nanocrystals, on the other hand, are composed of 100% drug and can be produced by a simple precipitation process, as long as they can be solubilized in a solvent miscible with antisolvent (MÜLLER; GOHLA; KECK, 2011a). A possible solvent for FBZ is dimethyl sulfoxide, a widely known solvent in *in vitro* experiments (ZHOU *et al.*, 2018) and quantification methods (LAURA *et al.*, 2015), which has already been reported for the preparation of FBZ for intravenous administration (MORENO *et al.*, 2004). Unfortunately, the extremely high boiling point of 189 °C (PUBCHEM,) hinders elimination through spray drying. Several solvents can be accepted without justification, including formic acid, a class 3 solvent; other commonly used substances, such as ethanol and acetone; and residual solvents in the range of 5,000 ppm (ICH, 2017). FBZ presents a high solubility in formic acid (340 mg/ml), which has already been explored by Vialpando and colleagues for obtaining amorphous FBZ formulations by spray drying with 9.8-18.2% loading through a 90:10 (v/v) solution of dichloromethane and formic acid (VIALPANDO *et al.*, 2016). Although this solvent is classified as class 3, regarded as less toxic and exhibits lower risk to human health, this amount would demand regulatory justification (THE UNITED STATES PHARMACOPEIA, 2020) and could impact downstream processability (VIALPANDO *et al.*, 2016). Through the nanoprecipitation method, the amount of formic acid could be reduced to less than 1% in the final nanosuspension for spray drying, and the need for a second organic solvent could be eliminated.

Therefore, FBZ was solubilized in formic acid and added to different steric stabilizer solutions (PVP, PVA, and poloxamer 188) at 0.5% (w/w) under sonication. In the nanoprecipitation process, the nanoparticles are smaller and more uniform when the solvent and antisolvent are more efficiently mixed and the diffusion of antisolvent in the system is more uniform (SINHA; MÜLLER; MÖSCHWITZER, 2013). As depicted in Table 5.4, poloxamer 188 provided the smallest particle size of 177.1 nm at 5 minutes. This could be due to the presence of amphiphilic block polymer, which in addition to the hydrophilic polyethylene oxide chains that provide steric stabilization, allows adsorption on the surface of nanocrystals by hydrophobic interactions with polypropylene oxide chains (TUOMELA; HIRVONEN; PELTONEN, 2016b). Poloxamer 188 is a nonionic copolymer (OWEN, S.C., 2006) that was

reported for the stabilization of different nanosuspension preparations, such as glimepiride, itraconazole and paclitaxel (GU *et al.*, 2013), and for orally inhaled powder preparations (SON; WORTH LONGEST; HINDLE, 2013). In addition to providing better stabilization, dropwise addition of FBZ solution in a higher stirring speed condition could favor a more efficient mixing, resulting in faster nucleation in smaller and more uniform particles.

Table 5.4. Flubendazole nanoparticle size and polydispersity index (PDI) optimization through univariate study of nanoprecipitation process parameters. The stabilizer concentration was fixed at 0.5% w/w; particle size and PDI values represent the mean of triplicate analyses.

Stabilizer	Dropping rate	Stirring speed (rpm)	Ultrasonication time (min)	Particle size (nm)	PDI
PVP	Dropwise	600	5	251.3 ± 3.2	0.220 ± 0.027
PVA	Dropwise	600	5	208.2 ± 2.3	0.247 ± 0.011
Poloxamer 188	Dropwise	400	5	193.4 ± 1.5	0.199 ± 0.012
		400	10	177.9 ± 2.9	0.197 ± 0.017
		600	5	177.1 ± 1.7	0.229 ± 0.004
		600	10	164.2 ± 0.8	0.215 ± 0.006
		800	5	181.1 ± 1.0	0.221 ± 0.005
		800	10	169.6 ± 1.1	0.187 ± 0.014
	One shot	600	5	332.6 ± 3.1	0.354 ± 0.045
		600	10	254.5 ± 4.1	0.338 ± 0.049

No expressive difference was found for the studied stirring speed range, but it was observed that higher speeds helped improve the dispersion of the FBZ solution as the drops were added. However, the incorporation of air was more likely to occur at 800 rpm, decreasing the efficiency of particle size reduction. Hence, a stirring speed of 600 rpm was selected.

5.3.2 Formation of dry inhalable microparticles

A systemic preclinical toxicity study of a new FBZ amorphous solid dispersion was conducted by Janssen Pharmaceutica to target filarial treatment through oral formulation (LACHAU-DURAND *et al.*, 2019). It exhibited good bioavailability, and no Cmax-related effects in cardiovascular and central nervous systems were detected; however, repeated dosing was necessary to maintain plasmatic levels and genotoxicity results, leading to toxicity, and the researchers concluded that no treatment regimen could be selected and justified for this aim

(LACHAU-DURAND *et al.*, 2019). In contrast, many studies have reported the potential of FBZ for the treatment of different types of cancer. *In vitro,* tests showed efficacy against myeloma, leukemia (SPAGNUOLO *et al.*, 2010), glioma (ZHOU, 2018), several lines of neuroblastoma (MICHAELIS *et al.*, 2015b) and breast cancer (ČÁŇOVÁ; ROZKYDALOVÁ; RUDOLF, 2017). Moreover, it suppressed tumor growth *in vivo* against xenograft models of leukemia and triple-negative and resistant types of breast cancer (ČÁŇOVÁ; ROZKYDALOVÁ; RUDOLF, 2017; KIM *et al.*, 2018). In those studies, FBZ is usually prepared for intravenous administration with polysorbate 80 and dimethyl sulfoxide (ČÁŇOVÁ; ROZKYDALOVÁ; RUDOLF, 2017; KIM *et al.*, 2018). Like FBZ, many drugs have limitations regarding safety and lack of efficacy in clinical trials, sometimes associated with dose-dependent systemic toxicity. To increase local concentration, dry inhalable particles were proposed as feasible formulations through spray drying FBZ nanosuspensions. As flubendazole spray-dried microparticles with increased concentrations showed greater cohesiveness, mannitol was added to the formulation as a carrier to improve flowability and particle dispersion (HAMISHEHKAR; RAHIMPOUR; JAVADZADEH, 2012).

Using poloxamer 188 as a stabilizer and previously discussed conditions for nanoprecipitation, a fractional factorial study was performed as shown in Table 5.5. The impact of each studied parameter was evaluated and is organized in Table 5.6.

Table 5.5. Factors and responses of fractional factorial design. Factors: flubendazole (FBZ) and poloxamer 188 concentration considering % w/w at the final dried product; inlet temperature (inlet T); atomization pressure; and feed flow rate. Responses: flubendazole particle size before (Z-ave before SD) and after spray drying (Z-ave after SD); yield; emitted dose (ED); final particle fraction (FPF); and mass median aerodynamic diameter (MMAD).

Run	Factors					Responses					
	FBZ (%)	Poloxamer 188 (%)	Inlet T (°C)	Atomization (MPa)	Feed flow rate (%)	Z-ave before SD (nm)	Z-ave after SD (nm)	Yield (%)	ED (%)	FPF (%)	MMAD (μm)
1	15	3.5	150	0.10	13.3	211.3	573.3	60.1	82.9	43.3	2.99
2	15	10.5	150	0.20	13.3	214.3	343.0	44.4	78.5	19.7	3.81
3	15	3.5	120	0.20	13.3	203.7	1218	23.1	95.2	33.0	3.29
4	15	10.5	120	0.20	6.6	216.2	327.5	31.8	67.5	27.3	3.24
5	10	7.0	135	0.15	9.9	189.2	384.9	50.7	74.6	41.1	3.07
6	5	10.5	120	0.10	6.6	188.4	252.6	58.8	87.5	14.3	3.65
7	5	10.5	120	0.20	13.3	202.1	798.8	33.5	94.0	15.3	3.94
8	10	7.0	135	0.15	9.9	169.6	333.2	50.8	68.5	31.6	3.18
9	15	3.5	150	0.20	6.6	217.0	593.8	36.7	71.2	21.2	2.79
10	5	3.5	150	0.20	13.3	197.4	430.4	43.8	51.5	23.2	3.46
11	5	3.5	120	0.10	13.3	176.1	1186.0	55.4	85.9	26.4	4.41
12	15	10.5	150	0.10	6.6	213.9	327.0	59.0	84.6	16.6	3.96
13	5	10.5	150	0.20	6.6	251.2	274.2	39.2	83.2	24.2	3.68
14	5	3.5	150	0.10	6.6	191.8	471.6	62.9	80.6	44.3	3.30
15	5	3.5	120	0.20	6.6	194.3	323.7	31.7	60.3	37.0	2.76
16	15	3.5	120	0.10	6.6	209.1	627.8	59.7	70.6	31.4	2.87
17	15	10.5	120	0.10	13.3	217.2	441.3	61.2	88.6	26.7	3.98
18	5	10.5	150	0.10	13.3	219.3	373.2	58.3	93.2	18.4	4.14

Table 5.6. Influence of parameters evaluated through fractional factorial design. Factors: (A) flubendazole (FBZ) and (B) poloxamer 188 concentration considering % w/w of the final dried product; (C) inlet temperature (inlet T); (D) atomization pressure; and (E) feed flow rate. Responses: yield; emitted dose (ED); final particle fraction (FPF); mass median aerodynamic diameter (MMAD); and flubendazole particle size after spray drying (Z-ave after SD).

	Yield	ED	FPF	MMAD	Z-ave after SD
A: FBZ Loading	-	-	-	-	-
B: Poloxamer 188	-	↑	↓↓	↑↑	↓↓
C: Inlet temperature	-	-	-	-	↓
D: Atomization pressure	-	↓	-	-	-
E: Feed flow rate	-	-	-	↑	↑↑
AB interaction	-	↓	-	-	-
AE interaction	-	-	↑	-	-
CE interaction	-	↓	-	-	↓

↓ and ↑ are used to represent $p < 0.05$ for decreasing or increasing the response, respectively, and ↓↓ and ↑↑ are used when $p < 0.005$.

5.3.3 Main effects

Poloxamer 188 was the only factor that caused a significant impact on all studied responses, contributing to FBZ stabilization in the final dried product and increasing the emitted dose. As previously reported, stabilizers do not favor aerosolization properties (BUTTINI *et al.*, 2018), and the capacity of behaving as a wetting agent (MERUVA *et al.*, 2020) could have contributed to microparticle aggregation and led to increased MMAD. Therefore, despite reducing electrostatic and facilitating the release of powder from the device, it also impaired FPF. The increase in MMAD is more expressive at a higher concentration (10.5%) of poloxamer 188 and lower atomization pressure (0.1 MPa), in which a larger droplet with an abrupt increase in viscosity in the drying droplet (C. ANANDHARAMAKRISHNAN, PADMA ISHWARYA S., 2015) could intensify microparticle aggregation. Although the inlet temperature range of 120 to 150 °C is much higher than its melting point (52 °C), the heated air promotes drying of the droplet and form particles within a few seconds, with minimum exposure (C. ANANDHARAMAKRISHNAN, PADMA ISHWARYA S., 2015). Additionally, outlet temperatures were not higher than 85 °C during all processes, with an average of 75 °C, and no interaction was found between stabilizer concentration and inlet temperature for the FPF response, reducing the probability that poloxamer 188 melting would impact FPF for the studied range.

The inlet temperature and feed flow rate were also significant. A higher inlet temperature (150 °C) and lower feed flow rate (6.6 g/min) led to a smaller FBZ particle size. Since FBZ exhibited poor water solubility, nanocrystals will likely be in close contact with poloxamer 188 while in suspension. As the solvent is removed by exposure to heated air, the saturation in the droplet surface increases along with viscosity, resulting in nanoparticle aggregation, as reported by Jog and Burgess (JOG; BURGESS, 2019). As the drying rate increases, it promotes drying before collision between particles, leading to minimized aggregation of FBZ nanoparticles. Therefore, conditions that contributed to the generation of smaller droplets and a fast drying rate were confirmed to decrease aggregation and consequent FBZ particle size. On the other hand, Kumar and colleagues reported that higher inlet temperatures (196 °C) contributed to an increase in indomethacin nanocrystal size, but this observation was explained by the generation of surface defects and amorphization due to proximity to the drug melting point of 158 °C (KUMAR; GOKHALE; BURGESS, 2014). Since FBZ has a high melting temperature of 238 °C (VIALPANDO *et al.*, 2016), this event was not observed, as preservation of the crystalline structure was confirmed later by XRPD and Rietveld refinement analysis (Figure 5.6).

Lower atomization pressure (0.1 MPa) showed no effect on FBZ particle size but favored an increase in emitted dose, revealing a parameter set for 5% FBZ and 3.5% poloxamer 188, with 471.6 nm, 80.6% ED and 44% FPF (Table 5.5). Since atomization pressure has a direct impact on droplet size, the final particles were expected to be smaller; however, no correlation was observed between MMAD and FPF, perhaps due to the studied range and reduced number of experiments. As the particle size decreases, an increase in electrostatic charges in the spray-dried product with adherence to equipment walls is commonly reported (Dobrowolski et al., 2018). These electrostatic charges also contribute to microparticle agglomeration, which could explain the observed decrease in ED. The particle formation mechanism depends on many variables, but as poloxamer 188 concentration showed a significant and opposite effect on established QTPPs, optimization would be necessary to increase FBZ loading.

5.3.4 Interactions

As the model applied is a fractional factorial study, interactions should be analyzed with caution since the discrimination power is not high. The poloxamer 188 concentration showed that a more comprehensive study was necessary to find an optimal amount for the formulation, which would simultaneously stabilize the FBZ particle size and not impair the aerosolization properties. Other main factors showed simpler behavior, indicating that a higher inlet

temperature, lower atomization pressure, and lower feed flow rate would favor the characteristics of interest.

Although FBZ did not directly influence responses, it revealed possible interactions between poloxamer concentration and feed flow rate that could influence ED and FPF. Therefore, the FBZ concentration was included in the next step of the response surface design experiments for formulation optimization, particularly aiming at higher drug loading.

5.3.5 Optimizing the formulation for high drug loading

The results obtained from the response surface design experiments are presented in Table 5.7. 3D response surface plots could be constructed for 4 responses from a combination of both presented designs (Figure 5.3). With an increased number of experiments, the impact of atomization pressure and inlet temperature on yield could also be distinguished, but ED was not significant.

Figure 5.3. 3D response surface plot for (A) particle size after spray drying; (B) yield; (C) FPF and (D) mass median aerodynamic diameter (MMAD), generated with a combination of results from fractional factorial (Table 5) and response surface methodology (Table 7) at chosen formulation (FBZ 15% w/w; poloxamer 188 3.5% w/w) and parameters (150 °C inlet temperature and 0.1 MPa atomization pressure).
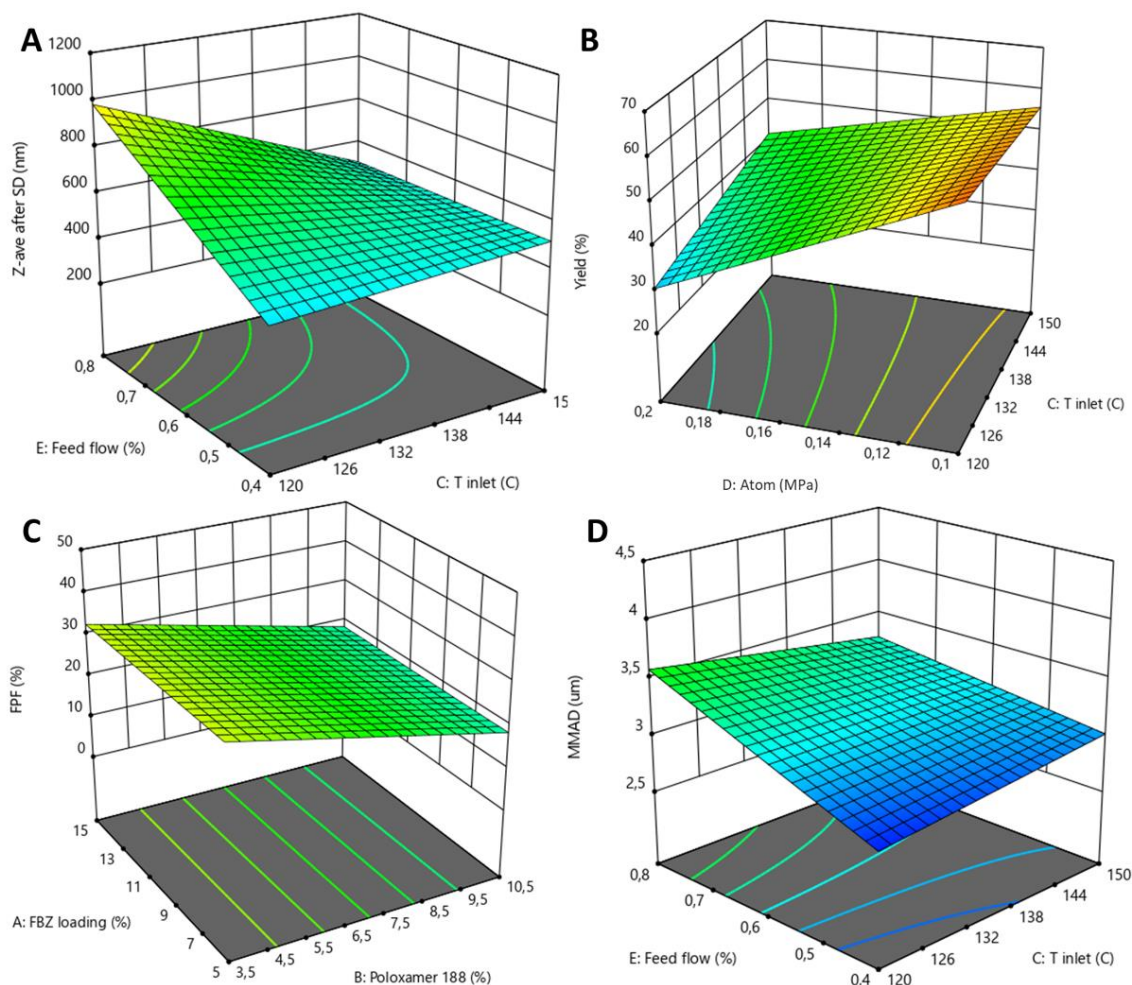
Source: elaborated by the author.

High inlet temperature and low atomization pressure seem to generate a higher yield. A higher inlet temperature contributes to an increase in the drying rate, minimizing moisture-related stickiness of the particles on the spray dryer walls. Some studies that report increased electrostatic forces for smaller particles used an electrostatic precipitator as a common procedure to increase the recovery of smaller particles (0.1 to 1.0 µm) after spray drying (DOBROWOLSKI *et al.*, 2018). Atomization pressure can directly influence the size of the final particle, as it dictates droplet size (HADIWINOTO; LIP KWOK; LAKERVELD, 2018b). Therefore, the decrease in yield generated by increasing atomization pressure can be explained by the loss of smaller particles that are not efficiently retained in the cyclone using a standard configuration.

Table 5.7. Factors and responses of response surface methodology. Factors: flubendazole (FBZ) and poloxamer 188 concentration considering % w/w at the final dried product. Responses: flubendazole particle size before (Z-ave before SD) and after spray drying (Z-ave after SD); yield; emitted dose (ED); final particle fraction (FPF); mass median aerodynamic diameter (MMAD).

Run	Factors		Responses					
	FBZ	Poloxamer 188	Z-ave before SD	Z-ave after SD	Yield	ED	FPF	MMAD
	(%)	(%)	(nm)	(nm)	(%)	(%)	(%)	(μm)
1	15.0	10.5	213.9	872.7	59.0	84.6	16.6	3.96
2	5.0	3.5	191.8	809.1	62.9	80.6	44.3	3.30
3	15.0	3.5	198.0	494.6	49.5	76.4	35.0	3.09
4	10.0	7.0	199.1	424.3	45.4	56.4	32.9	3.25
5	10.0	7.0	211.2	549.8	51.6	48.2	29.3	3.40
6	10.0	7.0	202.6	500.2	54.5	54.8	36.4	3.46
7	10.0	11.9	171.1	358.3	56.8	65.4	14.7	3.85
8	5.0	10.5	147.5	310.1	62.4	49.9	5.3	4.26
9	2.9	7.0	149.8	531.2	56.8	14.5	20.1	3.30
10	17.01	7.0	182.3	620.1	53.2	79.4	37.8	3.12
11	10.0	2.0	219.1	507.3	53.4	57.2	34.4	3.08

Combining all the response surfaces, it was possible to build an overlay plot (Figure 5.4) to clarify the final design space. Since FPF was modulated by poloxamer 188, based on previously established QTPPs, we set the following as the target to maximize FBZ concentration with a minimum negative impact on aerodynamic properties: final FBZ particle size of 480 nm, FPF lower than 28.5% and MMAD lower than 3.2 μm.

According to the obtained design space, concentrations of 15% FBZ and 5% poloxamer 188 were chosen to validate the model. The obtained results are organized in Table 8 and compared to the predicted values. With the good correlation of the model, most responses were close to the predicted values, but FPF (22.6%) was lower than expected.

Figure 5.4. Overlay plot showing the design space (yellow region) and experimental conditions (gray region). The desired condition was restricted considering FBZ particle size after spray drying (Z-ave after SD) smaller than 480 nm, fine particle fraction (FPF) higher than 28.5%, and mass median aerodynamic diameter (MMAD) smaller than 3.2 μm.
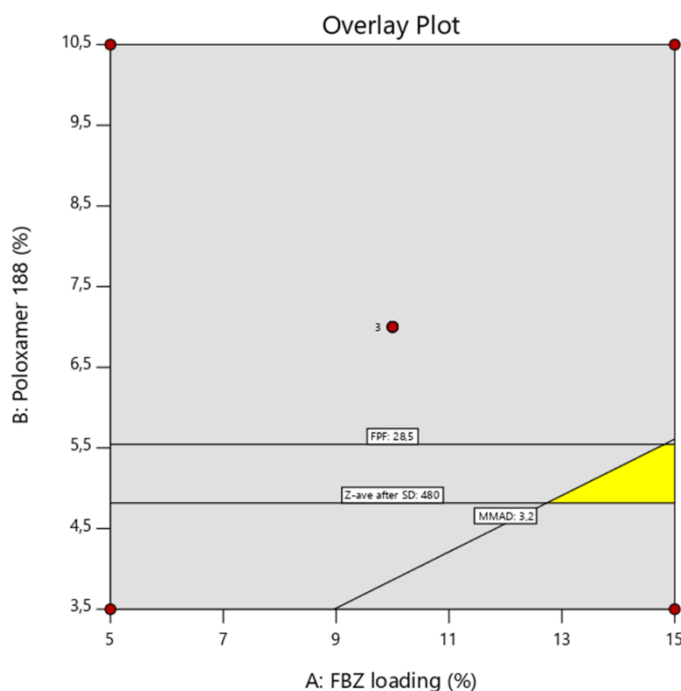
Source: elaborated by the author.

Table 5.8. Predicted vs. obtained responses for the chosen formulation and process parameters.

	Z-ave after SD (nm)	Yield (%)	FPF (%)	MMAD (μm)
Predicted	474.9	55.8	29.6	3.15
Observed	502.9	55.1	22.6	3.50

FBZ has exhibited promising potential against cancer cell lines (MICHAELIS *et al.*, 2015b), including resistant breast and leukemia cancer cell lines, with a reported IC90 of approximately 5 μM for lung cancer cells (MICHAELIS *et al.*, 2015b). As an anthelmintic, FBZ is commercially available for oral administration in humans but exhibits low bioavailability, with a reported maximal plasma concentration (Cmax) lower than 5 ng/ml even after the intake of 2 g (ČÁŇOVÁ; ROZKYDALOVÁ; RUDOLF, 2017). An intravenous administration preclinical study of a new amorphous solid dispersion with an equivalent 20 mg/kg (9.48% w/w) showed an increased Cmax of 473 ± 126 ng/mL in rats; however, there were concerns regarding efficacy in humans at safe exposure levels due to the tubulin binding-associated side effects and necessity of frequent administration of high doses (LACHAU-DURAND *et al.*, 2019). Dose reduction could be achieved by pulmonary administration of the obtained FBZ nanocrystals,

but a formulation with suitable aerosolization properties is essential to promote deep lung delivery and achieve the intended local effect.

Although many studies have administered lung cancer treatment through pulmonary delivery, the translation of preclinical studies to clinical trials is incipient, with no reported dry powder formulations (ROSIÈRE *et al.*, 2019b). Possible reasons include the toxicity concern regarding the delivery of a new drug to the lung and the lack of safety information on excipients (OSTERBERG; SEE, 2003). Therefore, we first focused on obtaining the simplest formulation consisting of a drug, stabilizer, and carrier that could deliver maximum FBZ loading. Poloxamer 188 is used in oral and intravenous and topical administration (MÜLLER; MAÈDER; GOHLA, 2000). Compared with polysorbate 80, an FDA-approved surfactant for pulmonary delivery (METZ, 2020), poloxamer 188 presented better results by the air-liquid interface method, with no detected toxicity (LINDENBERG *et al.*, 2019); after evaluation in different cell lines, the drug was considered safe for pulmonary applications (STEINER *et al.*, 2019). Mannitol was safely administered as a challenge test for asthmatic patients, and a phase III study concluded that the treatment could be regarded as safe and well tolerated at doses of approximately 150 mg of mannitol (BRANNAN *et al.*, 2005). Mannitol has already been approved in products that have reached the market, such as Bronchitol® and Exubera®, and belongs to the list of generally recognized safe products by the FDA (HERTEL; BIRK; SCHERLIESS, 2020). We successfully obtained a formulation of 5% FBZ with 3.5% poloxamer 188 and mannitol as carriers with good aerosolization properties. However, after a more comprehensive study through a response surface methodology, our results revealed a limitation regarding drug loading, which prevents more satisfactory performance. Since the FPF needed to be improved to meet the established QTPP, a force control agent that could reduce cohesive forces between particles, which would contribute to an enhanced inhalable fraction, was needed (YE; MA; ZHU, 2022a).

L-leucine, an essential amino acid, has been approved for oral and intravenous administration and shows great promise for its potential in inhalation applications as well. In a study on capreomycin dry powder, single doses of up to 60 mg of leucine were administered by inhalation to patients, and no alteration was observed; even after daily exposure during a 24-week treatment, L-leucine was observed to be well tolerated (ZILLEN *et al.*, 2021). Its use as a lubricant or force control agent, which was reported to increase aerosolization (SCHOUBBEN *et al.*, 2019), is widely described in the literature (ZILLEN *et al.*, 2021). To improve the aerosolization properties for higher FBZ loading, 10 and 20% L-leucine were added to the optimized formulations.

As seen in Table 5.9, L-leucine not only improved FPF (50.3%), ED (83.2%), and MMAD (2.9 μm) but also seemed to contribute to FBZ nanocrystal stabilization (388.6 nm). This contribution may result from the lubrication property exhibited by L-leucine while recovering microparticles and the protection against humidity, as previously described (MANGAL *et al.*, 2018). L-leucine is a weak surfactant that can improve dispersibility by acting on interparticle forces (VEHRING, 2008). With low water solubility (22 mg/ml) (VEHRING, 2008), saturation inside the droplet environment is reached sooner. This leads to crystallization and encapsulation of the polymer and other formulation components, which form a hydrophobic shell (JÜPTNER; SCHERLIESS, 2019) and further promote changes in morphology (ZILLEN *et al.*, 2021). This L-leucine shell also seemed to protect the FBZ nanoparticle interaction, which can explain the better stabilization.

One important factor that influences morphological changes during spray drying is the Peclet number (Pe), which is the ratio between the drying rate of a droplet and the diffusion rate of solutes from the edge to the center of a droplet (C. ANANDHARAMAKRISHNAN, PADMA ISHWARYA S., 2015). Assuming that the drying rate remains constant for the entire process, when the diffusion rate is much higher than the evaporation rate (Pe<<<1), particles can evenly redistribute during evaporation, leading to a solid particle of higher density (C. ANANDHARAMAKRISHNAN, PADMA ISHWARYA S., 2015; VEHRING, 2008). In contrast, when the evaporation rate is much higher than the capacity of particles to diffuse (Pe>>>1), species become trapped as the droplet surface recedes, leading to a rapid increase in viscosity with consequent shell formation (C. ANANDHARAMAKRISHNAN, PADMA ISHWARYA S., 2015; VEHRING, 2008). In this case, since we are spray-drying a nanosuspension, the presence of the suspended material contributes to a high Pe number and a thin shell formation (VEHRING, 2008), which can be confirmed by SEM images (Figure 5.5). No significant changes could be observed between the morphology of spray-dried placebo (Figure 5.5B) and the formulation containing 5% FBZ (Figure 5.5C). However, when the concentrations of FBZ and poloxamer 188 were increased to 15% to 1.5%, respectively, the concentration of suspended particles increased, and the smooth and round shapes became irregular and semicollapsed particles. Additionally, when increasing the L-leucine concentration and consequently reducing the mannitol concentration, the shape is subjected to further change; as a result, more collapsed raising-like structures are generated, which corroborates the previously reported observation (JÜPTNER; SCHERLIESS, 2019).

Figure 5.5. Scanning electron microscopy (SEM) of (A) flubendazole drug; (B) spray-dried placebo; (C) RUN 14 of fractional factorial DoE of 5% flubendazole and 3.5% poloxamer 188; (D) spray-dried batches of the optimized formulation with no addition of L-leucine; (E) addition of 10% L-leucine; and (F) addition of 20% L-leucine.
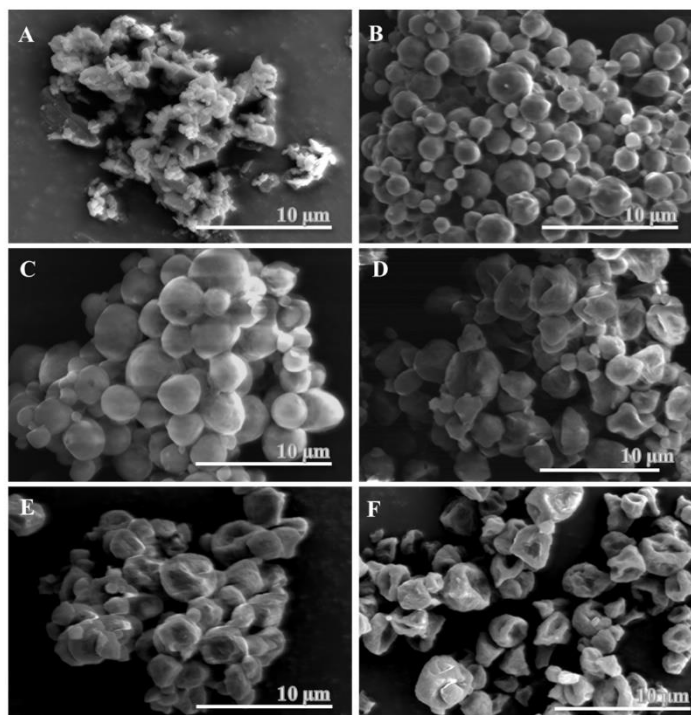
Source: elaborated by the author.

Table 5.9. Obtained particle size results and aerosolization performance after addition of different concentrations of L-leucine for the chosen formulation and spray drying conditions (flubendazole at 15% w/w and poloxamer 188 at 5% w/w, in which the weight difference was compensated with mannitol; 150 °C inlet temperature; 6.6 g/min feed flow rate and 0.1 MPa atomization pressure). Responses: flubendazole particle size before (Z-ave before SD) and after spray drying (Z-ave after SD), emitted dose (ED), fine particle fraction (FPF), and mass median aerodynamic diameter (MMAD).

L-Leucine (%)	Z-ave before SD (nm)	Z-ave after SD (nm)	ED (%)	FPF (%)	MMAD (µm)
0	174.5	502.9	43.5%	22.6%	3.5
10	177.0	437.1	61.6%	30.4%	3.1
20	174.4	388.6	83.2%	50.3%	2.9

5.3.6   Physicochemical characterization

The final optimized formulation (15% FBZ, 5% poloxamer 188, 20% L-leucine, and 60% mannitol) was tested for saturation solubility. This result (14.73 ± 2.3 µg/mL) showed a 3-fold increase compared with conventional FBZ (4.53 ± 0.1 µg/mL). This effect can be explained by the Ostwald-Freundlich equation, which correlates an exponential increase in solubility with solid particle radius reduction (MÜLLER; GOHLA; KECK, 2011a).

Substances that exhibit a long-range molecular arrangement with a regular pattern are classified as crystals (PELTONEN; STRACHAN, 2020). Molecular conformations and interactions minimize Gibbs free energy and are therefore more thermodynamically stable than irregular or disordered substances (e.g., amorphous dispersions) (PELTONEN; STRACHAN, 2020). This high-energy form with weaker bonding forces is easier to solubilize and consequently presents a higher dissolution rate (PELTONEN; STRACHAN, 2020) and is a commonly desired characteristic for a spray-dried product (JERMAIN; BROUGH; WILLIAMS, 2018, p.; SHETTY *et al.*, 2018b). A nanocrystal is an intermediary form in terms of organization and stability, providing an increase in solubility without affecting bioavailability (PELTONEN; STRACHAN, 2020).

The presence of L-leucine, mannitol, and FBZ was confirmed by Rietveld refinement for crystalline structures. Figure 5.6. Rietveld plot showing a good fit between calculated and observed patterns where blue arrows indicate the FBZ main peaks. presents the Rietveld plot from the refinement, indicating that the calculated and observed patterns are well-adjusted, which is confirmed by the agreement factors of $R_{wp} = 5.38\%$ and gof = 1.59. The quantitative phase analysis performed with refinement results reveals a mass proportion of 14.11% for FBZ, 21.59% for L-leucine, and 64.31% for mannitol, which confirms that the FBZ crystalline structure was preserved. The FBZ main peaks are indicated by the blue arrows.

Figure 5.6. Rietveld plot showing a good fit between calculated and observed patterns where blue arrows indicate the FBZ main peaks.
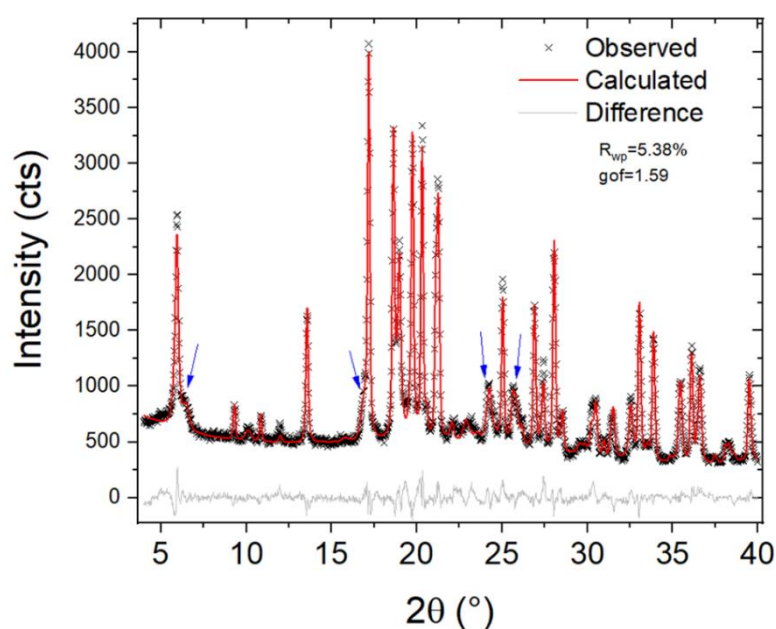
Source: elaborated by the author.

Lactose remains the most commonly used carrier for DPI (LITTRINGER *et al.*, 2012), but mannitol can provide stability advantages regarding degradation and humidity exposure; this was observed by Shetty and colleagues after they compared different spray-dried ciprofloxacin formulations obtained with different carriers (SHETTY *et al.*, 2018a). They observed a significantly lower water absorption for formulations with mannitol as a carrier (4.48% (w/w) between 0% and 60% RH) compared to lactose or trehalose (10% and 9% (w/w) between 0% and 60% RH, respectively) (SHETTY *et al.*, 2018a). The FBZ SD NC formulation is composed of nonhygroscopic components and exhibits favorable stability, as the water vapor sorption desorption isotherm (Figure 5.7) shows the beginning of water sorption at 30% RH, which increases in a more pronounced way at 60% RH. However, even at 80% RH, water sorption remains at 2% weight with a reversible loss according to the desorption cycle.

Figure 5.7. Water vapor sorption desorption isotherm for the dry powder formulation (SD FBZ NC).
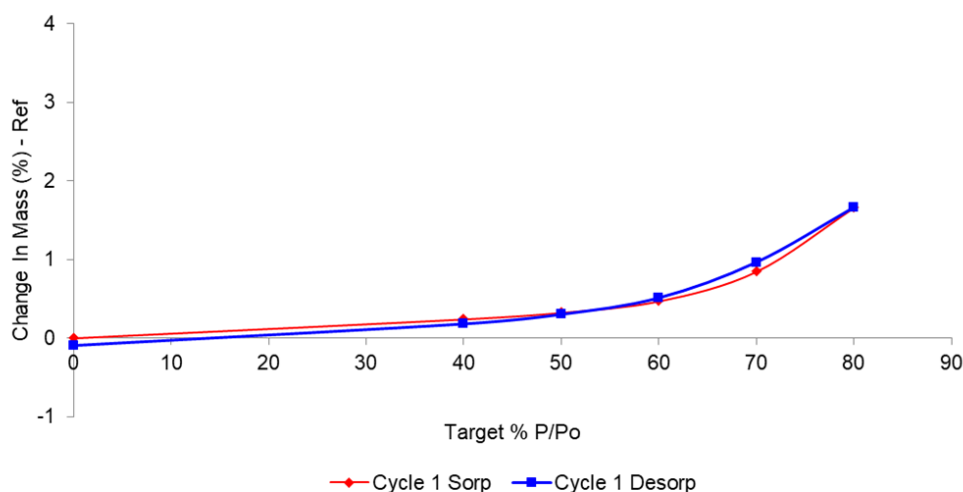
Source: elaborated by the author.

5.3.7 Cytotoxicity assay

The cytotoxicity of FBZ SD NC was evaluated with an Alamar Blue® assay in A549 lung cancer cells (Figure 5.8A). After 48 h of exposure, spray-dried placebo indicated that the used excipients exhibited no toxicity, as viability remained at 100%, but a plateau at 75% survival was observed for the 3,000 nM FBZ SD NC formulation.

Paclitaxel is a well-established drug for the treatment of lung cancer (HARDY *et al.*, 2010) and, as a tubulin-binding agent, presents a similar mechanism of action to FBZ (PARKER *et al.*, 2017). Cytotoxicity evaluation in A549 cells after 48 h showed a progressive reduction in cell viability. The maximum effect (approximately 50% of total cell viability) was observed

from 1000 nM, and no increase was observed with the subsequent concentration of 3000 nM, indicating that A549 cells are intrinsically resistant to paclitaxel (Figure 5.8B). However, when cells were previously exposed to the FBZ SD NC formulation, a marked 1,000-fold reduction in IC_{50} was observed. When the highest single agent (HSA) method was used to evaluate the effects of cytotoxicity at 300 nM for paclitaxel (57,86%) and the combined treatment (29,79%), the combination index was determined to be 3.5, suggesting that these concentrations exhibit a synergistic effect (DUARTE; VALE, 2022). Other studies revealed a synergistic effect of paclitaxel against A549 cells, such as the association with jasmine oil (ENGELBERG *et al.*, 2021). The DNA-PK inhibitor M3814 also potentiated the paclitaxel cytotoxic effect, but this major dose reduction with a relatively low concentration of FBZ SD NC could significantly contribute to lowering the adverse effects of a paclitaxel chemotherapy regimen.

Treatment cycles of drug combinations are a common clinical practice as a strategy to overcome drug resistance and increase effectiveness and have been reproduced in several studies *in vitro* to better explore and prevent failure in future clinical trials (PATWARDHAN *et al.*, 2021). The combination of paclitaxel and FBZ SD NC, a novel oral inhaled formulation, exhibits a synergistic effect on the cytotoxicity of tumor cells. Thus, compared with using paclitaxel alone, when paclitaxel is used in cells pretreated with FBZ SD NC, it leads to a more pronounced inhibitory effect on cell growth or induction of cell death, and repeated paclitaxel treatment cycles can improve the outcome. Under the 1-cycle paclitaxel regimen, administered at a dose of 1000 nM, approximately 30% of cells retained their viability. On the other hand, the 3-cycle chemotherapy regimen, which involves multiple rounds of paclitaxel treatment, resulted in a significantly lower cell viability rate of 15% compared to the 50% cell viability obtained without the presence of FBZ SD NC in the treatment protocol. The combination of paclitaxel and FBZ SD NC in a novel oral inhaled formulation seems to offer advantages in the treatment of lung cancer, as the cytotoxicity of tumor cells is enhanced with the lowest doses of paclitaxel. Therefore, this combination therapy might have the potential to reduce the adverse effects associated with paclitaxel. Additionally, it may help overcome chemoresistance, which is a common challenge in cancer treatment.

Our results showed that the effect on cell viability differed significantly for use of paclitaxel alone versus its association with FBZ SD NC in the treatment regimen. As observed in Figure 5.8C, the effect on cell viability for the same doses was increased, reaching 25% for the lowest concentration tested (1.0 nM). Under the 1-cycle paclitaxel regimen, administered at a dose of 1000 nM, approximately 30% of cells retained their viability. Conversely, the 3-cycle chemotherapy regimen, involving multiple rounds of paclitaxel treatment, exhibited a more

pronounced influence on cell viability. Following this regimen, only 15% of cells remained viable, implying a stronger inhibitory impact on cell growth or induction of cell death compared to that of the 1-cycle regimen. Furthermore, in the absence of FBZ SD NC in the treatment protocol, the maximum attainable effect is a 50% cell viability rate.

Here, we revealed that pairing paclitaxel and FBZ in a novel oral inhaled formulation (FBZ SD NC) exhibits a synergistic impact on the cytotoxicity of tumor cells. This novel treatment approach could potentially serve as a viable option for patients with lung cancer, offering a reduction in the adverse effects associated with paclitaxel and potentially overcoming chemoresistance.

Figure 5.8. Cytotoxicity in A549 cells after 48 h of exposure. (A) FBZ SD NC and placebo alone (*p<0.01, **p<0.005 compared with placebo); (B) paclitaxel alone and pretreatment with FBZ SD NC (1000 nM) (*p<0.05, **p<0.001, ****p<0.0001 compared with paclitaxel); (C) paclitaxel alone or in association with FBZ SD NC (1000 nM) as a single (1x) or 3-cycle treatment (3x) (*p<0.05, **p<0.01, ****p<0.0001 compared with paclitaxel (1x); # p<0.05 compared with FBZ SD NC + paclitaxel (1x)).
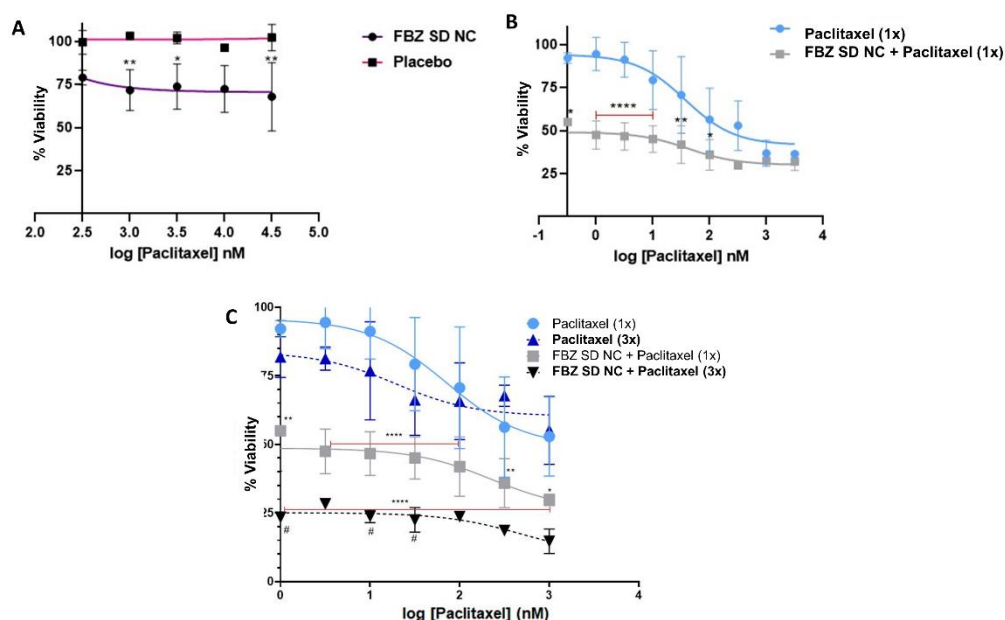
Source: elaborated by the author.

5.4 CONCLUSION

This study reported the development and characterization of an orally inhalable FBZ nanocrystal formulation with suitable aerosolization properties obtained through a rationale design. Along with the small particle size and increased saturated solubility, the formulation might increase the local concentration and bioavailability of this poorly soluble drug.

Combination with paclitaxel *in vitro* revealed a synergistic effect that was evinced after a 3-cycle treatment, with an impressive reduction in IC_{50} in A549 cells. A feasible formulation likely increases the chances of transposition to clinics, and all components used in the formulation are reported to have low toxicity. Furthermore, the process can be adjusted to a larger scale with minimum use of organic solvent. These results reaffirm the possibility of repurposing FBZ for lung cancer treatment with local delivery but suggest that FBZ would be better explored as an adjuvant for available cytotoxic agents, with great potential to assist dose reduction and consequently improve patients' quality of life by reducing adverse effects.

5.5 REFERENCES

ARNAUD-SAMPAIO, V. F.; BENTO, C. A.; GLASER, T.; ADINOLFI, E.; ULRICH, H.; LAMEU, C. P2X7 Receptor Isoform B Is a Key Drug Resistance Mediator for Neuroblastoma. **Frontiers in Oncology**, v. 12, p. 966404, 25 ago. 2022.

BEZZON, V. D. N.; FERREIRA, F. F.; SMITH, P.; BENMORE, C. J.; BYRN, S. R.; DE ARAUJO, G. L. B. Amorphous Dispersions of Flubendazole in Hydroxypropyl Methylcellulose: Formulation Stability Assisted by Pair Distribution Function Analysis. **International Journal of Pharmaceutics**, v. 600, p. 120500, maio 2021.

BRANNAN, J. D.; ANDERSON, S. D.; PERRY, C. P.; FREED-MARTENS, R.; LASSIG, A. R.; CHARLTON, B. The safety and efficacy of inhaled dry powder mannitol as a bronchial provocation test for airway hyperresponsiveness: a phase 3 comparison study with hypertonic (4.5%) saline. **Respiratory Research**, v. 6, n. 1, p. 144, 2005.

BUTTINI, F.; ROZOU, S.; ROSSI, A.; ZOUMPLIOU, V.; REKKAS, D. M. The Application of Quality by Design Framework in the Pharmaceutical Development of Dry Powder Inhalers. **European Journal of Pharmaceutical Sciences**, v. 113, p. 64–76, fev. 2018.

C. ANANDHARAMAKRISHNAN, PADMA ISHWARYA S. **Spray Drying Techniques for Food Ingredient Encapsulation**. [s.l.] John Wiley & Sons, Ltd, 2015. 312 p.

ČÁŇOVÁ, K.; ROZKYDALOVÁ, L.; RUDOLF, E. Anthelmintic Flubendazole and Its Potential Use in Anticancer Therapy. **Acta Medica (Hradec Kralove, Czech Republic)**, v. 60, n. 1, p. 5–11, 2017.

CHAFT, J. E.; RIMNER, A.; WEDER, W.; AZZOLI, C. G.; KRIS, M. G.; CASCONE, T. Evolution of Systemic Therapy for Stages I–III Non-Metastatic Non-Small-Cell Lung Cancer. **Nature Reviews Clinical Oncology**, v. 18, n. 9, p. 547–557, set. 2021.

DE ARAUJO, G. L. B.; FERREIRA, F. F.; BERNARDES, C. E. S.; SATO, J. A. P.; GIL, O. M.; DE FARIA, D. L. A.; LOEBENBERG, R.; BYRN, S. R.; GHISLENI, D. D. M.; BOU-CHACRA, N. A.; PINTO, T. J. A.; ANTONIO, S. G.; FERRAZ, H. G.; ZEMLYANOV, D.; GONÇALVES, D. S.; MINAS DA PIEDADE, M. E. A New Thermodynamically Favored Flubendazole/Maleic Acid Binary Crystal Form: Structure, Energetics, and *in Silico* PBPK Model-Based Investigation. **Crystal Growth & Design**, v. 18, n. 4, p. 2377–2386, 4 abr. 2018.

DE ASSIS, J. M. C.; BARBOSA, E. J.; BEZZON, V. D. N.; LOURENÇO, F. R.; CARVALHO, F. M. S.; MATOS, J. R.; ARACI BOU-CHACRA, N.; BENMORE, C. J.; BYRN, S. R.; COSTA, F. N.; DE

124

ARAUJO, G. L. B. Hot-melt extrudability of amorphous solid dispersions of flubendazole-copovidone: An exploratory study of the effect of drug loading and the balance of adjuvants on extrudability and dissolution. **International Journal of Pharmaceutics**, v. 614, p. 121456, 25 fev. 2022.

DE GROOT, P. M.; WU, C. C.; CARTER, B. W.; MUNDEN, R. F. The Epidemiology of Lung Cancer. **Translational Lung Cancer Research**, v. 7, n. 3, p. 220–233, jun. 2018.

DE SOUZA GONÇALVES, D.; YUKUYAMA, M. N.; MIYAGI, M. Y. S.; SILVA, T. J. V.; LAMEU, C.; BOU-CHACRA, N. A.; DE ARAUJO, G. L. B. Revisiting Flubendazole Through Nanocrystal Technology: Statistical Design, Characterization and Its Potential Inhibitory Effect on Xenografted Lung Tumor Progression in Mice. **Journal of Cluster Science**, v. 34, n. 1, p. 261–272, 1 jan. 2023.

DOBROWOLSKI, A.; STROB, R.; NIETFELD, J.; PIELOTH, D.; WIGGERS, H.; THOMMES, M. Preparation of Spray Dried Submicron Particles: Part B – Particle Recovery by Electrostatic Precipitation. **International Journal of Pharmaceutics**, v. 548, n. 1, p. 237–243, set. 2018.

DUARTE, D.; VALE, N. Evaluation of Synergism in Drug Combinations and Reference Models for Future Orientations in Oncology. **Current Research in Pharmacology and Drug Discovery**, v. 3, p. 100110, 2022.

DUMA, N.; SANTANA-DAVILA, R.; MOLINA, J. R. Non–Small Cell Lung Cancer: Epidemiology, Screening, Diagnosis, and Treatment. **Mayo Clinic Proceedings**, v. 94, n. 8, p. 1623–1640, ago. 2019.

ENGELBERG, S.; LIN, Y.; ASSARAF, Y. G.; LIVNEY, Y. D. Targeted Nanoparticles Harboring Jasmine-Oil-Entrapped Paclitaxel for Elimination of Lung Cancer Cells. **International Journal of Molecular Sciences**, v. 22, n. 3, p. 1019, 20 jan. 2021.

FUKUSHIGE, K.; TAGAMI, T.; NAITO, M.; GOTO, E.; HIRAI, S.; HATAYAMA, N.; YOKOTA, H.; YASUI, T.; BABA, Y.; OZEKI, T. Developing Spray-Freeze-Dried Particles Containing a Hyaluronic Acid-Coated Liposome–Protamine–DNA Complex for Pulmonary Inhalation. **International Journal of Pharmaceutics**, v. 583, p. 119338, 15 jun. 2020.

GU, Q.; XING, J. Z.; HUANG, M.; ZHANG, X.; CHEN, J. Nanoformulation of Paclitaxel to Enhance Cancer Therapy. **Journal of Biomaterials Applications**, v. 28, n. 2, p. 298–307, ago. 2013.

HADIWINOTO, G. D.; LIP KWOK, P. C.; LAKERVELD, R. A Review on Recent Technologies for the Manufacture of Pulmonary Drugs. **Therapeutic Delivery**, v. 9, n. 1, p. 47–70, jan. 2018.

HAMISHEHKAR, H.; RAHIMPOUR, Y.; JAVADZADEH, Y. The Role of Carrier in Dry Powder Inhaler. *Em*: SEZER, A. D. **Recent Advances in Novel Drug Carrier Systems**. [s.l.] InTech, 2012.

HARDY, D.; CORMIER, J. N.; XING, Y.; LIU, C.-C.; XIA, R.; DU, X. L. Chemotherapy-Associated Toxicity in a Large Cohort of Elderly Patients with Non-Small Cell Lung Cancer. **Journal of Thoracic Oncology**, v. 5, n. 1, p. 90–98, jan. 2010.

HERTEL, N.; BIRK, G.; SCHERLIESS, R. Particle Engineered Mannitol for Carrier-Based Inhalation – A Serious Alternative? **International Journal of Pharmaceutics**, v. 577, p. 118901, 15 mar. 2020.

ICH. Q3C — Tables and List Guidance for Industry. jun. 2017. Disponível em: <https://www.fda.gov/media/71737/download>. Acesso em: 3 maio. 2023.

JERMAIN, S. V.; BROUGH, C.; WILLIAMS, R. O. Amorphous solid dispersions and nanocrystal technologies for poorly water-soluble drug delivery – An update. **International Journal of Pharmaceutics**, v. 535, n. 1, p. 379–392, 15 jan. 2018.

JOG, R.; BURGESS, D. J. Comprehensive Quality by Design Approach for Stable Nanocrystalline Drug Products. **International Journal of Pharmaceutics**, v. 564, p. 426–460, jun. 2019.

JÜPTNER, A.; SCHERLIESS, R. Spray Dried Formulations for Inhalation—Meaningful Characterisation of Powder Properties. **Pharmaceutics**, v. 12, n. 1, p. 14, 21 dez. 2019.

KIM, Y.-J.; SUNG, D.; OH, E.; CHO, Y.; CHO, T.-M.; FARRAND, L.; SEO, J. H.; KIM, J. Y. Flubendazole Overcomes Trastuzumab Resistance by Targeting Cancer Stem-like Properties and HER2 Signaling in HER2-Positive Breast Cancer. **Cancer Letters**, v. 412, p. 118–130, jan. 2018.

KOSMIDIS, C.; SAPALIDIS, K.; ZAROGOULIDIS, P.; SARDELI, C.; KOULOURIS, C.; GIANNAKIDIS, D.; PAVLIDIS, E.; KATSAOUNIS, A.; MICHALOPOULOS, N.; MANTALOBAS, S.; KOIMTZIS, G.; ALEXANDROU, V.; TSIOUDA, T.; AMANITI, A.; KESISOGLOU, I. Inhaled Cisplatin for NSCLC: Facts and Results. **International Journal of Molecular Sciences**, v. 20, n. 8, p. 2005, 24 abr. 2019.

KUMAR, S.; GOKHALE, R.; BURGESS, D. J. Quality by Design Approach to Spray Drying Processing of Crystalline Nanosuspensions. **International Journal of Pharmaceutics**, v. 464, n. 1–2, p. 234–242, abr. 2014.

LACHAU-DURAND, S.; LAMMENS, L.; VAN DER LEEDE, B.; VAN GOMPEL, J.; BAILEY, G.; ENGELEN, M.; LAMPO, A. Preclinical Toxicity and Pharmacokinetics of a New Orally Bioavailable Flubendazole Formulation and the Impact for Clinical Trials and Risk/Benefit to Patients. **PLOS Neglected Tropical Diseases**, v. 13, n. 1, p. e0007026, 16 jan. 2019.

LAURA, C.; CELINA, E.; SERGIO, S. B.; GUILLERMO, D.; CARLOS, L.; LUIS, A. Combined Flubendazole-Nitazoxanide Treatment of Cystic Echinococcosis: Pharmacokinetic and Efficacy Assessment in Mice. **Acta Tropica**, v. 148, p. 89–96, ago. 2015.

LINDENBERG, F.; SICHEL, F.; LECHEVREL, M.; RESPAUD, R.; SAINT-LORANT, G. Evaluation of Lung Cell Toxicity of Surfactants for Inhalation Route. **Journal of Toxicology and Risk Assessment**, v. 5, n. 2, 15 maio 2019. Disponível em: <https://www.clinmedjournals.org/articles/ijtra/international-journal-of-toxicology-and-risk-assessment-ijtra-5-022.php?jid=ijtra>. Acesso em: 28 out. 2020.

LITTRINGER, E. M.; MESCHER, A.; SCHROETTNER, H.; ACHELIS, L.; WALZEL, P.; URBANETZ, N. A. Spray Dried Mannitol Carrier Particles with Tailored Surface Properties – The Influence of Carrier Surface Roughness and Shape. **European Journal of Pharmaceutics and Biopharmaceutics**, v. 82, n. 1, p. 194–204, 1 set. 2012.

MANGAL, S.; GAO, W.; LI, T.; ZHOU, Q. (Tony). Pulmonary delivery of nanoparticle chemotherapy for the treatment of lung cancers: challenges and opportunities. **Acta Pharmacologica Sinica**, v. 38, n. 6, p. 782–797, jun. 2017.

MANGAL, S.; NIE, H.; XU, R.; GUO, R.; CAVALLARO, A.; ZEMLYANOV, D.; ZHOU, Q. Physico-Chemical Properties, Aerosolization and Dissolution of Co-Spray Dried Azithromycin Particles with L-Leucine for Inhalation. **Pharmaceutical Research**, v. 35, n. 2, p. 28, fev. 2018.

MAY, S.; JENSEN, B.; WEILER, C.; WOLKENHAUER, M.; SCHNEIDER, M.; LEHR, C.-M. Dissolution Testing of Powders for Inhalation: Influence of Particle Deposition and Modeling of Dissolution Profiles. **Pharmaceutical Research**, v. 31, n. 11, p. 3211–3224, nov. 2014.

MERUVA, S.; THOOL, P.; GONG, Y.; KARKI, S.; BOWEN, W.; KUMAR, S. Role of Wetting Agents and Disintegrants in Development of Danazol Nanocrystalline Tablets. **International Journal of Pharmaceutics**, v. 577, p. 119026, mar. 2020.

METZ, J. Safety Assessment of Excipients (SAFE) for Orally Inhaled Drug Products. **ALTEX**, 2020. Disponível em: <https://www.altex.org/index.php/altex/article/view/1474>. Acesso em: 16 out. 2020.

MICHAELIS, M.; AGHA, B.; ROTHWEILER, F.; LÖSCHMANN, N.; VOGES, Y.; MITTELBRONN, M.; STARZETZ, T.; HARTER, P. N.; ABHARI, B. A.; FULDA, S.; WESTERMANN, F.; RIECKEN, K.; SPEK, S.; LANGER, K.; WIESE, M.; DIRKS, W. G.; ZEHNER, R.; CINATL, J.; WASS, M. N.; CINATL, J. Identification of Flubendazole as Potential Anti-Neuroblastoma Compound in a Large Cell Line Screen. **Scientific Reports**, v. 5, n. 1, p. 8202, 3 fev. 2015a.

MICHAELIS, M.; AGHA, B.; ROTHWEILER, F.; LÖSCHMANN, N.; VOGES, Y.; MITTELBRONN, M.; STARZETZ, T.; HARTER, P. N.; ABHARI, B. A.; FULDA, S.; WESTERMANN, F.; RIECKEN, K.; SPEK, S.; LANGER, K.; WIESE, M.; DIRKS, W. G.; ZEHNER, R.; CINATL, J.; WASS, M. N.; CINATL, J. Identification of Flubendazole as Potential Anti-Neuroblastoma Compound in a Large Cell Line Screen. **Scientific Reports**, v. 5, n. 1, p. 8202, jul. 2015b.

MORENO, L.; ALVAREZ, L.; MOTTIER, L.; VIRKEL, G.; SANCHEZ BRUNI, S.; LANUSSE, C. Integrated Pharmacological Assessment of Flubendazole Potential for Use in Sheep: Disposition Kinetics, Liver Metabolism and Parasite Diffusion Ability1. **Journal of Veterinary Pharmacology and Therapeutics**, v. 27, n. 5, p. 299–308, out. 2004.

MÜLLER, R. H.; GOHLA, S.; KECK, C. M. State of the Art of Nanocrystals – Special Features, Production, Nanotoxicology Aspects and Intracellular Delivery. **European Journal of Pharmaceutics and Biopharmaceutics**, v. 78, n. 1, p. 1–9, maio 2011.

MÜLLER, R. H.; MAÈDER, K.; GOHLA, S. Solid Lipid Nanoparticles (SLN) for Controlled Drug Delivery ± a Review of the State of the Art. **European Journal of Pharmaceutics and Biopharmaceutics**, p. 17, 2000.

OSTERBERG, R. E.; SEE, N. A. Toxicity of Excipients—A Food and Drug Administration Perspective. **International Journal of Toxicology**, v. 22, n. 5, p. 377–380, 1 set. 2003.

OWEN, S.C., R., R. C. **Handbook of Pharmaceutical Excipients**. 5th. ed. [s.l: s.n.]918 p.

PARKER, A. L.; TEO, W. S.; MCCARROLL, J. A.; KAVALLARIS, M. An Emerging Role for Tubulin Isotypes in Modulating Cancer Biology and Chemotherapy Resistance. **International Journal of Molecular Sciences**, v. 18, n. 7, p. 1434, 4 jul. 2017.

PATWARDHAN, G. A.; MARCZYK, M.; WALI, V. B.; STERN, D. F.; PUSZTAI, L.; HATZIS, C. Treatment Scheduling Effects on the Evolution of Drug Resistance in Heterogeneous Cancer Cell Populations. **npj Breast Cancer**, v. 7, n. 1, p. 60, 26 maio 2021.

PELTONEN, L.; STRACHAN, C. J. Degrees of Order: A Comparison of Nanocrystal and Amorphous Solids for Poorly Soluble Drugs. **International Journal of Pharmaceutics**, v. 586, p. 119492, ago. 2020.

PUBCHEM. **Dimethyl sulfoxide**. Disponível em: <https://pubchem.ncbi.nlm.nih.gov/compound/679>. Acesso em: 26 out. 2020.

ROSIÈRE, R.; BERGHMANS, T.; DE VUYST, P.; AMIGHI, K.; WAUTHOZ, N. The Position of Inhaled Chemotherapy in the Care of Patients with Lung Tumors: Clinical Feasibility and Indications According to Recent Pharmaceutical Progresses. **Cancers**, v. 11, n. 3, p. 329, 7 mar. 2019.

SCHOUBBEN, A.; VIVANI, R.; PAOLANTONI, M.; PERINELLI, D. R.; GIOIELLO, A.; MACCHIARULO, A.; RICCI, M. D-Leucine Microparticles as an Excipient to Improve the

Aerosolization Performances of Dry Powders for Inhalation. **European Journal of Pharmaceutical Sciences**, v. 130, p. 54–64, mar. 2019.

SHETTY, N.; AHN, P.; PARK, H.; BHUJBAL, S.; ZEMLYANOV, D.; CAVALLARO, A.; MANGAL, S.; LI, J.; ZHOU, Q. (Tony). Improved physical stability and aerosolization of inhalable amorphous ciprofloxacin powder formulations by incorporating synergistic colistin. **Molecular pharmaceutics**, v. 15, n. 9, p. 4004–4020, 4 set. 2018a.

SHETTY, N.; PARK, H.; ZEMLYANOV, D.; MANGAL, S.; BHUJBAL, S.; ZHOU, Q. (Tony). Influence of Excipients on Physical and Aerosolization Stability of Spray Dried High-Dose Powder Formulations for Inhalation. **International Journal of Pharmaceutics**, v. 544, n. 1, p. 222–234, jun. 2018b.

SINHA, B.; MÜLLER, R. H.; MÖSCHWITZER, J. P. Bottom-up Approaches for Preparing Drug Nanocrystals: Formulations and Factors Affecting Particle Size. **International Journal of Pharmaceutics**, v. 453, n. 1, p. 126–141, ago. 2013.

SON, Y.-J.; WORTH LONGEST, P.; HINDLE, M. Aerosolization Characteristics of Dry Powder Inhaler Formulations for the Excipient Enhanced Growth (EEG) Application: Effect of Spray Drying Process Conditions on Aerosol Performance. **International Journal of Pharmaceutics**, v. 443, n. 1–2, p. 137–145, 25 fev. 2013.

SPAGNUOLO, P. A.; HU, J.; HURREN, R.; WANG, X.; GRONDA, M.; SUKHAI, M. A.; DI MEO, A.; BOSS, J.; ASHALI, I.; BEHESHTI ZAVAREH, R.; FINE, N.; SIMPSON, C. D.; SHARMEEN, S.; ROTTAPEL, R.; SCHIMMER, A. D. The Antihelmintic Flubendazole Inhibits Microtubule Function through a Mechanism Distinct from Vinca Alkaloids and Displays Preclinical Activity in Leukemia and Myeloma. **Blood**, v. 115, n. 23, p. 4824–4833, 10 jun. 2010.

STEINER, V.; ÖHLINGER, K.; CORZO, C.; SALAR-BEHZADI, S.; FRÖHLICH, E. Cytotoxicity Screening of Emulsifiers for Pulmonary Application of Lipid Nanoparticles. **European Journal of Pharmaceutical Sciences**, v. 136, p. 104968, ago. 2019.

SUNG, H.; FERLAY, J.; SIEGEL, R. L.; LAVERSANNE, M.; SOERJOMATARAM, I.; JEMAL, A.; BRAY, F. Global Cancer Statistics 2020: GLOBOCAN Estimates of Incidence and Mortality Worldwide for 36 Cancers in 185 Countries. **CA: A Cancer Journal for Clinicians**, v. 71, n. 3, p. 209–249, maio 2021.

TAKI, M.; TAGAMI, T.; FUKUSHIGE, K.; OZEKI, T. Fabrication of Nanocomposite Particles Using a Two-Solution Mixing-Type Spray Nozzle for Use in an Inhaled Curcumin Formulation. **International Journal of Pharmaceutics**, v. 511, n. 1, p. 104–110, set. 2016.

TANEJA, S.; SHILPI, S.; KHATRI, K. Formulation and Optimization of Efavirenz Nanosuspensions Using the Precipitation-Ultrasonication Technique for Solubility Enhancement. **Artificial cells, nanomedicine, and biotechnology**, v. 44, n. 3, p. 978–984, maio 2016.

TANG, S.; QIN, C.; HU, H.; LIU, T.; HE, Y.; GUO, H.; YAN, H.; ZHANG, J.; TANG, S.; ZHOU, H. Immune Checkpoint Inhibitors in Non-Small Cell Lung Cancer: Progress, Challenges, and Prospects. **Cells**, v. 11, n. 3, p. 320, jan. 2022.

THE UNITED STATES PHARMACOPEIA. **USP 31 NF26s1_c601, General Chapters: <601> AEROSOLS, NASAL SPRAYS, METERED-DOSE INHALERS, AND DRY POWDER INHALERS,**. Disponível em: <http://www.uspbpep.com/usp31/v31261/usp31nf26s1_c601.asp>. Acesso em: 10 set. 2020.

THE UNITED STATES PHARMACOPEIA. <467> RESIDUAL SOLVENTS. v. 42, p. 23, 2020.

TUOMELA, A.; HIRVONEN, J.; PELTONEN, L. Stabilizing Agents for Drug Nanocrystals: Effect on Bioavailability. **Pharmaceutics**, v. 8, n. 2, p. 16, jun. 2016.

VEHRING, R. Pharmaceutical Particle Engineering via Spray Drying. **Pharmaceutical Research**, v. 25, n. 5, p. 999–1022, maio 2008.

VIALPANDO, M.; SMULDERS, S.; BONE, S.; JAGER, C.; VODAK, D.; VAN SPEYBROECK, M.; VERHEYEN, L.; BACKX, K.; BOEYKENS, P.; BREWSTER, M. E.; CEULEMANS, J.; NOVOA DE ARMAS, H.; VAN GEEL, K.; KESSELAERS, E.; HILLEWAERT, V.; LACHAU-DURAND, S.; MEURS, G.; PSATHAS, P.; VAN HOVE, B.; VERRECK, G.; VOETS, M.; WEUTS, I.; MACKIE, C. Evaluation of Three Amorphous Drug Delivery Technologies to Improve the Oral Absorption of Flubendazole. **Journal of Pharmaceutical Sciences**, v. 105, n. 9, p. 2782–2793, set. 2016.

YE, Y.; MA, Y.; ZHU, J. The Future of Dry Powder Inhaled Therapy: Promising or Discouraging for Systemic Disorders? **International Journal of Pharmaceutics**, v. 614, p. 121457, fev. 2022.

ZHOU, X. Flubendazole Inhibits Glioma Proliferation by G2/M Cell Cycle Arrest and pro-Apoptosis. p. 10, 2018.

ZHOU, X.; LIU, J.; ZHANG, J.; WEI, Y.; LI, H. Flubendazole Inhibits Glioma Proliferation by G2/M Cell Cycle Arrest and pro-Apoptosis. **Cell Death Discovery**, v. 4, n. 1, p. 1–10, 14 fev. 2018.

ZILLEN, D.; BEUGELING, M.; HINRICHS, W. L. J.; FRIJLINK, H. W.; GRASMEIJER, F. Natural and Bioinspired Excipients for Dry Powder Inhalation Formulations. **Current Opinion in Colloid & Interface Science**, v. 56, p. 101497, 1 dez. 2021.

CHAPTER 6   CONCLUSIONS

6.1 CONCLUSIONS

The most concerning statistic for lung cancer is that more than 50% of patients have metastasis by the time of diagnosis, and in Brazil, they represent a striking 87%. This condition directly translates into poor prognosis with only 5 to 10% being expected to survive more than 5 years, providing little to no hope to patients and their relatives. In addition to this perspective, the common understanding of how chemotherapy can spoil the quality of life due to serious adverse effects certainly does not contribute to seeking or starting a treatment. Immunotherapy was a breakthrough for the treatment of metastatic lung cancer, but only for patients with high expression of specific proteins, such as PD-L1. Meanwhile, improvements to already existing chemotherapy regimens could benefit all.

Through rationale development, FBZ nanocrystals were successfully obtained by precipitation in an aqueous solution, with minimum use of organic solvents. The subsequent spray drying with mannitol, l-leucine and poloxamer 188 provided a powder with suitable characteristics for inhalation and preserved crystalline state. This application of technology to improve an already known drug assists in clarifying the perspective that this approach can be used as a tool for repurposing poorly soluble drugs. Thus, the synergistic effect observed with association to paclitaxel could illustrate a first step towards inhalable chemotherapy, by using a less toxic active ingredient carried by few known excipients aiming adjuvant therapy.

Reduction of systemic exposure and the discomfort of a long intravenous infusion and higher efficacy due to local delivery are some of the benefits of inhalable chemotherapy. As this approach is still in its infancy, and DPIs rather than nebulization is even more recent, many challenges must be addressed on different fronts to provide momentum for development and better translation:

- An increasing number of pragmatic studies confirming the feasibility of suitable formulations could attract the attention of industries.
- Sponsors would be attracted to invest in product development.
- Suppliers would be compelled to invest in toxicity tests to provide new excipients for inhalation.
- Development of devices in combination with the final formulation to further improve specific aerosolization and increase delivery, considering patient needs.
- Improvements of biorelevant *in vitro* methods and protocols that would not dissociate evaluation of physical properties and efficacy.

- *In vivo* evaluation, combined with emerging *in silico* modeling for better adjusting extrapolation to humans.
- Better description of device specifications in leaflets, and explanation of differences among existing types to doctors to assure suitable prescription.
- Periodic guiding patients on the correct use of devices to maximize delivery and assure compliance with the treatment.

Naturally, inhaled chemotherapy might not benefit all stages or all histologic types and could be first proposed in association with a well stablished treatment. But is also interesting to broaden possibilities of inhalable administration as a form of delivering palliative care to patients.

CHAPTER 7   FUTURE DIRECTIONS

7.1 FUTURE DIRECTIONS

The obtained nanocrystal formulation showed great improvement in cytotoxicity when associated with paclitaxel against A549 lung cancer cells. But since a conventional culture hardly mimics the complex tumor microenvironment, additional tests that would continue to clarify FBZ efficacy for cancer treatment include:

- Evaluation of FBZ SD NC in more complex in vitro models, as 3D-cultures of A549 cells and microfluidic system with a fluid-dynamic bioreactor (MIVO®).

- Development of an *in silico* model using GastroPlus® to evaluate pharmacokinetics profile of the FBZ SD NC.

- Further synergic studies with established drugs can also serve as direction for development of new formulations.

FBZ shows potential against different types of cancer, therefore, depending on the systemic distribution of the formulation to be observed in a GastroPlus® model, FBZ SD NC could be evaluated *in vitro* against other type of cancer cell lines, as neuroblastoma and leukemia, since even greater response has been when compared to lung cancer (MICHAELIS *et al.*, 2015).

Lastly, a project that is already under development that aims better understanding of relationship of physical properties and *in vitro* efficacy is the SIMPATEC-USP (Simplified Impactor Developed at the University of São Paulo). After testing and validation, this low-cost apparatus can increase the feasibility of the study of inhalable formulations in academic institutions.

7.1.1 SIMPATEC-USP

FBZ nanocrystal formulation revealed a synergic effect when associated with paclitaxel, leading to a 1000-fold reduction of IC_{50}. The 3-cycle model combined treatment increased threshold of cytotoxicity by 25% for the same dose when compared to 3-cycle paclitaxel alone. Since the protocol involved resuspension of the spray dried powder in cell culture medium, it would be interesting to evaluate the impact of aerodynamic properties directly on efficacy. As cascade impactors as ACI and NGI are expensive and can be laborious to set up due to the multi-stages, we developed a novel low-cost single-stage impactor design that meets the pharmacopeial parameters (USP) for in vitro testing of dry powder inhalers (DPIs). The proposed simplified impactor, referred to as SIMPATEC-USP (Simplified Impactor Developed at the University of São Paulo), eliminates the multiple stages found in conventional cascade impactors, retaining the fraction of interest in a single stage within a Petri dish (Figure 7.1).

Figure 7.1. 3D-design of SIMPATEC-USP (Simplified Impactor Developed at the University of São Paulo).
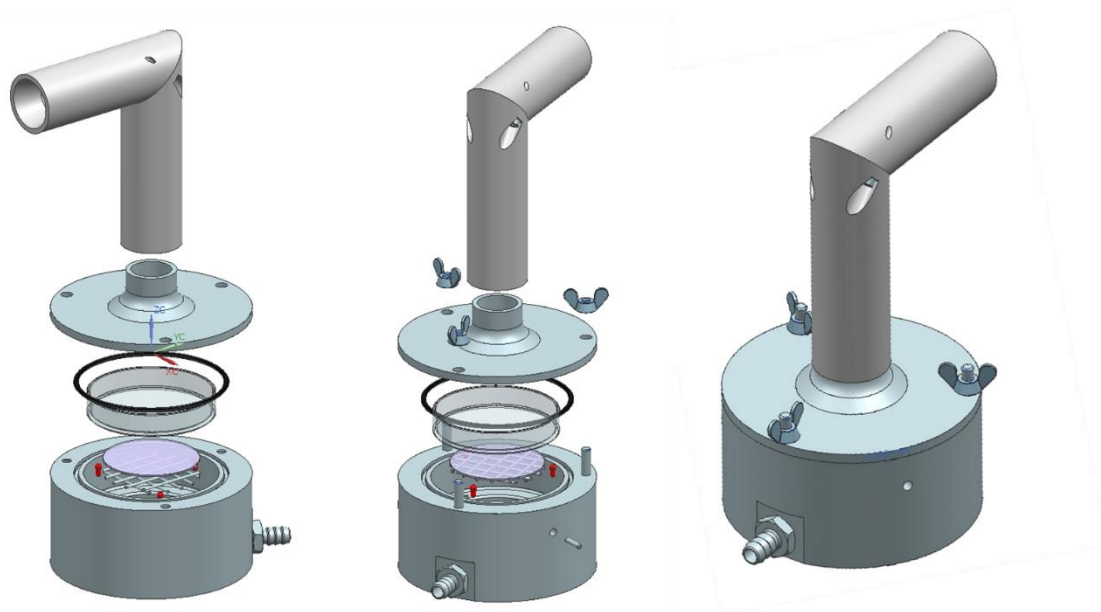
Source: elaborated by the author.

The designed impactor incorporates a unique closure system that simplifies assembly and disassembly, eliminating the need for cumbersome springs or fixing mechanisms. Based on a modified cascade impactor, the collection chamber is tailored to accommodate a glass Petri dish instead of a collection plate. The impactor utilizes the Petri dish as the collection medium, supported by filter paper for final filtration. This design facilitates convenient collection of viable product following inhaler aerosolization, rendering the impactor cost-effective compared to commercially available alternatives. The simplified impactor offers a quick method in early development for comparing the aerodynamic behavior of formulations, evaluating capsule retention and emitted dose uniformity, and assessing the performance of dry powder inhaler devices. Additionally, it enables the collection of samples for drug release and activity studies, as well as delivering formulations directly to Petri dishes containing a culture medium inoculated with test organisms for antibacterial activity screenings.

This low-cost impactor design offers a practical solution for pharmaceutical laboratories and academic institutions by significantly reducing the cost associated with in vitro testing of DPIs. Its implementation enables researchers to efficiently evaluate inhaler device performance and make formulation improvements during the early stages of product development.

This new affordable apparatus offers a practical solution for pharmaceutical laboratories and academic institutions for a rapid assessment of inhaler aerosolization performance, contributing to DOE analysis, identifying potential issues during early-stage product development, and preparing samples for an efficacy or dissolution test. The proposed impactor

serves as an accessible tool for quality control and research purposes, ultimately advancing the field of pulmonary drug delivery.

7.2 REFERENCES

MICHAELIS, M.; AGHA, B.; ROTHWEILER, F.; LÖSCHMANN, N.; VOGES, Y.; MITTELBRONN, M.; STARZETZ, T.; HARTER, P. N.; ABHARI, B. A.; FULDA, S.; WESTERMANN, F.; RIECKEN, K.; SPEK, S.; LANGER, K.; WIESE, M.; DIRKS, W. G.; ZEHNER, R.; CINATL, J.; WASS, M. N.; CINATL, J. **Identification of Flubendazole as Potential Anti-Neuroblastoma Compound in a Large Cell Line Screen.** Scientific Reports, v. 5, n. 1, p. 8202, 3 fev. 2015.